Enclosure 7

AREVA Report ANP-3224(NP)

Applicability of AREVA NP BWR Methods To Monticello

Revision 2

185 pages follow

ANP-3224NP
Revision 2

Applicability of AREVA NP BWR Methods to Monticello

June 2013

AREVA NP Inc.

AREVA

AREVA NP Inc.

ANP-3224NP
Revision 2

Applicability of AREVA NP BWR Methods to Monticello

AREVA NP Inc.

ANP-3224NP
Revision 2

Applicability of AREVA NP BWR Methods to Monticello

Record of Revision

Revision No.	Pages/Sections/ Paragraphs Changed	Brief Description / Change Authorization
002	Table D-1	Table D-1 revised to be consistent with proprietary document.
001	All	Minor typographic errors.
	A-29, G-6, G-7, and G-8	The figures have been marked as proprietary.
	D-9	Added proprietary marks in Table D-1.
	E-6	In the third paragraph fourth sentence "RODEX2 at 2,200 GWd/MTU" has been corrected to read "RODEX2 at 2 GWd/MTU."
000	All	This is a new document.

Contents

1.0 Introduction 1-1

2.0 Overview 2-1
2.1 SER Restriction by Topical Report 2-4
2-1 XN-NF-79-56(P)(A) Revision 1 and Supplement 1, "Gadolinia Fuel Properties for LWR Fuel Safety Evaluation," Exxon Nuclear Company, November 1981. 2-5
2-2 XN-75-32(P)(A) Supplements 1 through 4, "Computational Procedure for Evaluating Fuel Rod Bowing," Exxon Nuclear Company, October 1983. (Base document not approved.) 2-6
2-3 XN-NF-81-58(P)(A) Revision 2 and Supplements 1 and 2, "RODEX2 Fuel Rod Thermal-Mechanical Response Evaluation Model," Exxon Nuclear Company, March 1984. 2-7
2-4 XN-NF-81-51(P)(A), "LOCA-Seismic Structural Response of an Exxon Nuclear Company BWR Jet Pump Fuel Assembly," Exxon Nuclear Company, May 1986. 2-8
2-5 XN-NF-85-74(P)(A) Revision 0, "RODEX2A (BWR) Fuel Rod Thermal-Mechanical Evaluation Model" Exxon Nuclear Company, August 1986. 2-9
2-6 XN-NF-85-92(P)(A), "Exxon Nuclear Uranium Dioxide/Gadolinia Irradiation Examination and Thermal Conductivity Results," Exxon Nuclear Company, November 1986. 2-10
2-7 ANF-89-98(P)(A) Revision 1 and Supplement 1, "Generic Mechanical Design Criteria for BWR Fuel Designs," Advanced Nuclear Fuels Corporation, May 1995. 2-11
2-8 ANF-90-82(P)(A) Revision 1, "Application of ANF Design Methodology for Fuel Assembly Reconstitution," Advanced Nuclear Fuels Corporation, May 1995. 2-13
2-9 EMF-85-74(P) Revision 0 Supplement 1(P)(A) and Supplement 2(P)(A), "RODEX2A (BWR) Fuel Rod Thermal-Mechanical Evaluation Model," Siemens Power Corporation, February 1998. 2-14
2-10 EMF-93-177(P)(A) Revision 1, "Mechanical Design for BWR Fuel Channels," Framatome ANP, August 2005. 2-16
2-11 BAW-10247PA Revision 0, "Realistic Thermal-Mechanical Fuel Rod Methodology for Boiling Water Reactors," AREVA NP, February 2008. 2-18
2-12 XN-NF-80-19(P)(A) Volume 1 and Supplements 1 and 2, "Exxon Nuclear Methodology for Boiling Water Reactors - Neutronic Methods for Design and Analysis," Exxon Nuclear Company, March 1983. 2-21
2-13 XN-NF-80-19(P)(A) Volume 4 Revision 1, "Exxon Nuclear Methodology for Boiling Water Reactors: Application of

the ENC Methodology to BWR Reloads," Exxon Nuclear Company, June 1986. 2-23

2-14 EMF-CC-074(P)(A) Volume 1, "STAIF - A Computer Program for BWR Stability Analysis in the Frequency Domain," and Volume 2 "STAIF - A Computer Program for BWR Stability Analysis in the Frequency Domain - Code Qualification Report," Siemens Power Corporation, July 1994. 2-24

2-15 EMF-2158(P)(A) Revision 0, "Siemens Power Corporation Methodology for Boiling Water Reactors: Evaluation and Validation of CASMO-4/MICROBURN-B2," Siemens Power Corporation, October 1999. 2-26

2-16 EMF-CC-074(P)(A) Volume 4, Revision 0, "BWR Stability Analysis - Assessment of STAIF with Input from MICROBURN-B2," Siemens Power Corporation, August 2000. 2-28

2-17 BAW-10255PA Revision 2, "Cycle-Specific DIVOM Methodology Using the RAMONA5-FA Code," AREVA NP, May 2008. 2-30

2-18 XN-NF-79-59(P)(A), "Methodology for Calculation of Pressure Drop in BWR Fuel Assemblies," Exxon Nuclear Company, November 1983. 2-31

2-19 XN-NF-80-19(P)(A) Volume 3 Revision 2, "Exxon Nuclear Methodology for Boiling Water Reactors, THERMEX: Thermal Limits Methodology Summary Description," Exxon Nuclear Company, January 1987. 2-32

2-20 ANF-524(P)(A) Revision 2 and Supplements 1 and 2, "ANF Critical Power Methodology for Boiling Water Reactors," Advanced Nuclear Fuels Corporation, November 1990. 2-34

2-21 EMF-2245(P)(A) Revision 0, "Application of Siemens Power Corporation's Critical Power Correlations to Co-Resident Fuel," Siemens Power Corporation, August 2000. 2-36

2-22 EMF-2209(P)(A) Revision 3, "SPCB Critical Power Correlation," AREVA NP, September 2009. 2-37

2-23 ANP-10249PA Revision 1, "ACE/ATRIUM-10 Critical Power Correlation," AREVA NP, September 2009. 2-39

2-24 ANP-10298PA Revision 0, "ACE/ATRIUM 10XM Critical Power Correlation," AREVA NP, March 2010. 2-40

2-25 ANP-10307PA Revision 0, "AREVA MCPR Safety Limit Methodology for Boiling Water Reactors," AREVA NP, June 2011. 2-42

2-26 XN-CC-33(A) Revision 1, "HUXY: A Generalized Multirod Heatup Code with 10 CFR 50 Appendix K Heatup Option Users Manual," Exxon Nuclear Company, November 1975. 2-43

2-27 XN-NF-80-19(P)(A) Volumes 2, 2A, 2B and 2C, "Exxon Nuclear Methodology for Boiling Water Reactors: EXEM

BWR ECCS Evaluation Model," Exxon Nuclear Company, September 1982. 2-46
2-28 XN-NF-82-07(P)(A) Revision 1, "Exxon Nuclear Company ECCS Cladding Swelling and Rupture Model," Exxon Nuclear Company, November 1982. 2-47
2-29 XN-NF-84-105(P)(A) Volume 1 and Volume 1 Supplements 1 and 2, "XCOBRA-T: A Computer Code for BWR Transient Thermal-Hydraulic Core Analysis," Exxon Nuclear Company, February 1987. 2-48
2-30 ANF-913(P)(A) Volume 1 Revision 1 and Volume 1 Supplements 2, 3 and 4, "COTRANSA2: A Computer Program for Boiling Water Reactor Transient Analyses," Advanced Nuclear Fuels Corporation, August 1990. 2-51
2-31 ANF-91-048(P)(A), "Advanced Nuclear Fuels Corporation Methodology for Boiling Water Reactors EXEM BWR Evaluation Model," Advanced Nuclear Fuels Corporation, January 1993. 2-55
2-32 ANF-91-048(P)(A) Supplements 1 and 2, "BWR Jet Pump Model Revision for RELAX," Siemens Power Corporation, October 1997. 2-56
2-33 EMF-2292(P)(A) Revision 0, "ATRIUM™-10: Appendix K Spray Heat Transfer Coefficients," Siemens Power Corporation, September 2000. 2-57
2-34 EMF-2361(P)(A) Revision 0, "EXEM BWR-2000 ECCS Evaluation Model," Framatome ANP, May 2001. 2-58

3.0 References 3-1

Appendix A Neutronic Methods A-1

A.1 Cross Section Representation A-1

A.2 Applicability of Uncertainties A-4

A.3 Fuel Cycle Comparisons A-8

A.4 Bypass Voiding A-10

A.5 Fuel Assembly Design A-12

Appendix B Non-Linear Stability B-1

B.1 Bypass voiding B-1

B.2 Applicability of ATWS-I B-2

Appendix C Application of AREVA Methodology for Mixed Cores C-1

C.1 Discussion C-1

C.2 Shutdown Margin C-5

C.3 Assembly Liftoff C-6

Appendix D Void-Quality Correlations D-1

D.1 AREVA Void Quality Correlations D-1

D.2 Void Quality Correlation Uncertainties D-4

D.3 Biasing of the Void-Quality Correlation D-5

D.4 Void-Quality Correlation Uncertainty Summary D-7

Appendix E Fuel Conductivity Degradation E-1

E.1 Introduction E-1

E.2 Disposition of Licensing Safety Analysis for Monticello ATRIUM 10XM Fuel E-1

E.3 Assessment of Analyses for Monticello ATRIUM 10XM Fuel E-2

E.3.1 Anticipated Operational Occurrence Analyses E-2

E.3.2 Loss of Coolant Accident Analyses E-4

E.3.2.1 Responses to NRC Requests E-5

E.3.3 Overpressurization Analyses E-6

E.3.3.1 Res*ponses to NRC Requests* E-7

E.3.4 Stability Analyses E-8

E.3.5 Fire Event Analyses E-8

Appendix F COTRANSA2 Cross Section Representation F-1

Appendix G Extending SPCB/GE14 Low Pressure Boundary G-1

Tables

Table 2-1 AREVA Operating/Licensing Experience 2-2
Table E-1 Impact of TCD on PCT E-9
Table E-2 Monticello Cycle 28 Overpressurization Biases and Results E-10

Figures

Figure 2-1 Comparison of AREVA Benchmark Data and Typical Monticello Reactor Conditions 2-3
Figure A-2 Microscopic Fast Cross Section of U-235 from Base Depletion and Branches A-15
Figure A-3 Microscopic Thermal Cross Section of U-235 at Beginning of Life A-16
Figure A-4 Microscopic Fast Cross Section of U-235 at Beginning of Life A-16
Figure A-5 Microscopic Thermal Cross Section of U-235 Comparison of Quadratic Fit with Explicit Calculations at Various Void Fractions A-17
Figure A-6 Microscopic Fast Cross Section of U-235 Comparison of Quadratic Fit with Explicit Calculations at Various Void Fractions A-17
Figure A-7 Macroscopic Diffusion Coefficient (Fast and Thermal) Comparison of Quadratic Fit with Explicit Calculations at Various Void Fractions A-18
Figure A-8 Microscopic Thermal Cross Section of U-235 at 70 GWd/MTU A-19
Figure A-9 Quadratic Interpolation Illustration of Microscopic Thermal Cross Section of U-235 ..... A-20
Figure A-10 Illustration of Final Quadratic Interpolation for Microscopic Thermal Cross Section of U-235 ..... A-20
Figure A-11 Comparison of k-infinity from MICROBURN-B2 Interpolation Process with CASMO-4 Calculations at Intermediate Void Fractions of 0.2, 0.6 and 0.9 ..... A-21
Figure A-12 Comparison of k-infinity from MICROBURN-B2 Interpolation Process with CASMO-4 Calculations at 0.4 Historical Void Fractions and 0.9 Instantaneous Void Fraction A-21
Figure A-13 Delta k-infinity from MICROBURN-B2 Interpolation Process with CASMO-4 Calculations at 0.4 Historical Void Fraction and 0.9 Instantaneous Void Fraction A-22

Figure A-14 Comparison of Interpolation Process Using Void Fractions of 0.0, 0.4 and 0.8 and Void Fractions of 0.0, 0.45 and 0.9 ..... A-22
Figure A-15 EMF-2158(P)(A) TIP Statistics by Axial Level A-23
Figure A-16 EMF-2158(P)(A) 2-D TIP Statistics for C-Lattice Plants vs. Core Power A-23
Figure A-17 EMF-2158(P)(A) 2-D TIP Statistics for C-Lattice Plants vs. Core Average Void Fraction A-24
Figure A-18 EMF-2158(P)(A) 2-D TIP Statistics for C-Lattice Plants vs. Core Power/Flow Ratio A-24
Figure A-19 EMF-2158(P)(A) 2-D TIP Statistics for D-Lattice Plants vs. Core Power A-25
Figure A-21 EMF-2158(P)(A) 2-D TIP Statistics for D-Lattice Plants vs. Core Power/Flow Ratio A-26
Figure A-22 EMF-2158(P)(A) 3-D TIP Statistics for C-Lattice Plants vs. Core Power A-26
Figure A-23 EMF-2158(P)(A) 3-D TIP Statistics for C-Lattice Plants vs. Core Average Void Fraction A-27
Figure A-24 EMF-2158(P)(A) 3-D TIP Statistics for C-Lattice Plants vs. Core Power/Flow Ratio A-27
Figure A-25 EMF-2158(P)(A) 3-D TIP Statistics for D-Lattice Plants vs. Core Power A-28
Figure A-26 EMF-2158(P)(A) 3-D TIP Statistics for D-Lattice Plants vs. Core Average Void Fraction A-28
Figure A-27 EMF-2158(P)(A) 3-D TIP Statistics for D-Lattice Plants vs. Core Power/Flow Ratio A-29
Figure A-28 Quad Cities Unit 1 Pin by Pin Gamma Scan Results A-29
Figure A-29 Maximum Assembly Power in Topical Report EMF-2158(P)(A) A-30
Figure A-30 Maximum Exit Void Fraction in Topical Report EMF-2158(P)(A) A-30
Figure A-31 Maximum Assembly Power Observed from Recent Operating Experience A-31
Figure A-32 Void Fractions Observed from Recent Operating Experience A-31
Figure A-33 Axial Power and Void Profile Observed from Recent Design Experience A-32
Figure A-34 Nodal Void Fraction Histogram Observed from Recent Design Experience A-32
Figure A-35 Maximum Assembly Power in an EPFOD Monticello Design A-33
Figure A-36 Maximum Exit Void Fraction in an EPFOD Monticello Design A-33
Figure A-37 Monticello EPFOD Design Axial Profile of Power and Void Fraction A-34

Figure A-38 Monticello EPFOD Design Nodal Void Fraction Histogram A-34
Figure A-39 Hypothetical MICROBURN-B2 Multi-Channel Average Bypass Void Distribution A-35
Figure B-1 Relative Power for Case 1 Base Global Oscillation B-9
Figure B-2 Relative Power for Case 2 Base Regional Oscillation B-9
Figure B-3 Relative Power for Case 3 Global Oscillation B-10
Figure B-4 Relative Power for Case 4 Regional Oscillation B-10
Figure B-5 Relative Power for Case 5 Regional Oscillation With Decreased Subcriticality B-11
Figure B-6 Relative Power for Case 6 Mitigated Global Oscillation B-11
Figure B-7 Relative Power for Case 7 Mitigated Regional Oscillation B-12
Figure B-8 Relative Power for Case 8 Late-Mitigated Global Oscillation B-12
Figure B-9 Relative Power for Case 9 Late-Mitigated Regional Oscillation B-13
Figure B-10 Inlet Mass Flow Rate for Case 1 Base Global Oscillation B-13
Figure B-11 Inlet Mass Flow Rate for Case 2 Base Regional Oscillation B-14
Figure B-12 Inlet Mass Flow Rate for Case 3 Global Oscillation B-14
Figure B-13 Inlet Mass Flow Rate for Case 4 Regional Oscillation B-15
Figure B-14 Inlet Mass Flow Rate for Case 5 Regional Oscillation With Decreased Subcriticality B-15
Figure B-15 Inlet Mass Flow Rate for Case 6 Mitigated Global Oscillation B-16
Figure B-16 Inlet Mass Flow Rate for Case 7 Mitigated Regional Oscillation B-16
Figure B-17 Inlet Mass Flow Rate for Case 8 Late-Mitigated Global Oscillation B-17
Figure B-18 Inlet Mass Flow Rate for Case 9 Late-Mitigated Regional Oscillation B-17
Figure B-19 Exit Void Fraction for Case 1 Base Global Oscillation B-18
Figure B-20 Exit Void Fraction for Case 2 Base Regional Oscillation B-18
Figure B-21 Exit Void Fraction for Case 3 Global Oscillation B-19
Figure B-22 Exit Void Fraction for Case 4 Regional Oscillation B-19
Figure B-23 Exit Void Fraction for Case 5 Regional Oscillation With Decreased Subcriticality B-20
Figure B-24 Exit Void Fraction for Case 6 Mitigated Global Oscillation B-20
Figure B-25 Exit Void Fraction for Case 7 Mitigated Regional Oscillation B-21
Figure B-26 Exit Void Fraction for Case 8 Late-Mitigated Regional Oscillation B-21
Figure B-27 Exit Void Fraction for Case 9 Late-Mitigated Regional Oscillation B-22
Figure B-28 Void Fraction in Selected Nodes for Case 1 Base Global Oscillation B-22

Figure B-29 Void Fraction in Selected Nodes for Case 2 Base Regional Oscillation B-23

Figure B-30 Void Fraction in Selected Nodes for Case 3 Global Oscillation B-23

Figure B-31 Void Fraction in Selected Nodes for Case 4 Regional Oscillation B-24

Figure B-32 Void Fraction in Selected Nodes for Case 5 Regional Oscillation With Decreased Subcriticality B-24

Figure D-1 Validation of [ ] using FRIGG-2 and FRIGG-3 Void Data D-11

Figure D-2 Validation of [ ] using ATRIUM-10 and ATRIUM 10XM Void Data D-11

Figure D-3 Validation of Ohkawa-Lahey using FRIGG-2 and FRIGG-3 Void Data D-12

Figure D-4 Validation of Ohkawa-Lahey using ATRIUM-10 and ATRIUM 10XM Void Data D-12

Figure D-5a FRIGG Test Cross Section D-13

Figure D-5b GE14 (left) and ATRIUM-10 (right) Top Cross Section D-13

Figure D-6 Modified Void Fraction Correlation Comparison to ATRIUM-10 Test Data D-14

Figure D-7 [ ] Void Fraction Comparison to ATRIUM-10 Test Data D-14

Figure G-1 The Influence of System Pressure on Critical Heat Flux G-4

Figure G-2 Normalized Critical Power versus Pressure G-5

Figure G-3 ATRIUM-10 Test STS-17.8 Critical Power versus Pressure G-6

Figure G-4 SPCB Correlation Critical Power as Function of Pressure and Flow Rate G-7

Figure G-5 SPCB/GE14 Correlation With Alternative Treatment of Low Pressure Boundary G-8

Nomenclature

Acronym	Definition
BWR	Boiling Water Reactor
CHF	Critical Heat Flux
EPU	Extended Power Uprate
EPFOD	Extended Power/Flow Operating Domain
LHGR	Linear Heat Generation Rate
LOCA	Loss of Coolant Accident
LRNB	Load Reject with no Bypass
KATHY	**KA**rlstein **T**hermal **HY**draulic test facility
MAPLHGR	Maximum Average Planar Linear Heat Generation Rate
MCPR	Minimum Critical Power Ratio
NRC	Nuclear Regulatory Commission
OLMCPR	Operating Limit Minimum Critical Power Ratio
PHTF	Richland Portable Hydraulic Test Facility
RAI	Request for Additional Information
SER	Safety Evaluation Report
SLMCPR	Safety Limit Minimum Critical Power Ratio

1.0 Introduction

This document reviews the AREVA NP* licensing methodologies to demonstrate that they are applicable to operation of the Monticello Nuclear Power Generating Station including Extended Power Uprate (EPU) conditions. EPU conditions refer to power uprate to 120% of the originally licensed rated thermal power.

* AREVA NP Inc. is an AREVA company.

2.0 Overview

The first step in determining the applicability of current licensing methods to EPU conditions for Monticello was a review of current AREVA BWR topical reports to identify SER restrictions on the BWR methodology. This review identified that there are no SER restrictions on power level or flow for the AREVA topical reports. The review also indicated that there are no SER restrictions on the parameters most impacted by the increased power level: steam flow, feedwater flow, jet pump M-ratio, and core average void fraction.

The AREVA methodologies are characterized by technically rigorous treatment of phenomena and are very well benchmarked (>100 cycles of operation plus gamma scan data for ATRIUM™-10*). Recent operating experience is tabulated in Table 2-1. The table present the reactor operating conditions and in particular the average and hot assembly powers for both US and European applications. As can be seen from this information, the average and peak bundle powers in this experience base exceed that associated with the power uprate for Monticello.

The validity of AREVA methods to the Monticello core design are further illustrated by combining both test data and assembly conditions used in the qualification of MICROBURN-B2 (Topical Report 2-15) in Figure 2-1. The data is presented in terms of the key physical phenomena (e.g. fluid exit quality and assembly flow) as they relate closely to the exit void fractions.

The increased steam flow from power uprate comes from increased power in normally lower power assemblies in the core, operating at higher power levels. High powered assemblies in uprated cores will be subject to the same LHGR, MAPLHGR, MCPR, and cold shutdown margin limits and restrictions as high powered assemblies in non-uprated cores.

The similarity of operating conditions between current and uprate conditions assures that the methods used to compute reactivity and power distributions remain valid. Furthermore, the characteristics computed by the steady-state core simulator and used in safety analyses remain valid.

---

* ATRIUM is a trademark of AREVA NP.

Table 2-1 AREVA Operating/Licensing Experience

Reactor	Reactor Size, #FA	Power, MWt (% Uprated)*	Ave. Bundle Power, MWt/FA	Approximate Peak Bundle Power, MWt/FA	Fuel/Cycle Licensing†	Uprate Comments
A	592	2575 (0.0)	4.4	7.2	X	
B	592	2575 (0.0)	4.4	7.4	X	
C	532	2292 (0.0)	4.3	7.3	(X)	
D	840	3690 (0.0)	4.4	7.5	X	Licensing only through Cycle 20
E	500	2500 (15.7)	5.0	8.0	X	For 3 operating cycles.
F	444	1800 (5.9)	4.1	7.3	X	
G	676	2928 (8.0)	4.3	7.6	(X)	
H	700	3300 (9.3)	4.7	8.0	(X)	
I	784	3840 (0.0)	4.9	8.1	(X)	
J	624	3237 (11.9)	5.2	7.8	(X)	
K	648	3600 (14.7)	5.6	8.6	(X)	With ATRIUM 10XM
L	648	2500 (10.1)	3.9	6.9	(X)	
M	624	3091 (6.7)	5.0	7.7	X	
N	800	3898 (1.7)	4.9	7.7	X	
O	764	3489 (5.0)	4.6	7.2	X	
P	560	2923 (20.0)	5.2	8.0	X	
Q	764	3952 (20.0)	5.2	7.7	X	
Monticello‡	484	2004 (20.0)	4.1	7.3		

* Latest power uprates.

† (x)=currently fuel licensing only (Europe).

‡ Monticello added for comparison purposes only, i.e., not in the Operating Experience database.

Figure 2-1 Comparison of AREVA Benchmark Data and Typical Monticello Reactor Conditions

2.1 *SER Restriction by Topical Report*

The NRC has approved the following licensing topical reports that describe the methods and assumptions used by AREVA to demonstrate the adequacy of BWR fuel system design for Monticello. These reports address mechanical design criteria, required mechanical and thermal conditions, nuclear design criteria and required fuel and thermal conditions used in licensing analyses, thermal and hydraulic criteria and thermal conditions used in steady-state and transient licensing analyses, AOO and accident analyses. The purpose of each topical report and the restrictions that have been placed on the methods presented are described in the following pages.

2-1 XN-NF-79-56(P)(A) Revision 1 and Supplement 1, "Gadolinia Fuel Properties for LWR Fuel Safety Evaluation," Exxon Nuclear Company, November 1981.

- Purpose: Justify gadolinia fuel properties for up to 5 wt% gadolinia loading in uranium dioxide fuel.

- SER Restrictions:

  1. The concentration of gadolinia is limited to 5 wt%.

  2. The report is acceptable based on a commitment to acquire more data for gadolinia bearing rods.

- Implementation of SER Restrictions:

  1. This SER restriction is no longer applicable. The limit on gadolinia concentration was increased to 8 wt% in Topical Report 2-6 with the application of RODEX2 and RODEX2A.

  2. The additional data was gathered and was provided to the NRC in Reference 1.

- Observations:

  1. The limitation on the concentration of gadolinia was raised to 8 wt% by the Topical Report 2-6. Additional data was gathered on gadolinia from Prairie Island, Tihange, and other reactors.

  2. The topical report is no longer referenced in conjunction with the RODEX4 methodology. The gadolinia concentration limit increased to 10 wt% in Topical Report 2-11 and an updated thermal conductivity correlation is used.

2-2 XN-75-32(P)(A) Supplements 1 through 4, "Computational Procedure for Evaluating Fuel Rod Bowing," Exxon Nuclear Company, October 1983. (Base document not approved.)

- Purpose: Develop an empirical method for determining fuel rod bow.
- SER Restrictions: The technical evaluation of the methodology was limited to the fuel designs, exposures, and conditions stated in the topical report and, in part, on assumptions made in formulating the methodology. It was recommended that Exxon continue fuel surveillance to ensure confidence in the assumptions and bases.
- Implementation of SER Restrictions: The application of the rod bow model to higher burnup and other fuel designs was approved in Topical Report 2-9.
- Observations: AREVA has continued to gather data from fuel surveillance and CPR experiments.

  XN-NF-75-32(P)(A) continues to be applicable. Through approval of Topical Reports 2-1 and 2-9, XN-NF-75-32(P)(A) applies up to 54,000 MWd/MTU for ATRIUM-9 and ATRIUM-10 designs. The ATRIUM 10XM design that is being supplied to Monticello shares the same fuel rod support structure as the ATRIUM-9 and ATRIUM-10 and the rod diameter falls between the ATRIUM-9 and ATRIUM-10 designs. Therefore, the rod bow behavior is expected to be very similar to the two approved designs.

2-3 XN-NF-81-58(P)(A) Revision 2 and Supplements 1 and 2, "RODEX2 Fuel Rod Thermal-Mechanical Response Evaluation Model," Exxon Nuclear Company, March 1984.

- Purpose: Provide an analytical capability to predict BWR and PWR fuel thermal and mechanical conditions for normal core operation and to establish initial conditions for power ramping, non-LOCA and LOCA analyses.

- SER Restrictions:

  1. The NRC concluded that the RODEX2 fission gas release model was acceptable to burnups up to 60 MWd/KgU. This implies a burnup limit of 60 MWd/KgU (nodal basis).

  2. The creep correlation accepted by the NRC is the one with the designation MTYPE = 0.

- Implementation of SER Restrictions:

  1. This restriction no longer applies. The exposure limits for BWR fuel were increased to 54 MWd/kgU for an assembly and to 62 MWd/kgU for a rod in Topical Report 2-9. These exposure limits are reflected in engineering guidelines.

  2. This restriction is implemented in the engineering guidelines and through computer code controls (defaults, override warning messages).

- Observations: The computer code that is used to perform analyses is now called RODEX2-2A. The NRC approved models, RODEX2 or RODEX2A, are chosen by input. A single code is maintained in order to assure that the NRC approved models are implemented correctly. RODEX2 is the fuel performance code that provides input to BWR LOCA and transient thermal-hydraulic methodologies.

  RODEX2 and RODEX2A may be used to model fuel with up to 8% gadolinia loading (See Topical Report 2-6).

2-4 XN-NF-81-51(P)(A), "LOCA-Seismic Structural Response of an Exxon Nuclear Company BWR Jet Pump Fuel Assembly," Exxon Nuclear Company, May 1986.

- Purpose: Develop a methodology for performing LOCA-Seismic structural analyses of BWR jet pump fuel assemblies.

- SER Restrictions: The allowable stress values reported for BWR jet pump fuel channel and assembly components are acceptable and licensees referencing the topical report for other non-GE manufactured channels are required to show that the calculated allowable stresses for seismic and LOCA loading conditions are bounded by those in the topical report.

- Implementation of SER Restrictions: This restriction is no longer applicable. The requirements for fuel channels are now described in Topical Report 2-10.

- Observations: The analyses reported were for an 8x8 fuel assembly. The channeled fuel assembly seismic analysis was performed using the response spectrum method of dynamic analysis in the NASTRAN finite element program (Reference 2). Current analyses make use of the KWUSTOSS dynamic analysis code for fuel channels (with fuel assembly) as described in Topical Report 2-10. The LOCA seismic criteria are specified in Topical Report 2-7.

2-5 XN-NF-85-74(P)(A) Revision 0, "RODEX2A (BWR) Fuel Rod Thermal-Mechanical Evaluation Model" Exxon Nuclear Company, August 1986.

- Purpose: The purpose of this topical report was to obtain NRC approval of a modification of the RODEX2 (Topical Report 2-3) fission gas release model for application to BWRs. This code version was named RODEX2A.

- SER Conclusions / Restrictions:

  1. The code RODEX2A is acceptable for mechanical analyses but RODEX2 must continue to be used for LOCA and transient analysis input generation.

  2. The RODEX2A calculation of fuel rod pressure must be performed to a minimum burnup of 50 MWd/kgU using the approved power history.

- Implementation of SER Restrictions:

  1. This SER restriction is implemented in engineering guidelines.

  2. The code RODEX2A was approved to a rod average burnup of 62 MWd/kgU in Topical Report 2-9. The analyzed burnup for all current designs is greater than 58 MWd/kgU.

- Observations: The RODEX2A code was approved to a maximum rod average burnup of 62 MWd/kgU in Topical Report 2-9.

2-6 XN-NF-85-92(P)(A), "Exxon Nuclear Uranium Dioxide/Gadolinia Irradiation Examination and Thermal Conductivity Results," Exxon Nuclear Company, November 1986.

- Purpose: Justify gadolinia fuel properties for up to 8 wt % gadolinia loading in uranium dioxide fuel to be used in BWR fuel designs. The topical report applies with the application of the RODEX2 and RODEX2A methodology.

- SER Restrictions: Based on a commitment to confirm the fission gas release model with in-reactor data, the gadolinia fuel properties are acceptable for licensing applications up to 8 wt% gadolinia concentration.

- Implementation of SER Restrictions: The SER restriction on 8 wt% gadolinia is implemented in engineering guidelines.

- Observations:

  1. In-reactor fission gas release test results (Reference 1) were provided to the NRC. The thermal conductivity model supersedes the previously approved model (Topical Report 2-1).

  2. With the use of RODEX4, the gadolinia concentration limit is increased to 10 wt%. In addition, an updated thermal conductivity model is provided. This topical report does not need to be referenced with the application of RODEX4.

- Clarifications: NRC concurrence with a clarification related to the topical report was requested in Reference 3. The NRC concurrence with the clarification was provided in Reference 4. The clarification was with respect to the use of one conductivity equation for UO_2-only fuel and a separate gadolinia-bearing fuel conductivity equation for all gadolinia concentrations greater than zero wt%.

2-7 ANF-89-98(P)(A) Revision 1 and Supplement 1, "Generic Mechanical Design Criteria for BWR Fuel Designs," Advanced Nuclear Fuels Corporation, May 1995.

- Purpose: Establish a set of design criteria which assures that BWR fuel will perform satisfactorily throughout its lifetime.

- SER Restrictions:

  1. Peak pellet burnup shall not be increased beyond 60,000 MWd/MTU unless axial growth and fretting wear data have been collected from lead test assemblies of the modified design.

  2. Exposure beyond 60,000 MWd/MTU peak pellet must be approved by the NRC.

  3. Approval does not extend to the development of additive constants for ANFB to co-resident fuel.

  4. For each application of the mechanical design criteria, AREVA must document the design evaluation and provide a summary of the evaluation for the NRC.

- Implementation of SER Restrictions:

  The revised SER restrictions on burnup are implemented in engineering guidelines.

  1. The NRC approved higher burnup values as presented in Topical Report 2-9.

  2. The exposure limit was extended to a rod-average burnup of 62 GWd/MTU by the approval of Topical Report 2-9.

  3. The ANFB correlation is no longer used.

  4. It was clarified in References 5 and 6 that this requirement applies to generic evaluations that are independent of plant specific evaluations. The NRC concurred with this in Reference 7.

- Observations:

1. The application of the processes and criteria described in this topical report do not require prior NRC approval.

2. With the use of RODEX4, some fuel rod design criteria are updated. The RODEX4 LTR (Topical Report 2-11) references this topical report for the remaining fuel rod criteria.

3. The mechanical design of the fuel channel is performed using the criteria and methods described and approved in Topical Report 2-10.

4. The design methodology for the reconstitution of a BWR fuel assembly complies with Topical Report 2-8.

2-8 ANF-90-82(P)(A) Revision 1, "Application of ANF Design Methodology for Fuel Assembly Reconstitution," Advanced Nuclear Fuels Corporation, May 1995.

- Purpose: Develop a methodology to justify reinsertion of irradiated fuel assemblies, which have been reconstituted with replacement rods, into a reactor core. Replacement rods can be fuel rods containing natural uranium pellets, water rods, and inert rods containing Zircaloy or stainless steel inserts.

- SER Restrictions: The reconstitution methodology is acceptable for reload licensing applications with the following conditions:

  1. BWR reconstituted assemblies are limited to 9 rods per assembly.

  2. The seismic LOCA analysis will be reassessed if the reconstructed weight drops below a proprietary value.

- Implementation of SER Restrictions: The SER restrictions are implemented in engineering guidelines.

- Observations: The reconstitution methodology is applicable to all fuel designs.

  The SER restrictions on the number of replacement rods apply only to inert rods containing Zircaloy or stainless steel inserts.

  NOTE: Extension of this Methodology for use with the SPCB or ACE CPR correlations would require Licensees to perform a 10 CFR 50.59 evaluation/justification or a plant specific methodology approval within a License Amendment Request.

2-9 EMF-85-74(P) Revision 0 Supplement 1(P)(A) and Supplement 2(P)(A), "RODEX2A (BWR) Fuel Rod Thermal-Mechanical Evaluation Model," Siemens Power Corporation, February 1998.

- Purpose: Extend the exposure limits of the RODEX2A (Topical Report 2-5) code, which is a version of RODEX2 that includes a fission gas release model specific to BWR fuel designs.

- SER Restrictions: RODEX2A is acceptable for steady state licensing applications to 62,000 MWd/MTU rod-average burnup and the fuel rod growth, fuel assembly growth, and fuel channel growth models and analytical methods are acceptable for ATRIUM-9 and -10 fuel designs up to 54,000 MWd/MTU assembly-average burnup.

- Implementation of SER Restrictions: The SER restrictions on burnup are implemented in engineering guidelines.

- Observations: The RODEX2A code, which is used for BWR fuel design applications, is a derivative of AREVA's base fuel performance code RODEX2.

  In the approved topical report, the NRC acknowledges the following observations as correct:

  1. Steady state analyses of maximum wall thinning from oxidation for end of life conditions will be performed.
  2. The growth correlations reviewed are applicable to all AREVA 9x9 fuel designs.
  3. Transient strain is to be calculated with the version of RODEX referenced in XN-NF-81-58(P)(A) Revision 2 Supplement 1 (Topical Report 2-3). Strain is limited to 1.0% and the limit is reduced at high exposures.
  4. Steady state strain is to be calculated with RODEX2A and is limited to 1%.
  5. RODEX2A is to be used to calculate fuel temperatures for fuel melt analyses.
  6. RODEX2 shall be used as the base fuel performance code to interface with the AREVA LOCA and transient thermal-hydraulic methodologies. The RODEX2 code was also approved for BWR analyses to 62 GWd/MTU rod average burnup.

  The topical report provides a review of the fuel assembly mechanical methodology (e.g., component stress, fuel liftoff) and justifies an increased assembly exposure limit of 54

MWd/kgU. This also includes an extension of the rod bow methodology (Topical Report 2-2) to the 54 MWd/kgU burnup level for ATRIUM-9 and ATRIUM-10 fuel.

With the use of RODEX4, some of the fuel rod criteria present in this topical report were updated. For example, the transient strain limit and the corrosion limit were changed. However, the RODEX4 topical report references this topical report for other fuel rod-related design criteria such as those for cladding steady-state stresses.

- Clarifications: NRC concurrence with clarifications related to this topical report was requested in References 8 and 9. The NRC concurrence with these clarifications was provided in Reference 10. The clarification was associated with applying the exposure limits to only the full length fuel rods and not the part length fuel rods.

2-10 EMF-93-177(P)(A) Revision 1, "Mechanical Design for BWR Fuel Channels," Framatome ANP, August 2005.

- Purpose: Demonstrate that analytical methods are adequate to perform evaluations which ensure that fuel channels perform as designed for normal operations and during anticipated operational occurrences and that for postulated accident loadings channel damage does not prevent control blade insertion and assembly coolability is maintained.

- SER Restrictions: Subject to certain conditions, the analyses conducted by AREVA are acceptable for licensing applications.

  1. The fuel channel Topical Report (TR) methods and criteria may be applied to fuel channel designs similar to the configuration of a square box with radiused corners open at the top and bottom ends. The wall thickness shall fall within the range of current designs. The channels shall be fabricated from either Zircaloy-2 or Zircaloy-4. AREVA will not use Zircaloy material for channels which has less strength than specified in the TR, and if the strength of material is greater than that in the TR, AREVA will not take credit for the additional strength without staff review.

  2. Updates to channel bulge and bow data are permitted without review by the NRC staff; however, AREVA shall resubmit the channel bulge and bow data statistics if the two-sigma upper and lower bounds change by more than one standard deviation.

  3. This TR is approved using the ABAQUS or ANSYS codes in the deformation analysis. The use of other codes in the deformation analysis, i.e., NASTRAN, is beyond the current approval.

  The following restrictions are carried over from EMF-93-177(P)(A) Revision 0; for specific plant applications the following conditions are to be met:

  4. The allowable differential pressure loads and accident loads should bound those of the specific plant.

  5. Lattice dimensions should be compatible to those used in the analyses reported such that the minimum clearances with control blades continue to be acceptable.

6. Maximum equivalent exposure and residence time should not exceed the values used in the analyses.

- Implementation of SER Restrictions: The SER restrictions are implemented in engineering guidelines.

- Observations: The methodology approved is appropriate for exposures and minor dimensional changes beyond those evaluated and reported in the topical. Use of the methodology to extended exposure must be validated against the original design criteria.

  The Reference 11 letter was provided to the NRC to inform them that Revision 0 of the topical report had been used to confirm the fuel channel design met the design criteria at an approved assembly exposure for which results had not been previously provided. No NRC response was requested.

2-11 BAW-10247PA Revision 0, "Realistic Thermal-Mechanical Fuel Rod Methodology for Boiling Water Reactors," AREVA NP, February 2008.

- Purpose: Provide an analytical capability to predict BWR fuel thermal and mechanical conditions for normal core operation and to establish initial conditions for power ramping, and non-LOCA. At this time RODEX4 is not approved for use with LOCA analyses.

- SER Restrictions:

  1. Due to limitations within the FGR model, the analytical fuel pellet grain size shall not exceed 20 microns 3-D when the as-manufactured fuel pellet grain size could exceed 20 microns 3-D.

  2. RODEX4 shall not be used to model fuel above incipient fuel melting temperatures.

  3. The hydrogen pickup model within RODEX4 is not approved for use.

  4. Due to the empirical nature of the RODEX4 calibration and validation process, the specific values of the equation constants and tuning parameters derived in TR BAW-10247(P), Revision 0 (as updated by RAI responses) become inherently part of the approved models. Thus, these values may not be updated without necessitating further NRC review.

  5. RODEX4 has no crud deposition model. Due to the potential impact of crud formation on heat transfer, fuel temperature, and related calculations, RODEX4 calculations must account for a design basis crud thickness. The level of deposited crud on the fuel rod surface should be based upon an upper bound of expected crud and may be based on plant-specific history. Specific analyses would be required if an abnormal crud or corrosion layer (beyond the design basis) is observed at any given plant. For the purpose of this evaluation, an abnormal crud/corrosion layer is defined by a formation that increases the calculated fuel average temperature by more than 25°C beyond the design basis calculation.

- Implementation of SER Restrictions:

  1. The RODEX4 methodology is automated using the AUTOFROST and AUTOPOSTFROST codes. In RODEX4 fuel rod thermal-mechanical analyses, AUTOFROST is used to prepare RODEX4 inputs and set up the RODEX4 runs. AUTOFROST has internal automatic checks to ensure the proper grain size is input that meets SER requirements. (Note: Both RODEX4 and the manufacturing specifications define the grain size using the MLS (mean line intercept) method instead of a 3-D measurement. The equivalent MLS grain size is on the order of 12.8 μm.)

  2. Fuel melting is a fuel rod thermal-mechanical design criterion. No fuel design is allowed that would exceed fuel melting temperature. Thus RODEX4 will not be applied above fuel melting.

  3. AUTOPOSTFROST, the post-processor of AUTOFROST/RODEX4 runs, writes hydrogen pickup calculation results to output with the qualifier "for information only".

  4. The model parameters documented in BAW-10247PA have been programmed into AUTOFROST as default values. By default, the automation will override user inputs of model parameters with the approved values.

  5. Because the crud deposition is plant specific and operation dependent, and thus so are the RODEX4 calculations/applications. This requirement was implemented in a guideline by requiring that liftoff measurement data and/or visual examinations be examined to characterize plant crud conditions. If crud conditions (total liftoff) indicate higher than normal crud levels, then a heat transfer coefficient must be estimated and input to account for the added thermal resistance as required by the SER. Available data for the Monticello plant indicate that crud levels are normal and no added crud input is necessary.

- Observations: RODEX4 is approved for modeling BWR fuel rods with the following conditions:

  a. Peak rod average burnup limit of 62 GWd/MTU (full length rod).

  b. Solid UO_2 fuel pellet with a maximum gadolinia content of 10.0 weight percent.

c. CWSR Zr-2 fuel clad material.

A regulatory commitment was made to the NRC during the first application of RODEX4 that restricts the maximum external oxidation to a proprietary limit. Until further data are available, it is expected that applications of RODEX4 for other plants will require the same limitation until data to support a higher limit is obtained. The limit is included in the fuel rod analysis engineering guideline. Monticello equilibrium and Cycle 28 RODEX4 calculations were performed that include calculations of the maximum cladding oxidation. The oxidation predictions for Cycle 28 were shown to satisfy the more restrictive oxidation limit.

RODEX4 is not yet approved for use with LOCA analyses.

2-12 XN-NF-80-19(P)(A) Volume 1 and Supplements 1 and 2, "Exxon Nuclear Methodology for Boiling Water Reactors - Neutronic Methods for Design and Analysis," Exxon Nuclear Company, March 1983.

- Purpose: Development of BWR core analysis methodology which comprises codes for fuel neutronic parameters and assembly burnup calculations, reactor core simulation, diffusion theory calculations, core and channel hydrodynamic stability predictions, and producing input for nuclear plant transient analysis. Procedures for applying the codes for control rod drop, control rod withdrawal and fuel misloading events (mis-location and mis-rotation) have been established.

- SER Restrictions: No restrictions

- Implementation of SER Restrictions: None

- Observations: Portions of this topical report have been superseded by subsequently approved codes or methodologies. Superseded and currently applicable portions are identified below:

Superseded Portions:

Fuel Assembly Depletion Model - XFYRE replaced with CASMO-4 (see Topical Report 2-15).

Core Simulator – XTGBWR replaced with MICROBURN-B2 (see Topical Report 2-15).

Diffusion Theory Model - XDT replaced with CASMO-4 (see Topical Report 2-15).

Stability Analysis - COTRAN replaced with STAIF (see Topical Report 2-16).

Control Rod Withdrawal - XTGBWR replaced with MICROBURN-B2 (see Topical Report 2-15).

Fuel Misloading Analysis – XFYRE replaced with CASMO-4 and XTGBWR replaced with MICROBURN-B2. These analyses are performed to verify that the offsite dose due to such events does not exceed a small fraction of 10 CFR 100 guidelines as described and

approved in Topical Report 2-13. For plants that have implemented Alternate Source Term (AST), 10 CFR 100 is superseded by 10 CFR 50.67.

Applicable Portions:

Control Rod Drop Accident – This analysis is performed using COTRAN.

Control Rod Withdrawal – This analysis determines the change in CPR (ΔCPR) for error rod patterns. In addition a check is made that the LHGR does not exceed the transient (PAPT) LHGR limit.

Neutronic Reactivity Parameters – These parameters are determined as described in the topical report but using the most recently approved codes.

Void Reactivity Coefficient – Method used to calculate core void reactivity coefficient is the same but MICROBURN-B2 is used instead of XTGBWR.

Doppler Reactivity Coefficient – Method used to calculate the core average Doppler coefficient is the same but CASMO-4 is used instead of XFYRE.

Scram Reactivity – Method used is the same except MICROBURN-B2 is used instead of XTGBWR.

Delayed Neutron Fraction – Calculated using CASMO-4 instead of XFYRE.

Prompt Neutron Lifetime – Calculated using CASMO-4 instead of XFYRE.

Recent interaction with the NRC has requested a more in-depth description of the cross section methodology and the applicability of the uncertainties presented in this topical report to modern fuel designs. This is discussed in detail in Appendix A.

2-13 XN-NF-80-19(P)(A) Volume 4 Revision 1, "Exxon Nuclear Methodology for Boiling Water Reactors: Application of the ENC Methodology to BWR Reloads," Exxon Nuclear Company, June 1986.

- Purpose: Summarize the types of BWR licensing analyses performed, identify each with approved computer codes and methodologies, and develop a reload reporting format.
- SER Restrictions: Conditions imposed were based on pending approvals of outstanding topical reports which have been subsequently approved.
- Implementation of SER Restrictions: This restriction is no longer applicable (because of subsequent approvals).
- Observations: Many of the codes and methodologies referenced have changed or have been replaced since the report was approved.
- Clarifications: AREVA provided a clarification related to the topical report in References 5 and 6. The clarification was associated with the use of power and flow dependent LHGR multipliers to establish LHGR limits that provide adequate margin during events initiated from off-rated conditions.

2-14 EMF-CC-074(P)(A) Volume 1, "STAIF - A Computer Program for BWR Stability Analysis in the Frequency Domain," and Volume 2 "STAIF - A Computer Program for BWR Stability Analysis in the Frequency Domain - Code Qualification Report," Siemens Power Corporation, July 1994.

- Purpose: Provide a methodology for the determination of the thermal-hydraulic stability of BWRs, including reactivity feedback effects.

- SER Restrictions:

  1. The core model must be divided into a minimum of 24 axial nodes.

  2. The core model must be divided into a series of radial nodes (i.e., thermal-hydraulic regions or channels) in such a manner that:

     a) No single region can be associated with more than 20 percent of the total core power generation. This requirement guarantees a good description of the radial power shape, especially for the high power channels.
     b) The core model must include a minimum of three regions for every bundle type that accounts for significant power generation.
     c) The model must include a hot channel for each significant bundle type with the actual conditions of the hot channel.

  3. Each of the thermal-hydraulic regions must have its own axial power shape to account for 3-D power distributions. For example, high power channels are likely to have more bottom peaked shapes.

  4. The collapsed 1-D cross sections must represent the actual conditions being analyzed as closely as possible, including control rod positions.

  5. The STAIF calculation must use the "shifted Nyquist" or complex pole search feature to minimize the error at low decay ratio conditions.

- Implementation of SER Restrictions: The SER restrictions are implemented in the code and the user's manual for STAIF. The requirements will automatically be satisfied if the code defaults are used and the MICROBURN-B2 STAIF guideline is followed.

- Observations: Stability analysis procedures described in Topical Report 2-12 were superseded by the approval of the STAIF code (Topical Reports 2-14 and 2-16).

Volume 1 of EMF-CC-074 presents the STAIF code theory, which for the most part remains applicable for the STAIF version applied to Monticello. A description of the changes and expanded qualification against separate effect test and reactor data are presented in Topical Report 2-16.

2-15 EMF-2158(P)(A) Revision 0, "Siemens Power Corporation Methodology for Boiling Water Reactors: Evaluation and Validation of CASMO-4/MICROBURN-B2," Siemens Power Corporation, October 1999.

- Purpose: Replace the MICBURN-3/CASMO-3G bundle depletion codes and the MICROBURN-B simulator code with the codes CASMO-4 and MICROBURN-B2, respectively.

- SER Restrictions:

  1. The CASMO-4/MICROBURN-B2 code systems shall be applied in a manner that predicted results are within the range of the validation criteria (Tables 2.1 and 2.2) and measurement uncertainties (Table 2.3) presented in EMF-2158(P).

  2. The CASMO-4/MICROBURN-B2 code system shall be validated for analyses of any new fuel design which departs from current orthogonal lattice designs and/or exceed gadolinia and U-235 enrichment limits.

  3. The CASMO-4/MICROBURN-B2 code system shall only be used for BWR licensing analyses and BWR core monitoring applications.

  4. The review of the CASMO-4/MICROBURN-B2 code system should not be construed as a generic review of the CASMO-4 or MICROBURN-B2 computer codes.

  5. The CASMO-4/MICROBURN-B2 code system is approved as a replacement for the CASMO-3G/MICROBURN-B code system used in NRC-approved AREVA BWR licensing methodology and in AREVA BWR core monitoring applications. Such replacements shall be evaluated to ensure that each affected methodology continues to comply with its SER restrictions and/or conditions.

  6. AREVA shall notify any customer who proposes to use the CASMO-4/MICROBURN-B2 code system independent of any AREVA fuel contract that conditions 1 through 4 above must be met. AREVA's notification shall provide positive evidence to the NRC that each customer has been informed by AREVA of the applicable conditions for using the code system.

- Implementation of SER Restrictions: The SER restrictions relevant to methodology used by AREVA are implemented in engineering guidelines.

  1. Application of the CASMO-4/MICROBURN-B2 code system for the Monticello units involves the following models:

     - Control blade B-10 depletion
     - Explicit neutronic treatment of the spacer grids
     - Explicit water rod hydraulics
     - Explicit neutronic treatment of the plenum above the PLFR's

     Application of these models has been evaluated for the Monticello benchmark and AREVA cycles relative to the LTR statistics. The results of the statistical analysis demonstrated that these models meet the approved methodology validation criteria and measurement uncertainties presented in EMF-2158(P)(A).

  2. The ATRIUM 10XM fuel has an orthogonal lattice design and the nuclear design does not exceed the Gadolinia concentration or U-235 enrichment limits.

  3. Monticello is a General Electric BWR-4; therefore, the analyses in the calculation package meet this SER restriction.

  4. CASMO-4 and MICROBURN-B2 are being used in a manner consistent with the original approval.

  5. CASMO-4/MICROBURN-B2 does not violate the SER restrictions of separate methodologies used in the licensing analyses.

  6. This licensing analysis is being performed by AREVA through a fuel contract between AREVA and Xcel Energy. Xcel Energy has been provided a copy of the topical report which includes the SER and all clarifications. Training sessions have been conducted with Xcel Energy personnel to assure that they are familiar with the application of the methodology.

- Observations: None.

2-16 EMF-CC-074(P)(A) Volume 4, Revision 0, "BWR Stability Analysis - Assessment of STAIF with Input from MICROBURN-B2," Siemens Power Corporation, August 2000.

- Purpose: Document and justify enhancements to the STAIF code including the capability to accept input from the code MICROBURN-B2. Justify a modification to the approved stability criteria for STAIF in conjunction with input from both MICROBURN-B and MICROBURN-B2. The STAIF code is used to perform stability analysis for BWRs.

- SER Restrictions:

  The SER concludes that the STAIF code is acceptable for best-estimate decay ratio calculations. This conclusion applies to the three types of instabilities relevant to BWR operation, which are quantified by the hot-channel, core-wide, and out-of-phase decay ratios. The staff estimates that STAIF decay ratio calculations for the decay ratio range of 0.0 to 1.1 are accurate within:

  +/- .2 for the hot-channel decay ratio
  +/- .15 for the core-wide decay ratio
  +/- .2 for the out-of-phase decay ratio

  The staff concludes that the proposed modification of the E1A acceptance criteria for region-validation calculations is acceptable because it provides the intended protection against instabilities outside the E1A regions. The following E1A region-validation criteria are acceptable for the STAIF code:

  The calculated hot-channel decay ratio must be lower than .8.
  The calculated core-wide decay ratio must be lower than .85.
  The calculated out-of-phase decay ratio must be less than .8.

- Implementation of SER Restrictions: The SER restrictions are implemented in engineering guidelines.

- Observations: The NRC stated in Reference 12, that the revised stability criteria is applicable to calculations with the STAIF code with input from either MICROBURN-B or MICROBURN-B2.

EMF-CC-074(P)(A), Volume 4, approves the use of the STAIF frequency domain code with the use of the MICROBURN-B2 core simulator used for Monticello licensing analyses.

2-17 BAW-10255PA Revision 2, "Cycle-Specific DIVOM Methodology Using the RAMONA5-FA Code," AREVA NP, May 2008.

- Purpose: Document and justify the use of the RAMONA5-FA code for performing cycle-specific DIVOM calculations.

- SER Restrictions:

  1. If a reduced scope of parameter variations is used to define the cycle-specific DIVOM slope as described in Section 7 of the TR, the scope must be justified and documented for NRC staff review.

  2. The NRC staff imposes a condition to perform a full code review of RAMONA5-FA, including constitutive relations, numerics, neutronic methods, and benchmarks before RAMONA5-FA can be used to calculate DIVOM curves in EFW operating domains without the 10 percent penalty on DIVOM slopes, as noted in Limitation and Condition No.3 below.

  3. The NRC staff imposes an interim 10 percent penalty on DIVOM slopes calculated using the RAMONA5-FA methodology under EFW conditions. This is an interim restriction that will be revised when the full RAMONA5-FA Code review is completed.

- Implementation of SER Restrictions: The SER restrictions are implemented in engineering guidelines.

- Observations: None.

  SER restrictions 2 and 3 state that all DIVOM analyses performed in the EFW (MELLLA+) domain need to impose an interim 10% penalty on DIVOM slopes. This penalty was to remain until the NRC staff had the opportunity to perform a full code review of RAMONA5-FA. The NRC has since performed a full code review of RAMONA5-FA and has issued a new SE removing the 10% penalty on MELLLA+ DIVOM calculations. The new SE documenting the removal of this penalty is given in Reference 52. Appendix B presents additional information on non-linear stability performance and application to Monticello.

2-18 XN-NF-79-59(P)(A), "Methodology for Calculation of Pressure Drop in BWR Fuel Assemblies," Exxon Nuclear Company, November 1983.

- Purpose: Develop a methodology for determining the BWR assembly pressure drop which determines the assembly coolant flow and which varies with total recirculating flow and reactor power.

- SER Restrictions: No restrictions.

- Implementation of SER Restrictions: None.

- Observations: This methodology continues to be used and incorporates experimental pressure drop data for new fuel and spacer designs.

  The continued applicability of XN-NF-79-59 for Monticello has been established through the qualification of the methodology against ATRIUM 10XM single and two phase pressure drop measurements. The PHTF measurements of the ATRIUM 10XM fuel in combination with the geometric data for the design are used to determine the component loss coefficients. Pressure drop measurements during the KATHY CHF measurements provide the two-phase data to demonstrate continued applicability of the closure relations for two-phase flow. The determination of loss coefficients for both the ATRIUM 10XM and GE14 assemblies are utilized to predict the flow distribution and impact on critical power performance in a mixed core as described in Appendix C.

  AREVA has also expanded the qualification of the void correlations used in the design codes. The void correlations are discussed in Appendix D.

2-19 XN-NF-80-19(P)(A) Volume 3 Revision 2, "Exxon Nuclear Methodology for Boiling Water Reactors, THERMEX: Thermal Limits Methodology Summary Description," Exxon Nuclear Company, January 1987.

- Purpose: Provide an overall methodology for determining a MCPR operating limit. The methodology comprises CHF correlations, fuel hydraulic characteristics, safety limit analyses, AOO analyses, and statistical combination of uncertainties.

- SER Restriction: Monitoring systems other than POWERPLEX®*CMSS may be used provided that the associated power distribution uncertainties are identified and appropriate operating parameters compatible with ENC transient safety analyses are monitored. Whatever monitoring system is used should be specifically identified in plant submittals.

- Implementation of SER Restriction: The SER restriction is implemented in engineering guidelines.

- Observations: Although Topical Report 2-19 only discusses applications to ENC 8x8 and 9x9 fuel types, the overall methodology is applicable to other AREVA fuel designs when appropriate CHF correlations are implemented. Subsequent to the approval of this topical report, AREVA developed and the NRC approved the use of generic design criteria for new fuel designs (Topical Report 2-7). In the SER/TER for Topical Report 2-7, the NRC concurred with the continued applicability of the methodology in Topical Report 2-19 (with the exception of the CHF correlation) for demonstrating compliance with thermal hydraulic design criteria.

- Some of the computer codes referenced in the topical report have been superseded by other NRC-approved codes (e.g., COTRANSA with COTRANSA2, XTGBWR with MICROBURN-B2) and the XN-3 CHF correlation has been supplemented with the NRC-approved SPCB CHF correlation (see Topical Report 2-22) and ACE critical power correlations (see Topical Report 2-23 and Topical Report 2-24).

---

* POWERPLEX is a trademark registered in the U.S. and various other countries.

The SER states "Based on the similarity of the computational models of the two codes (XCOBRA and XCOBRA-T) and the NRC approval of the XCOBRA-T code (Topical Report 2-29), we find the use of the steady-state code [ ] acceptable in this context." XCOBRA continues to be applied for steady-state analyses.

2-20 ANF-524(P)(A) Revision 2 and Supplements 1 and 2, "ANF Critical Power Methodology for Boiling Water Reactors," Advanced Nuclear Fuels Corporation, November 1990.

- Purpose: Provide a methodology for the determination of the SLMCPR.

- SER Restrictions:

  1. The NRC approved MICROBURN-B power distribution uncertainties should be used in the SLMCPR determination.

  2. Since the ANFB correlation uncertainties depend on fuel design, in plant-specific applications the uncertainty value used for the ANFB additive constants should be verified. [

     ]

  3. The CPR channel bowing penalty for non-ANF fuel should be made using conservative estimates of the sensitivity of local power peaking to channel bow.

  4. The methodology for evaluating the effect of fuel channel bowing is not applicable to reused second-lifetime fuel channels.

- Implementation of SER Restrictions: SER restrictions 1 and 2 are implemented in engineering guidelines and automation tools. Restrictions 3 and 4 are implemented in engineering guidelines.

- Observations: The critical power methodology is a general methodology which may be used with all AREVA developed CHF correlations that include additive constants and additive constant uncertainties.

  Power distribution uncertainties for MICROBURN-B2 and other AREVA core simulator codes approved by the NRC will be used in the CPR methodology.

  As additive constants and additive constant uncertainties are fuel type specific, they do not change for each plant specific application, as noted in SER restriction 2.

ANF-524 presents a general methodology that is applicable to Monticello. The specific methodology applied for Monticello is approved in Topical Report 2-25.

2-21 EMF-2245(P)(A) Revision 0, "Application of Siemens Power Corporation's Critical Power Correlations to Co-Resident Fuel," Siemens Power Corporation, August 2000.

- Purpose: Present and justify the use of AREVA critical power correlations to co-resident fuel (non-AREVA manufactured).

- SER Restrictions: Technology transfer to licensees who may be responsible for using these processes will be accomplished through AREVA and licensee procedures consistent with the requirements of GL 83-11, Supplement 1. This process includes the performance of an independent benchmarking calculation by AREVA for comparison to licensee-generated results to verify that the application of AREVA CHF correlations is properly applied for the first application by a licensee.

- Implementation of SER Restrictions: The SER restriction is implemented in engineering work practices.

- Observations:

  An integral component of AREVA licensing of mixed cores, as described in Appendix C, is the development of the critical power correlation for the co-resident fuel design. For Monticello, the SPCB correlation (Topical Report 2-22) was used to characterize the GE14 critical power performance based on calculated CPR data provided by Xcel Energy and the alternate (indirect) approach described in this LTR. Conservative application of the SPCB correlation for co-resident fuel to low pressures is discussed in Appendix G.

2-22 EMF-2209(P)(A) Revision 3, "SPCB Critical Power Correlation," AREVA NP, September 2009.

- Purpose: Present and justify a critical power correlation applicable for the ATRIUM-9B and ATRIUM-10 fuel design.

- SER Restrictions:

  1. The SPCB correlation is applicable to Framatome ANP, Inc. ATRIUM-9B and ATRIUM-10 fuel design with a design local peaking factor no greater than 1.5.

  2. If in the process of calculating the MCPR safety limit, the local peaking factor exceeds 1.5, an additional uncertainty of 0.026 for ATRIUM-9B and 0.021 for ATRIUM-10 will be imposed on a rod by rod basis.

  3. The SPCB correlation range of applicability is 571.4 to 1432.2 psia for pressure, 0.087 to 1.5 Mlb/hr-ft^2 for inlet mass velocity and 5.55 to 148.67 Btu/lbm for inlet subcooling.

  4. Technology transfer will be accomplished only through the process described in Reference 13, which includes the performance of an independent bench-marking calculation by FANP for comparison to the licensee-generated results to verify that the new CHF correlation (SPCB) is properly applied for the first application by the licensee.

  5. Application of this correlation and the proposed revisions to fuel designs other than the ATRIUM-9B and ATRIUM-10 designs require prior staff approval.

  Note: restrictions 1 – 4 are from Revision 1.

- Implementation of SER Restrictions: SER restrictions 1 and 5 are implemented in engineering guidelines. Restriction 2 is implemented in engineering guidelines and automation tools. Restriction 3 is directly implemented in engineering computer codes. Restriction 4 is implemented in engineering work practices.

- Observations: The purpose of Revision 2 was to modify the SPCB critical power correlation in the region of the uranium blanket at the top of the fuel. The purpose of Revision 3 was to make corrections to the correlation additive constants to account for an error in the KATHY loop operation.

- Clarifications: NRC concurrence with a clarification related to this topical report (Revision 1) was requested in References 14 and 15. The NRC concurrence with the clarification was provided in Reference 16. The clarification discusses the actions taken when the calculation values fall outside the correlation bounds.

  For Monticello, the SPCB correlation is applied to the co-resident GE14 fuel design based on the alternate (indirect) approach defined in Topical Report 2-21. The correlation bounds are monitored by AREVA methods and when appropriate NRC approved actions are taken by the code when the operating conditions fall outside the correlation bounds.

2-23 ANP-10249PA Revision 1, "ACE/ATRIUM-10 Critical Power Correlation," AREVA NP, September 2009.

- Purpose: Present and justify a new critical power correlation applicable for the ATRIUM-10 fuel design.

- SER Restrictions:

  1. The ACE/ATRIUM-10 methodology may only be used to perform evaluations for AREVA ATRIUM-10 fuel. The ACE/ATRIUM-10 correlation may also be used to evaluate the performance of co-resident fuel in mixed cores as described in Section 3 of the safety evaluation report.

  2. ACE/ATRIUM-10 shall not be used outside its range of applicability defined by the range of the test data from which it was developed and the additional justifications provided by AREVA. This range is listed in Table 2.1.

  Note: restrictions 1 and 2 are from Revision 0.

- Implementation of SER Restrictions:

  SER restriction 1 is implemented in engineering guidelines. Restriction 2 is directly implemented in the engineering software implementing the ACE correlation, ACELIB, for mass flow, pressure, and inlet subcooling. For maximum local peaking, the restriction is implemented via neutronics bundle design guidelines.

- Observations: The purpose of Revision 1 was to make corrections to the correlation additive constants to account for an error in the KATHY loop operation. A revision to the ACE correlation that removes potentially non-physical behavior is under review by the U.S. NRC.

  ANP-10249(P)(A) presents the theory behind the ACE correlation. For Monticello, the correlation was revised based on the ATRIUM 10XM test data per Topical Report 2-24.

2-24 ANP-10298PA Revision 0, "ACE/ATRIUM 10XM Critical Power Correlation," AREVA NP, March 2010.

- Purpose: Present and justify a new critical power correlation applicable for the ATRIUM 10XM fuel design.

- SER Restrictions:

  1. Since ACE/ATRIUM 10XM was developed from test assemblies designed to simulate ACE/ATRIUM 10XM fuel, the methodology may only be used to perform evaluations for fuel of that type without further justification.

  2. ACE/ATRIUM 10XM shall not be used outside its range of applicability defined by the range of the test data from which it was developed and the additional justifications provided by AREVA in this submittal. This range is listed in Table 2.1.

- Implementation of SER Restrictions:

  SER restriction 1 is implemented in engineering guidelines. Restriction 2 is directly implemented in the engineering software implementing the ACE correlation, ACELIB, for mass flow, pressure, and inlet subcooling. For maximum local peaking, the restriction is implemented via neutronics bundle design guidelines.

- Observations: A revision to the ACE correlation that removes potentially non-physical behavior is under review by the U.S. NRC.

  ANP-10298(P)(A) presents the qualification of the ACE correlation form to the ATRIUM 10XM fuel design that will be loaded in the Monticello reactor. Subsequent to approval of the LTR, a weakness was identified in the use of assembly average K-factor values to account for rod local peaking, rod location and bundle geometry effects. The K-factor methodology was modified in Reference 36 in response to deficiencies found in the axial averaging process and the additive constants were revised as a result of the change to the K-factor model.

  The K-factor parameter is described in detail in Section 3.1 of Reference 36.

At the time of the creation of this document, Reference 36 had not yet been generically approved. Reference 23 presents the ACE/ATRIUM 10XM critical power correlation that will be used in licensing analyses for Monticello in the interim. The correlation presented in Reference 23 is exactly the same as that presented in Reference 36.

The correlation bounds are monitored by AREVA methods and when appropriate NRC approved actions are taken by the code when the operating conditions fall outside the correlation bounds.

2-25 ANP-10307PA Revision 0, "AREVA MCPR Safety Limit Methodology for Boiling Water Reactors," AREVA NP, June 2011.

- Purpose: Present and justify a new methodology for determining the safety limit minimum critical power ratio (SLMCPR) to incorporate the ACE critical power correlations (Topical Reports 2-23 and 2-24) and a realistic fuel channel bow model approved in Topical Report 2-11.

- SER Restrictions: There are no specific SER restrictions.

- Implementation of SER Restrictions: None.

- Observations: For non-typical situations, such as abnormal bow situations, transition cores, and new channel designs, the channel bow model will be applied in a conservative manner through use of **[ ]** according to Topical Report 2-11.

  Two modifications were made to the SAFLIM3D analyses to support the determination of the Monticello MCPR Safety Limit. The first change was associated with the implementation of the improved K-factor Model for the ACE/ATRIUM 10XM Critical Power Correlation (Reference 23) in SAFLIM3D. The second was to address a concern with the application of the fuel channel bow standard deviation when the fluence gradient is computed to exceed the bound of the channel measurement database. As a consequence, the fuel channel bow standard deviation component of the channel bow model uncertainty used by ANP-10307PA to determine the Safety Limit Minimum Critical Power Ratio was increased by the ratio of channel fluence gradient to the channel fluence gradient bound of the channel measurement database, when applied to channels with fluence gradients outside the bounds of the measurement database from which the model uncertainty was determined.

  Since Monticello will perform core monitoring with the GARDEL CMS, uncertainty values for SAFLIM3D calculation will be taken from uncertainty analyses performed for the GARDEL CMS.

2-26 XN-CC-33(A) Revision 1, "HUXY: A Generalized Multirod Heatup Code with 10 CFR 50 Appendix K Heatup Option Users Manual," Exxon Nuclear Company, November 1975.

- Purpose: Develop a planar heat transfer model which includes rod-to-rod radiation. This code also includes the BULGEX model for the calculation of fuel rod strains and ballooning.

- SER Restrictions:

  1. The staff, however, will require that a conservative reduction of 10% be made in the (spray heat transfer) coefficients specified in 10 CFR 50 Appendix K for 7x7 assemblies when applied to ENC 8x8 assemblies.

  2. In each individual plant submittal employing the Exxon model the applicant will be required to properly take rod bowing in account.

  3. Since GAPEX is not identical to HUXY in radial noding or solution scheme, it is required that the volumetric average fuel temperature for each rod be equal to or greater than that in the approved version of GAPEX. If it is not, the gap coefficient must be adjusted accordingly.

  4. It has been demonstrated that the (2DQ local quench velocity) correlation gives hot plane quench time results that are suitably conservative with respect to the available data when a coefficient behind the quench front of 14000 Btu/(hr-ft^2-°F) is used.

  5. It (Appendix K) requires that heat production from the decay of fission products shall be 1.2 times the value given by K. Shure as presented in ANS 5.1 and shall assume infinite operation time for the reactor.

  6. It is to be assumed for all these heat sources (fission heat, decay of actinides and fission product decay) that the reactor has operated continuously at 102% of licensed power at maximum peaking factors allowed by Technical Specifications.

  7. For small and intermediate size breaks, the applicability of the fission power curve used in the calculations will be justified on a case by case basis. This will include justification

of the time of scram (beginning point in time of the fission power decrease) and the rate of fission power decrease due to voiding, if any.

8. The rate of (metal water) reaction must be calculated using the Baker-Just equation with no decrease in reaction rate due to the lack of steam. This rate equation must be used to calculate metal-water reactions both on the outside surface of the cladding, and if ruptured, on the inside surface of the cladding. The reaction zone must extend axially at least three inches.

9. The initial oxide thickness (that affects the zirconium-water reaction rate) used should be no larger than can be reasonably justified, including consideration of the effects of manufacturing processes, hot-functional testing and exposure.

10. Exxon has agreed to provide calculations on a plant by plant basis to demonstrate that the plane of interest assumed for each plant is the plane in which peak cladding temperatures occur for that plant.

- Implementation of SER Restrictions: SER restrictions 1, 2, 3, 4, 6, 7, 9, and 10 are implemented in engineering guidelines. Restrictions 5 and 8 are directly implemented in engineering computer codes.

  NOTE: The Cross-string method of developing radiation heat transfer view factors used in the HUXY code has been replaced with the Ray-trace method which produces a direct finite element evaluation of view factors. This modification was included in the Monticello specific LOCA analyses.

- Observations: [

]

For Monticello, all SER restrictions are addressed through engineering guidelines or software implementation. One concern has been raised by the NRC with respect to application of this LTR to Monticello, exposure dependent Thermal Conductivity Degradation (TCD). The evaluation of thermal conductivity degradation for the Monticello LOCA analyses is presented in Appendix E. This appendix demonstrates that there is no PCT impact associated with thermal conductivity degradation due to the conservatisms in the AREVA LOCA methodology (Topical Report 2-34) that result in limiting PCTs early in life.

2-27 XN-NF-80-19(P)(A) Volumes 2, 2A, 2B and 2C, "Exxon Nuclear Methodology for Boiling Water Reactors: EXEM BWR ECCS Evaluation Model," Exxon Nuclear Company, September 1982.

- Purpose: Provide an evaluation model methodology for licensing analyses of postulated LOCAs in jet pump BWRs. The methodology was developed to comply with 10 CFR 50.46 criteria and 10 CFR 50 Appendix K requirements.

- SER Restrictions: Counter-current flow limit correlation coefficients used in FLEX for new fuel designs that vary from fuel cooling test facility (FCTF) measured test configurations must be justified.

- Implementation of SER Restrictions: The FLEX computer code is no longer used. This was replaced in Topical Report 2-34.

- Observations: RELAX and FLEX, which are key computer codes in the methodology, have been subsequently modified as described in Topical Reports 2-31 and 2-32, which documents the revised EXEM BWR Model, and in Topical Report 2-34 which documents EXEM BWR-2000 in which the RELAX code replaced FLEX. The EXEM BWR-2000 model supersedes the prior evaluation model.

  As described in the Monticello specific LOCA reports, a plant specific methodology derived from the Topical Report 2-34 methodology was applied for the ATRIUM 10XM fuel introduction.

2-28 XN-NF-82-07(P)(A) Revision 1, "Exxon Nuclear Company ECCS Cladding Swelling and Rupture Model," Exxon Nuclear Company, November 1982.

- Purpose: Incorporate the swelling and rupture models described in NUREG-0630 (Reference 18) which comply with 10 CFR 50 Appendix K requirements into the HUXY code (Topical Report 2-26).

- SER Restrictions: No restrictions.

- Implementation of SER Restrictions: None.

- Observations: The swelling and rupture model is currently applicable.

  The swelling and rupture models described in NUREG-0630 which comply with 10 CFR 50 Appendix K requirements were applied in the Monticello plant specific LOCA methodology.

2-29 XN-NF-84-105(P)(A) Volume 1 and Volume 1 Supplements 1 and 2, "XCOBRA-T: A Computer Code for BWR Transient Thermal-Hydraulic Core Analysis," Exxon Nuclear Company, February 1987.

- Purpose: Provide a capability to perform analyses of transient heat transfer behavior in BWR assemblies.

- SER Restrictions:

  1. XCOBRA-T was found acceptable for the analysis of only the following licensing basis transients:

     a) Load rejection without bypass
     b) Turbine trip without bypass
     c) Feedwater controller failure
     d) Steam isolation valve closure without direct scram
     e) Loss of feedwater heating or inadvertent high pressure coolant injection (HPCI) actuation
     f) Flow increase transients from low-power and low-flow operation

  2. XCOBRA-T analyses that result in any calculated downflow in the bypass region will not be considered valid for licensing purposes.

  3. XCOBRA-T licensing calculations must use NRC approved default options for void-quality relationship and two-phase multiplier correlations.

  4. The use of XCOBRA-T is conditional upon a commitment by ENC to a follow-up program to examine the XCOBRA-T void profile against experimental data from other sources.

- Implementation of SER Restrictions: SER restrictions 1, 2, and 3 are implemented in engineering guidelines. SER restriction 3 is also implemented through code controls (defaults, override warning messages). Restriction 4 was subsequently addressed in Reference 19 and no further action is required.

- Observations: The XCOBRA-T computer code implements both the SPCB (Topical Report 2-22) and the ACE/ATRIUM 10XM (Topical Report 2-24) correlations to determine

transient conditions at which the hot channel experiences dryout. Both of these correlations have defined ranges of applicability and a fundamental aspect of implementing these correlations into the transient simulator was to implement correlation bounds checking. The bounds checking routine does not allow a calculation outside the range of applicability.

- Clarifications: NRC concurrence with an interpretation of the contents of the topical report was requested in References 20 and 21. The NRC concurrence with the interpretation was provided in Reference 22. The interpretation was with regard to a commitment to perform critical heat flux ratio evaluations at every node in the hot channel.

  In order to assess the margin to the critical heat flux in every node, the transient heat flux is compared to the corresponding critical heat flux. For SPCB and ATRIUM 10XM the critical heat flux or critical power is computed based on correlation specific local peaking factors (F-effective for SPCB and K-Factor arrays for ACE/ATRIUM 10XM) by MICROBURN-B2 based on pin power reconstruction methods. The method for computing these local peaking factors for each rod type in the assembly are described in Topical Report 2-22 and Topical Report 2-24). XCOBRA-T calculates the transient response for the average fuel rod surface heat flux in the hot assembly using a fuel rod heat conduction model, the power generated in the fuel rod, and the fluid conditions at the surface of the rod. The power generated in the fuel rod is described in Reference 19 Section 2.5.5. The power generated in each axial section of a fuel rod is calculated using Equation 2.130 from Reference 19. Although Reference 19 states that Equation 2.130 is calculated for each axial node, the equation itself does not denote which variables are axially dependent. Because the equation is for each axial node, the variables for heat generation rate, axial peaking factor, and number of rods are axial dependent. At the time Reference 19 was prepared, the number of rods at each axial plane was a constant for the fuel designs being supplied. For the ATRIUM 10XM fuel design with part length fuel rods (PLFRs), the number of rods became axial dependent and the code was modified to make application of Equation 2.130 correct and consistent with the NRC-approved Reference 19. For application to modern fuel designs, a better definition of the variable Nr in Equation 2.130 would be "number of *heated* rods per assembly *at the axial plane*" (italic indicates added text). For assembly axial nodes with PLFRs containing UO_2, the PLFRs are included in the variable Nr. For assembly axial nodes in the plena region of the PLFRs and above the PLFRs, Nr does not include the PLFRs. Equation 2.130 is

correctly applied for all axial planes when the variable Nr is the number of heated rods at the axial plane.

NRC concurrence with clarifications related to SER and TER issues concerning the topical report was requested in References 5 and 6. The NRC concurrence with these clarifications was provided in Reference 7. These references clarify that XCOBRA-T is approved for the analysis of the following events:

SRP Section	Chapter 15 Analysis
15.1.1 – 15.1.3	Decrease in Feedwater Temperature, Increase in Feedwater Flow, and Increase in Steam Demand
15.2.1 – 15.2.5	Loss of External Load, Turbine Trip, Loss of Condenser Vacuum, Closure of Main Steam Isolation Valve (BWR), and Steam Pressure Regulator Failure (Closed)
15.2.7	Loss of Normal Feedwater Flow
15.3.1-15.3.2	Loss of Forced Reactor Coolant Flow Including Trip of Pump Motor and Flow Controller Malfunctions
15.3.3-15.3.4	Reactor Coolant Pump Rotor Seizure and Reactor Coolant Pump Shaft Break
15.4.4 – 15.4.5	Startup of an Inactive Loop or Recirculation Loop at an Incorrect Temperature, and Flow Controller Malfunction Causing an Increase in BWR Core Flow Rate
15.5.1	Inadvertent Operation of ECCS that Increases Reactor Coolant Inventory
15.6.1	Inadvertent Opening of a PWR Pressure Relief Valve and BWR Pressure Relief Valve
15.8	Anticipated Transients Without Scram (the Initial Pressurization Only)

2-30 ANF-913(P)(A) Volume 1 Revision 1 and Volume 1 Supplements 2, 3 and 4, "COTRANSA2: A Computer Program for Boiling Water Reactor Transient Analyses," Advanced Nuclear Fuels Corporation, August 1990.

- Purpose: Develop an improved computer program for analyzing BWR system transients.

- SER Restrictions: The staff reviewed the subject safety evaluations and identified the following limitations that apply to COTRANSA2:

  1. Use of COTRANSA2 is subject to limitations set forth for methodologies described and approved for XCOBRA-T and COTRAN.

  2. The COTRANSA2 code is not applicable to the analysis of any transient for which lateral flow in a bundle is significant and nonconservative in the calculation of system response.

  3. For those analyses in which core bypass is modeled, the effect of a computed negative flow in the core bypass region should be shown to make no significant non-conservative contribution in the system response.

  4. Licensing applications referencing the COTRANSA2 methodology must include confirmation that sensitivity to the time step selection has been considered in the analysis.

- Implementation of SER Restrictions: SER restrictions 1, 2, and 4 are implemented in engineering guidelines. Restriction 3 is implemented in engineering guidelines and automation tools.

- Observations: The COTRANSA2 SER restrictions are similar to those for XCOBRA-T (Topical Report 2-29).

- Clarifications: NRC concurrence with clarifications related to SER and TER issues concerning the topical report was requested in References 5 and 6. The NRC concurrence with these clarifications was provided in Reference 7. These references clarify that COTRANSA2 is approved for the analysis of the following events:

SRP Section	Chapter 15 Analysis
15.1.1 – 15.1.3	Decrease in Feedwater Temperature, Increase in Feedwater Flow, and Increase in Steam Demand
15.2.1 – 15.2.5	Loss of External Load, Turbine Trip, Loss of Condenser Vacuum, Closure of Main Steam Isolation Valve (BWR), and Steam Pressure Regulator Failure (Closed)
15.2.7	Loss of Normal Feedwater Flow
15.3.1-15.3.2	Loss of Forced Reactor Coolant Flow Including Trip of Pump Motor and Flow Controller Malfunctions
15.3.3-15.3.4	Reactor Coolant Pump Rotor Seizure and Reactor Coolant Pump Shaft Break
15.4.4 – 15.4.5	Startup of an Inactive Loop or Recirculation Loop at an Incorrect Temperature, and Flow Controller Malfunction Causing an Increase in BWR Core Flow Rate
15.5.1	Inadvertent Operation of ECCS that Increases Reactor Coolant Inventory
15.6.1	Inadvertent Opening of a PWR Pressure Relief Valve and BWR Pressure Relief Valve
15.8	Anticipated Transients Without Scram (the Initial Pressurization Only)

The Monticello COTRANSA2 plant model is constructed from information provided by Xcel Energy. This includes the homologous pump curves used by COTRANSA2 and an assessment of the pump inertia against the data provided by the licensee. The performance data from the licensee also includes information on the safety and relief valves. The safety and relief valves (SRVs) are modeled in COTRANSA2 as a single mass sink from the steam line node where they are located. SRVs with the same setpoint are modeled as a combined valve in COTRANSA2. The net flow is the sum of the flow of each valve in parallel. Multiple SRVs are used in COTRANSA2 to represent banks of SRVs with different setpoints.

The SRVs are opened to relieve pressure when calculated pressure in the steam line node containing the valves reaches the opening setpoint pressure. The valve position is based on time since the valve setpoint was exceeded, the valve opening delay, and the valve stroke time.

Full open valve flow (*W*) is calculated as:

[ ]

The COTRANSA2 input for [ ] is adjusted to account for the total pressure loss in the SRV branch from the main steam line to the SRV.

As noted in the table above, the COTRANSA2 computer program assessed the system response to both the ASME over-pressure event and the peak vessel pressure for Anticipated Transients Without Scram. The ASME over-pressure event and the ATWS are not limiting with respect to 10 CFR 50.46 criteria. The ATWS event is significantly less limiting than the loss of coolant accident relative to 10 CFR 50.46 acceptance criteria. Furthermore, the ATWS overpressurization event is not used to establish operating limits for critical power; therefore, critical power correlations are not a factor in the analyses. While dryout might occur on limiting (high power) channels of the core during the ATWS event, these channels are not modeled in COTRANSA2 analyses. For the ATWS overpressurization analysis, ignoring dryout for the hot channels is conservative in that it maximizes the heat transferred to the coolant and results in a higher calculated pressure.

As described in Appendix E, the peak vessel pressure response is impacted by the use of the legacy fuel rod models from RODEX2 which does not address thermal conductivity degradation with exposure. Appendix E presents the evaluation of thermal conductivity degradation, and when coupled with penalties associated with both the Doppler mismatch between MICROBURN-B2 and COTRANSA2 and uncertainties in the void/quality correlation, demonstrates that the Monticello reactor maintains margin to the required peak vessel pressure limits.

In addition, Appendix F provides a description of the cross section treatment in COTRANSA2 that is used for Extended Power Uprate conditions to better simulate the reactivity characteristics of the MICROBURN-B2 three dimensional core simulator.

2-31 ANF-91-048(P)(A), "Advanced Nuclear Fuels Corporation Methodology for Boiling Water Reactors EXEM BWR Evaluation Model," Advanced Nuclear Fuels Corporation, January 1993.

- Purpose: Update the RELAX system blowdown code and FLEX refill code by reducing code instabilities and improving their predictive capabilities.

- SER Restrictions:

  1. The modified Dougall-Rohsenow heat transfer correlation has been shown to yield conservative results for many experimental measurements. The applicant used a suitable multiplier in the comparison calculations. Licensees will use this multiplier in licensing calculations.

  2. The revised model is valid within the range of applicability of the modified Dougall-Rohsenow heat transfer correlation.

  3. The staff requires that the revised evaluation model be protected with appropriate quality assurance procedures.

  4. The phase separation models will be limited to the models used in the topical report.

  5. The revised evaluation model will be limited to jet pump plant applications.

- Implementation of SER Restrictions: SER restrictions 1 and 2 are directly implemented in engineering computer codes. Restriction 3 is implemented in engineering work practices. Restriction 4 is implemented in engineering guidelines and automation tools. Restriction 5 is implemented in engineering guidelines.

- Observations: The RELAX code, with the jet pump update from ANF-91-048(P)(A) Supplements 1 and 2, and FLEX models were approved. This evaluation model has subsequently been superseded by EXEM BWR-2000 (Topical Report 2-34).

2-32 ANF-91-048(P)(A) Supplements 1 and 2, "BWR Jet Pump Model Revision for RELAX," Siemens Power Corporation, October 1997.

- Purpose: Modify the jet pump model in the RELAX blowdown code to better predict jet pump performance for all ranges of LOCA conditions.
- SER Restrictions: No restrictions imposed.
- Implementation of SER Restrictions: None.
- Observations: The jet pump model was approved.

2-33 EMF-2292(P)(A) Revision 0, "ATRIUM™-10: Appendix K Spray Heat Transfer Coefficients," Siemens Power Corporation, September 2000.

- Purpose: Justify the use of 10 CFR 50 Appendix K convective heat transfer coefficients during loss of coolant accident spray cooling for the ATRIUM-10 fuel design.
- SER Restrictions: None.
- Implementation of SER Restrictions: None.
- Observations: None.

AREVA made a commitment in Topical Report 2-7, to justify the use of 10 CFR 50 Appendix K convective heat transfer coefficients when the lattice array changes (e.g. 8x8, 9x9, 10x10, etc.). This report justified the continued conservatism for 10x10 arrays and is therefore applicable to the ATRIUM 10XM design for Monticello.

2-34 EMF-2361(P)(A) Revision 0, "EXEM BWR-2000 ECCS Evaluation Model," Framatome ANP, May 2001.

- Purpose: Describes an evaluation model for licensing analyses of postulated LOCAs in jet pump BWRs. The methodology complies with 10 CFR 50.46 and 10 CFR 50 Appendix K.
- SER Restrictions: The staff concluded that the EXEM BWR-2000 Evaluation Model was acceptable for referencing in BWR LOCA analysis, with the limitation that the application of the revised evaluation model be limited to jet pump applications.
- Implementation of SER Restrictions: The SER restriction is implemented in engineering guidelines.
- Observations: Replace the FLEX code by the code RELAX in the BWR LOCA methodology.

The Monticello specific methodology is a variant of the methodology described in this LTR. The Monticello specific methodology included:

- a conservative calculation procedure as described in the LOCA analyses reports;
- modifications to address thermal conductivity degradation as described in Appendix E; and
- the Ray-trace view factor methodology as noted in Topical Report 2-26.

3.0 References

1. Letter, R. A. Copeland (Siemens Nuclear Power) to R. C. Jones (NRC), "No Subject," RAC:050:91, May 13, 1992.

2. NASA SP-221, *The NASTRAN Theoretical Manual*, 1969.

3. Letter, James F. Mallay (SPC) to Document Control Desk (NRC), "Clarification of Methodology for Analyzing Gadolinia-Bearing Fuel," NRC:98:053, August 31, 1998.

4. Letter, Stuart A. Richards (NRC) to James F. Mallay (SPC), "Siemens Power Corporation Re: Request for Concurrence on Safety Evaluation Report Clarifications (MA6160)," November 3, 2000.

5. Letter, James F. Mallay (SPC) to Document Control Desk (NRC), "Request for Concurrence on SER Clarifications," NRC:99:030, July 28, 1999.

6. Letter, James F. Mallay (SPC) to Document Control Desk (NRC), "Revisions to Attachment 1 of Letter NRC:99:030, Request for Concurrence on SER Clarifications," NRC:99:045, October 12, 1999.

7. Letter, Stuart Richards (NRC) to James F. Mallay (SPC), "Siemens Power Corporation Re: Request for Concurrence on Safety Evaluation Report Clarifications (TAC No. MA6160)," May 31, 2000.

8. Letter, James F. Mallay (Framatome ANP) to Document Control Desk (NRC), "Clarification of Exposure Limit Applicable to Framatome ANP BWR Fuel," NRC:02:029, June 27, 2002.

9. Letter, James F. Mallay (Framatome ANP) to Document Control Desk (NRC), "Clarification of Exposure Limit Applicable to Framatome ANP BWR Fuel," NRC:02:041, September 4, 2002.

10. Letter, William H. Ruland (NRC) to James F. Mallay (Framatome ANP), "EMF-85-74(P)(A), Revision 0, Supplement 1 and Supplement 2, "RODEX2A (BWR) Fuel Rod Thermal-Mechanical Evaluation Model" – Clarification of Exposure Limit Applicable to Framatome ANP BWR Fuel (TAC No. MB6335)," December 17, 2002.

11. Letter, James F. Mallay (SPC) to Document Control Desk (NRC), "Assessment of Fuel Channel Design Calculations," NRC:99:031, July 23, 1999.

12. Letter, S. A. Richards (NRC) to James F. Mallay (SPC), "Supplement to Safety Evaluation and Technical Evaluation Report Clarifications for EMF-CC-074(P), Volume 4, Revision 0, 'BWR Stability Analysis Assessment of STAIF with Input from MICROBURN-B2' (TAC No. MA7221)," November 30, 2000.

13. Letter, James F. Mallay (SPC) to Document Control Desk (NRC), "SER Condition for EMF-2209(P) Revision 1, 'SPCB Critical Power Correlation'," NRC:00:024, April 24, 2000.

14. Letter, James F. Mallay (Framatome ANP) to Document Control Desk (NRC), "BWR CHF Bounds Checking," NRC:01:023, June 12, 2001.

15. Letter, James F. Mallay (Framatome ANP) to Document Control Desk (NRC), "BWR CHF Correlation Bounds Checking," NRC:02:003, January 11, 2002.

16. Letter, William H. Ruland (NRC) to James F. Mallay (Framatome ANP), "Safety Evaluation for BWR CHF Correlation Bounds Checking Clarifications Relating to Topical Reports EMF-1997(P)(A) Revision 0 and EMF-2209(P)(A) Revision 1 (TAC No. MB3107)," July 2, 2002.

17. *Standard Review Plan for the Review of Safety Analysis Reports for Nuclear Power Plants*, NUREG-0800, U.S. Nuclear Regulatory Commission, July 1981.

18. *Cladding Swelling and Rupture Models for LOCA Analysis*, NUREG-0630, U.S. Nuclear Regulatory Commission, April 1980.

19. XN-NF-84-105(P)(A) Volume 1 Supplement 4, *XCOBRA-T: A Computer Code for BWR Transient Thermal-Hydraulic Core Analysis – Void Fraction Model Comparison to Experimental Data*, Advanced Nuclear Fuels Corporation, June 1988.

20. Letter, James F. Mallay (SPC) to USNRC, "Clarification of SRP Chapter 15 Analyses Performed with XCOBRA-T and Checking of CHF Limits for Pump Seizure During SLO," NRC:98:037, June 3, 1998.

21. Letter, Don Curet (SPC) to USNRC, "Equilibrium Quality Limits for Hench-Levy Limit Line Correlation," NRC:98:044, June 25, 1998.

22. Letter, Cynthia A. Carpenter (NRC) to James F. Mallay (SPC), "Modification to Procedures for Use of XCOBRA-T," June 10, 1999.

23. ANP-3138(P) Revision 0, *Monticello Improved K-factor Model for ACE/ATRIUM 10XM Critical Power Correlation*, AREVA NP, August 2012.

24. EMF-2158(P)(A) Revision 0, *Siemens Power Corporation Methodology for Boiling Water Reactors: Evaluation and Validation of CASMO-4/MICROBURN-B2*, Siemens Power Corporation, October 1999.

25. XN-NF-85-67(P)(A) Revision 1, *Generic Mechanical Design for Exxon Nuclear Jet Pump BWR Reload Fuel*, Exxon Nuclear Company, September 1986.

26. NEDO-32047-A, "ATWS Rule Issues Relative to BWR Core Thermal-Hydraulic Stability," June 1995.

27. ANP-10262PA, Revision 0, *Enhanced Option III Long Term Stability Solution*, May 2008.

28. NEDO-32164 Revision 0, "Mitigation of BWR Core Thermal-Hydraulic Instabilities in ATWS," December 1992.

29. Wulff, W., H. S. Cheng, A.N. Mallen, and U.S. Rohatgi, "BWR Stability Analysis with the BNL Engineering Plant Analyzer," NUREG/CR-5816, October 1992.

30. March-Leuba, J., D.G. Cacuci, and R.B. Perez, "Nonlinear Dynamics and Stability of Boiling Water Reactors: Part I -- Qualitative Analysis," Nuclear Science and Engineering: 93, 111-123 (1986).

31. March-Leuba, J., "Density-Wave Instabilities in Boiling Water Reactors," NUREG/CR-6003, September 1992.

32. Farawila, Y.M., and D.W. Pruitt, "A Study of Nonlinear Oscillation and Limit Cycles in Boiling Water Reactors – I: The Global Mode," Nuclear Science and Engineering: 154, 302-315 (2006).

33. Farawila, Y.M., and D.W. Pruitt, "A Study of Nonlinear Oscillation and Limit Cycles in Boiling Water Reactors – II: The Regional Mode," Nuclear Science and Engineering: 154, 316-327 (2006).

34. EMF-2245(P)(A) Revision 0, *Application of Siemens Power Corporation's Critical Power Correlations to Co-Resident Fuel*, Siemens Power Corporation, August 2000.

35. ANP-10298PA, Revision 0, *ACE/ATRIUM 10XM Critical Power Correlation*, AREVA NP Inc., March 2010.

36. ANP-10298PA Revision 0 Supplement 1P Revision 0, *Improved K-Factor Model for ACE/ATRIUM 10XM Critical Power Correlation*, AREVA NP, December 2011.

37. ANF-913 (P)(A) Volume 1 Revision 1 and Volume 1 Supplements 2, 3, and 4, *COTRANSA2: A Computer Program for Boiling Water Reactor Transient Analyses*, Advanced Nuclear Fuels Corporation, August 1990.

38. N. Zuber and J. A. Findlay, "Average Volumetric Concentration in Two-Phase Flow Systems," J. Heat Transfer, 1965.

39. P. Coddington and R. Macian, "A Study of the Performance of Void Fraction Correlations Used In the Context of Drift-Flux Two-Phase Flow Models," Nuclear Engineering and Design, 215, 199-216, June 2002.

40. [
]

41. K. Ohkawa and R. T. Lahey, Jr., "The Analysis of CCFL Using Drift-Flux Models," Nuclear Engineering and Design, 61, 1980.

42. S. Misu et al., "The Comprehensive Methodology for Challenging BWR Fuel Assembly and Core Design used at FANP," proceedings on CD-ROM, PHYSOR 2002, Seoul, Korea, October 7-10, 2002.

43. O. Nylund et al., "Hydrodynamic and Heat Transfer Measurements on A Full-Scale Simulated 36-Rod Marviken Fuel Element with Non-Uniform Radial Heat Flux Distribution," FRIGG-3, R-494/RL-1154, November 1969.

44. J. Skaug et al., "FT-36b, Results of void Measurements," FRIGG-PM-15, May 1968.

45. O. Nylund et al., "Hydrodynamic and Heat Transfer Measurements on A Full-Scale Simulated 36-Rod Marviken Fuel Element with Uniform Heat Flux Distribution," FRIGG-2, R-447/RTL-1007, May 1968.

46. Letter, R. Gardner to NRC, "Informational Transmittal Regarding Requested White Paper on the Treatment of Exposure Dependent Fuel Thermal Conductivity Degradation in RODEX Fuel Performance Codes and Methods," NRC:09:069, ML092010160, July 14, 2009.

47. Letter, T. J. McGinty (NRC) to P. Salas (AREVA), "Nuclear Fuel Thermal Conductivity Degradation Evaluation for Light Water Reactors Using AREVA Codes and Methods (TAC No. ME5178)," March 23, 2012.

48. Letter, P. Salas (AREVA) to NRC, "Response to NRC Letter Regarding Nuclear Fuel Thermal Conductivity Degradation Evaluation for Light Water Reactors Using AREVA Codes and Methods," NRC:12:023, April 27, 2012.

49. ANP-10300P, Revision 0, *AURORA-B: An Evaluation Model for Boiling Water Reactors; Application to Transient and Accident Scenarios*, (ML100040158) December 2009.

50. NEDO-32465-A, "Reactor Stability Detect and Suppress Solutions Licensing Basis Methodology for Reload Applications," August 1996.

51. ANP-3212 Revision 0, *Monticello LOCA-ECCS Analysis MAPLHGR Limits for ATRIUM™ 10XM Fuel*, AREVA NP, May, 2013.

52. EMF-3028P-A Volume 2 Revision 4, *RAMONA5-FA: A Computer Program for BWR Transient Analysis in the Time Domain Volume 2: Theory Manual*, AREVA NP, March, 2013.

53. J. G. Collier and J. R. Thome, "Convective Boiling and Condensation," Third Edition, Oxford University Press, 1996.

54. R. T. Lahey, Jr., and F. J. Moody, "The Thermal-hydraulics of a Boiling Water Nuclear Reactor," American Nuclear Society, 1977.

Appendix A Neutronic Methods

A.1 Cross Section Representation

CASMO-4 performs a multi-group [ ] spectrum calculation using a detailed heterogeneous description of the fuel lattice components. Fuel rods, absorber rods, water rods/channels and structural components are modeled explicitly. The library has cross sections for [ ] materials including [ ] heavy metals. Depletion is performed with a predictor-corrector approach in each fuel or absorber rod. The two-dimensional transport solution is based upon the [ ]. The solution provides pin-by-pin power and exposure distributions, homogeneous multi-group (2) micro-scopic cross sections as well as macro-scopic cross sections. Discontinuity factors are determined from the solution. [ ] gamma transport calculation are performed. The code has the ability to perform [ ] calculations with different mesh spacings. Reflector calculations are easily performed.

MICROBURN-B2 performs microscopic fuel depletion on a nodal basis. The neutron diffusion equation is solved with a full two energy group method. A modern nodal method solution using discontinuity factors is used along with a [ ]. The flux discontinuity factors are [ ]. A multilevel iteration technique is employed for efficiency. MICROBURN-B2 treats a total of [ ] heavy metal nuclides to account for the primary reactivity components. Models for nodal [ ] are used to improve the accurate representation of the in-reactor configuration. A full three-dimensional pin power reconstruction method is utilized. TIP (neutron and gamma) and LPRM response models are included to compare calculated and measured instrument responses. Modern steady state thermal hydraulics models define the flow distribution among the assemblies. [ ] based upon CASMO-4 calculations are used for the in-channel fluid conditions as well as in the bypass and water rod regions. Modules for the calculation of CPR, LHGR and MAPLHGR are implemented for direct comparisons to the operating limits.

MICROBURN-B2 determines the nodal macroscopic cross sections by summing the contribution of the various nuclides.

$$\Sigma_x(\rho,\Pi,E,R)=\sum_{i=1}^{I} N_i\sigma_x^i(\rho,\Pi,E,R)+\Delta\Sigma_x^b(\rho,\Pi,E,R)$$

where:

Σ_x = nodal macroscopic cross section

$\Delta\Sigma_x^b$ = background nodal macroscopic cross section $(D, \Sigma_f, \Sigma_a, \Sigma_r)$

N_i = nodal number density of nuclide "i"

σ_x^i = microscopic cross section of nuclide "i"

I = total number of explicitly modeled nuclides

ρ = nodal instantaneous coolant density

Π = nodal spectral history

E = nodal exposure

R = control fraction

The functional representations of σ_x^i and $\Delta\Sigma_x^b$ come from 3 void depletion calculations with CASMO-4. Instantaneous branch calculations at alternate conditions of void and control state are also performed. The result is a multi-dimensional table of microscopic and macroscopic cross sections that is shown in and Figure A-2.

At BOL the relationship is fairly simple; the cross section is only a function of void fraction (water density) and the reason for the variation is the change in the spectrum due to the water density variations. At any exposure point, a quadratic fit of the three CASMO-4 data points is used to represent the continuous cross section over instantaneous variation of void or water density. This fit is shown in Figure A-3 and Figure A-4.

Detailed CASMO-4 calculations confirm that a quadratic fit accurately represents the cross sections as shown in Figure A-5, Figure A-6, and Figure A-7.

With depletion the isotopic changes cause other spectral changes. Cross sections change due to the spectrum changes. Cross sections also change due to self-shielding as the concentrations change. These are accounted for by the void (spectral) history and exposure parameters. Exposure variations utilize a piecewise linear interpolation over tabulated values at [ ] exposure points. The four dimensional representation can be reduced to three dimensions (see Figure A-8) by looking at a single exposure.

Quadratic interpolation is performed in each direction independently for the most accurate representation. Considering the case at 70 GWd/MTU with an instantaneous void fraction of 70% and a historical void fraction of 60%, Figure A-9 and Figure A-10 illustrate the interpolation

process. The table values from the library at 0, 40 and 80 % void fractions are used to generate 3 quadratic curves representing the behavior of the cross section as a function of the historical void fraction for each of the tabular instantaneous void fractions (0, 40 and 80 %).

The intersection of the three quadratic lines with the historical void fraction of interest are then used to create another quadratic fit in order to obtain the resultant cross section as shown in Figure A-10.

The results of this process for all isotopes and all cross sections in MICROBURN-B2 were compared for an independent CASMO-4 calculation with continuous operation at 20, 60 and 90% void and are presented in Figure A-11. Branch calculations at 90% void from a 40% void depletion were performed for multiple exposures. The results show very good agreement for the whole exposure range as shown in Figure A-12.

At the peak reactivity point, multiple comparisons were made (Figure A-13) to show the results for various instantaneous void fractions.

[

]

Void fraction has been used for the previous illustrations; however MICROBURN-B2 uses water density rather than void fraction in order to account for pressure changes as well as sub-cooled density changes. This transformation does not change the basic behavior as water density is proportional to void fraction. MICROBURN-B2 uses spectral history rather than void history in order to account for other spectral influences due to actual core conditions (fuel loading, control rod inventory, leakage, etc.) The Doppler feedback due to the fuel temperature is modeled by accumulating the Doppler broadening of microscopic cross sections of each nuclide.

$$\Delta\Sigma_x = (\sqrt{T_{eff}} - \sqrt{T_{ref}})\sum_i^I \frac{\partial\sigma_x^i}{\partial\sqrt{T_i}} N_i$$

where:

T_{eff} = Effective Doppler Fuel Temperature
T_{ref} = Reference Doppler Fuel Temperature
σ_x^i = Microscopic Cross Section (fast and thermal absorption) of nuclide "i"
N_i = Density of nuclide "i"

The partial derivatives are determined from branch calculations performed with CASMO-4 at various exposures and void fractions for each void history depletion. The tables of cross sections include data for [ ] states. The process is the same for [ ] states. Other important feedbacks to nodal cross sections are lattice [ ] and instantaneous [ ] between lattices of different [ ]. These feedbacks are modeled in detail.

The methods used in CASMO-4 are state of the art. The methods used in MICROBURN-B2 are state of the art. The methodology accurately models a wide range of thermal hydraulic conditions including EPU and extended power/flow operating map conditions.

A.2 Applicability of Uncertainties

The TIPs directly measure the local neutron flux from the surrounding four fuel assemblies. Thus, the calculated bundle power distribution uncertainty will be closely related to the calculated TIP uncertainty. However, the bundle powers in the assemblies surrounding a TIP are not independent. If a bundle is higher in power, neutronic feedback increases the power in the nearby assemblies, thus producing a positive correlation between nearby bundles. The gamma scan data provides the means to determine this correlation according to the EMF-2158(P)(A) (Reference 24) methodology. A smaller correlation coefficient implies that there is less correlation between nearby bundle powers, thus, there would be a larger bundle power distribution uncertainty.

The EMF-2158(P)(A) data was re-evaluated by looking at the deviations between measured and calculated TIP response for each axial level. The standard deviation of these deviations at each axial plane are presented in Figure A-15 and demonstrate that there is no significant trend vs. axial position, which indicates no significant trend vs. void fraction. This same data was evaluated for trends based upon the core conditions at the time of each TIP scan. The core parameters of interest that were evaluated include core thermal power, the core average void

fraction and the ratio between core power and core flow. The 2D standard deviations for "C" and "D" lattice plants are presented in Figure A-16 through Figure A-21, while the 3D standard deviations are presented in Figure A-22 through Figure A-27. This evaluation of the data indicates that there is no significant trend in the data associated with these plant parameters.

Parameters such as fuel density, part length rods, active fuel length, fuel pellet diameter and fuel cladding diameter are all inputs to the methodology. The methodology explicitly accounts for such changes in design parameters. The changes in these parameters for the ATRIUM 10 XM fuel are insignificant relative to the changes that have been included in the validation of the methodology that demonstrate the methodology's capability to evaluate these parameters. Fuel designs including 7X7, 8X8, 9X9 and 10X10 with corresponding changes in pellet and cladding diameters were presented in the topical report, EMF-2158(P)(A) "Siemens Power Corporation Methodology for Boiling Water Reactors: Evaluation and Validation of CASMO-4/MICROBURN-B2."

To compare core physics models to the gamma scan results, the calculated pin power distribution is converted into a Ba140 density distribution. A rigorous mathematical process using CASMO-4 pin nuclide inventory and MICROBURN-B2 nodal nuclide inventory is used.

Gamma scan comparisons for 9X9-1 and ATRIUM-10 fuel were presented in the topical report, EMF-2158(P)(A), in Section 8.2.2. Figures 8.18 through 8.31 showed very good comparisons between the calculated and measured relative Ba-140 density distributions for both radial and axial values.

The Quad Cities assembly gamma scan data was used to determine the correlation coefficient which accounts for the correspondence between the assembly powers of adjacent assemblies. This correspondence is quantified by a conservative multiplier to the uncertainty in the TIP measurements. In order to conservatively account for this correspondence, the bundle power uncertainty is increased due to the radial TIP uncertainty by a multiplier based on the correlation coefficient. The correlation coefficient is statistically calculated and shown in Figure 9.1 and Figure 9.2 of EMF-2158(P)(A). It indicates a less than perfect correlation between powers of neighboring bundles. The conservative multiplier is calculated as follows:

[ ]

The calculated TIP uncertainty would normally be expected to be slightly larger than the calculated power uncertainty due to the TIP model. The Quad Cities gamma scan comparison shows the 2-D radial power uncertainty of [ ] (see Section 9.6 of EMF-2158(P)(A)). The D-Lattice plant calculated radial TIP uncertainty is [ ]. The data indicates that the calculated TIP uncertainty is indeed larger than the calculated power uncertainty. The use of the correlation coefficient to increase the calculated power uncertainty is a very conservative approach resulting from the statistical treatment. The types of fuel bundles (8x8, 9x9, or 10x10) loaded in the core has no effect on the reality of the physical model which precludes the possibility of the calculated power uncertainty to be larger than the calculated TIP uncertainty. The accuracy of the MICROBURN-B2 models is demonstrated by comparisons between measured and calculated TIP's as well as comparison of calculated and measured Lanthanum-140 activation. The accuracy of the MICROBURN-B2 models was further validated with detailed axial pin by pin gamma scan measurements of 9X9-1 and ATRIUM-10 fuel assemblies in the reactor designated as KWU-S. These measurements demonstrated the continued accuracy of the MICROBURN-B2 models with modern fuel assemblies. Details of these measurements are provided in Section 8.2.2 of the topical report, EMF-2158(P)(A).

The AREVA SAFLIM2 code is used to calculate the number of expected rods in boiling transition (BT) for a specified value of the SLMCPR (i.e., SLMCPR is an input, not a calculated result). The extremes of the two correlation coefficients from the Quad Cities assembly gamma scan data sets [ )] discussed in section C.2 were used for a sensitivity study of the MCPR safety limit. An analysis of the safety limit was performed with SAFLIM2 using an input SLMCPR of 1.08 and the base RPF uncertainty. The number of boiling transition (BT) rods was calculated to be 60 from this analysis. The analysis was repeated in a series of SAFLIM2 calculations using the increased RPF uncertainty and performed by iterating on the input value of SLMCPR. Different values for the SLMCPR input were used until the number of BT rods calculated by SAFLIM2 was the same as the base case (60 rods). A SLMCPR input value of [ ] resulted in 60 rods in BT when the increased RPF uncertainty was input.

The difference in SLMCPR input [ ] for the two cases that resulted in the same number of BT rods is a measure of the safety limit sensitivity to the increased RPF uncertainty.

The only input parameters that changed between the two SAFLIM2 analyses were the SLMCPR and the RPF uncertainty. For each analysis, 1000 Monte Carlo trials were performed. To minimize statistical variations in the sensitivity study, the same random number seed was used and all bundles were analyzed for both analyses. As discussed above, 60 rods were calculated to be in BT in both analyses.

This sensitivity study was performed to quantify the sensitivity of SLMCPR to an increase in RPF uncertainty and did not follow the standard approach used in SLMCPR licensing analyses. In standard licensing calculations, the SLMCPR is not input at a precision greater than the hundredths decimal place. As a result, the increased RPF uncertainty would result [ ] in SLMCPR licensing analyses depending on how close the case was to the acceptance criterion prior to the increase in RPF uncertainty.

Gamma scanning provides data on the relative gamma flux from the particular spectrum associated with La140 gamma activity. The relative gamma flux corresponds to the relative La140 concentration. Based upon the time of shutdown and the time of the gamma scan the Ba140 relative distribution at the time of shutdown is determined. This Ba140 relative distribution is thus correlated to the pin or assembly power during the last few weeks of operation. The data presented in the topical report, EMF-2158(P)(A), includes both pin and assembly Ba140 relative density data. The assembly gamma scan data was taken at Quad Cities after the operation of cycles 2, 3 and 4. Some of this data also included individual pin data. This data was from 7X7 and 8X8 fuel types. Additional fuel pin gamma scan data was taken at the Gundremingen plant for ATRIUM-9 and ATRIUM-10 fuel. This data is also presented in the topical report.

Pin-by-pin Gamma scan data is used for verification of the local peaking factor uncertainty. Quad Cities measurements presented in the topical report EMF-2158(P)(A) have been re-evaluated to determine any axial dependency. Figure A-28 presents the raw data including measurement uncertainty and demonstrates that there is no axial dependency. The more recent Gamma scans performed by KWU, presented in the topical report EMF-2158(P)(A) and re-arranged by axial level in Table A-1 indicate no axial dependency. Full axial scans were performed on 16 fuel rods. Comparisons to calculated data show excellent agreement at all

axial levels. The dip in power associated with spacers, observed in the measured data, is not modeled in MICROBURN-B2. There is no indication of reduced accuracy at the higher void fractions.

CASMO-4 and MCNP calculations have been performed to compare the fission rate distribution statistics to Table 2-1 of the topical report EMF-2158(P)(A) which is shown in Table A-2. The fission rate differences at various void fractions demonstrate that CASMO-4 calculations have very similar uncertainties relative to the MCNP results for all void fractions. These fission rate differences also meet the criteria of the topical report EMF-2158(P)(A) for all void fractions.

Data presented in these figures and tables demonstrate that the AREVA methodology is capable of accurately predicting reactor conditions for fuel designs operated under the current operating strategies and core conditions.

A.3 Fuel Cycle Comparisons

AREVA has reviewed the data presented in EMF-2158(P)(A) with regard to the maximum assembly power (Figure A-29) and maximum exit void fraction (Figure A-30) to determine the range of data previously benchmarked.

Fuel loading patterns and operating control rod patterns are constrained by the minimum critical power ratio (MCPR) limit, which consequently limits the assembly power and exit void fraction regardless of the core power level. Operating data from several recent fuel cycle designs has been evaluated and compared to that in the topical report EMF-2158(P)(A). Maximum assembly power and maximum void fraction are presented in Figure A-31 and Figure A-32.

In order to evaluate some of the details of the void distribution a current design calculation was reviewed in more detail. Figure A-33 and Figure A-34 present the following parameters at the point of the highest exit void fraction (at 9336 MWd/MTU cycle exposure) in cycle core design for a BWR-6 reactor with ATRIUM-10 fuel. Another measure of the thermal hydraulic conditions is the population distribution of the void fractions. These are representative figures for a high power density plant.

- Core average void axial profile
- Axial void profile of the peak assembly

- Histogram of the nodal void fractions in core

The actual core designs used for each cycle will have slightly different power distributions and reactivity characteristics than any other cycle. Conclusions from analyses that are dependent on the core design (loading pattern, control rod patterns, fuel types) are re-confirmed as part of the reload licensing analyses performed each cycle. Cycle-specific reload licensing calculations will continue to be performed for all future EPFOD cycles using NRC approved methodologies consistent with the current processes.

Monticello operating under EPFOD conditions (Figure A-35 and Figure A-36) can be compared to the equivalent data of the topical report EMF-2158(P)(A). Comparison of Figure A-29 vs. Figure A-35 and Figure A-30 vs. Figure A-36 shows that EPFOD operation in the standard power/flow map is within the range of the original methodology approval for assembly power and exit void fraction. From a neutronic perspective, moderator density (void fraction) and exposure cause the greatest variation in cross sections. NRC-approved exposure limits for ATRIUM 10XM fuel evaluated with AREVA methods are unchanged for EPFOD conditions. Reactor conditions for Monticello with power uprate are not significantly different from that of current experience and are bounded by the experience for the important parameters.

The axial profile of the power and void fraction of the limiting assembly and core average values are presented in Figure A-37 for a Monticello EPFOD cycle design. These profiles demonstrate that the core average void fraction and the maximum assembly power void fractions are bounded by the topical report data and are consistent with recent experience on other reactors.

Figure A-38 presents a histogram of the void fraction for EPFOD conditions. This histogram was taken at the point of maximum exit void fraction expected during the cycle. The distribution of voids is shifted slightly toward the 70 -80 % void fraction levels. The population of nodes experiencing 85 -90% voids is still small.

The neutronic and thermal hydraulic conditions predicted for the EPFOD operation are bounded by the data provided in the topical report EMF-2158(P)(A) so the isotopic validation continues to be applicable to EPFOD operation.

The AREVA methodology [ ] the reactivity coefficients that are used in the transient analysis. Conservatisms in the methodology are used to produce conservative results that bound the uncertainties in the reactivity coefficients. Data

presented in these referenced figures indicate that there are no significant differences between EPFOD and non-EPFOD conditions that have an impact on the reactivity coefficients.

The core bypass water is modeled in the AREVA steady-state core simulator, transient simulator, LOCA and stability codes as [ ].

The steady-state core simulator, MICROBURN-B2, explicitly models the assembly specific flow paths through the lower tie-plate flow holes and the channel seals in addition to a [ ] core support plate. The numerical solution for the individual flow paths is computed based on a general parallel channel hydraulic solution that imposes a constant pressure drop across the core fuel assemblies and the bypass region. This solution scheme incorporates [ ] that is dependent on the [ ].

The MICROBURN-B2 state-point specific solution for bypass flow rate and [ ] is then used as initial conditions in the transient and LOCA analyses. When the reactor operates on high rod-lines at low flow conditions, the in-channel pressure drop decreases to a point where a solid column of water cannot be supported in the bypass region, and voiding occurs in the core bypass. For these conditions (in the region of core stability concerns) the neutronic feedback of bypass voiding [

]

[

]

The level of bypass boiling for a given state-point is a direct result of the hydraulic solution. The potential for boiling increases as the power/flow ratio increases or the inlet sub-cooling decreases. The licensing methodology utilizes [

] to specifically determine a bounding local bypass void distribution in the core. The model is conservative in that it [

]. The capability of this model to predict localized bypass boiling is demonstrated in Figure A-39 for the worst statepoint in the equilibrium.

Bypass voiding is of greatest concern for stability analysis due to its direct impact on the fuel channel flow rates and the axial power distributions. The reduced density head in the core bypass due to boiling results in a higher bypass flow rate and consequently a lower hot channel flow rate. This lower hot channel flow rate and a more bottom-peaked power distribution (due to lower reactivity in the top of the core due to boiling in the bypass region) destabilize the core through higher channel decay ratios. AREVA stability methods directly model these phenomena to assure that the core stability is accurately predicted.

CASMO-4 has the capability to specify the density of the moderator in the bypass and in-channel water rods, [

].

Bypass voiding is not significant during full power, steady-state EPFOD operation for Monticello so there is no impact on steady-state analyses. For transient conditions it is conservative to ignore the density changes as additional voiding aids in shutting down the power generation.

For Monticello, a 100% power / 100% flow statepoint (120% of the original licensed thermal power) was assessed. Even with the conservative multi-channel model, there was minimal bypass boiling at the EPU power level. This assessment assures that the limiting transients at the uprated thermal power are not adversely affected by bypass boiling. As the flow is reduced along the 100% power line, the decrease in flow is compensated by increased sub-cooling which more than compensates for the decrease in flow. When flow is further reduced along the

highest rod line, boiling in the bypass is calculated to begin. This is in the area of stability concerns where the boiling in the bypass is modeled explicitly. For normal operation at 100% power boiling in the bypass is not expected to occur, so there is no impact on the lattice local peaking or the LPRM response.

A.5 Fuel Assembly Design

No fuel design modifications have been made for EPFOD operation, neither mechanical nor thermal hydraulic. The maximum allowed enrichment level of any fuel pellet is 4.95 wt% U-235. A description of fuel enrichments on both a lattice basis and an assembly basis for the first reload of ATRIUM 10XM fuel in Monticello is provided in Table A-3.

All new and spent fuel at Monticello is stored in the Spent Fuel Storage Pool (SFSP) and in accordance with Technical Specification 4.3.1.1 must maintain a subcritical multiplication factor (keff) of less than 0.95 when flooded with non-borated water. A SFSP criticality analysis has been performed for Monticello that confirms that this requirement is met for ATRIUM 10XM fuel designs. This analysis applies to both units which have the same high density storage rack configuration, as detailed in Section 10.2 of the UFSAR. A reload specific evaluation is performed to verify that the specific bundle designs being loaded remain bounded by the criticality analysis.

Table A-1 KWU-S Gamma Scan Benchmark Results from EMF-2158(P)(A)

Table A-2 Comparison of CASMO-4 and MCNP results for ATRIUM-10 Design

Table A-3 Fuel Enrichment Description for the Initial Monticello EPFOD ATRIUM 10XM Fuel Cycle Design

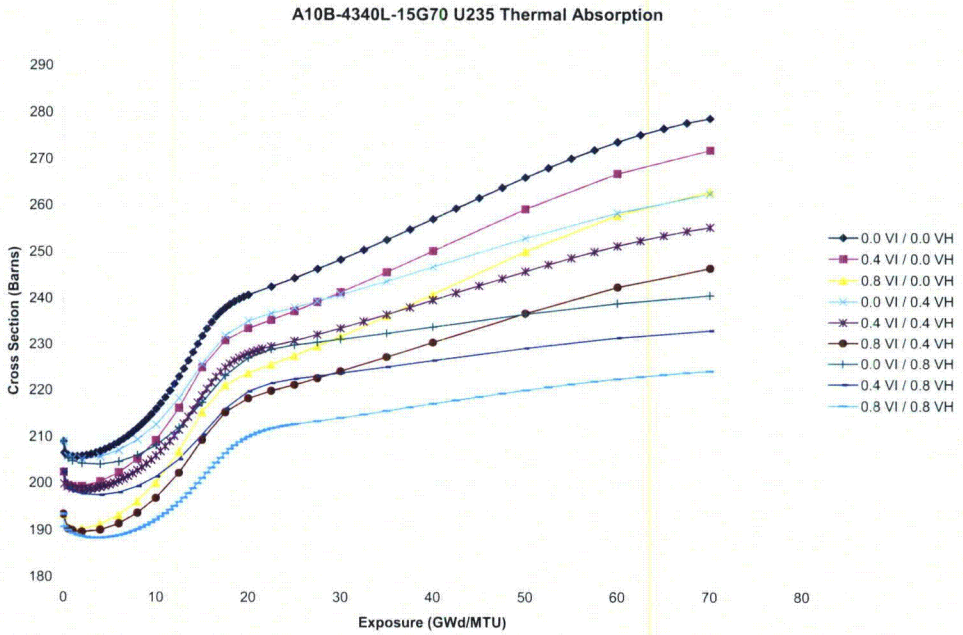

Figure A-1 Microscopic Thermal Cross Section of U-235 from Base Depletion and Branches

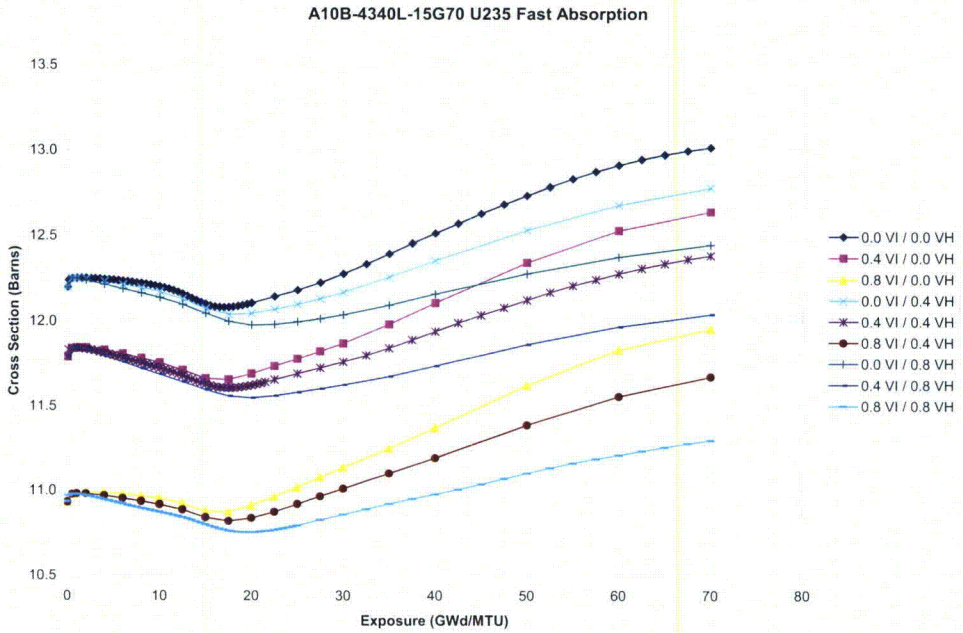

Figure A-2 Microscopic Fast Cross Section of U-235 from Base Depletion and Branches

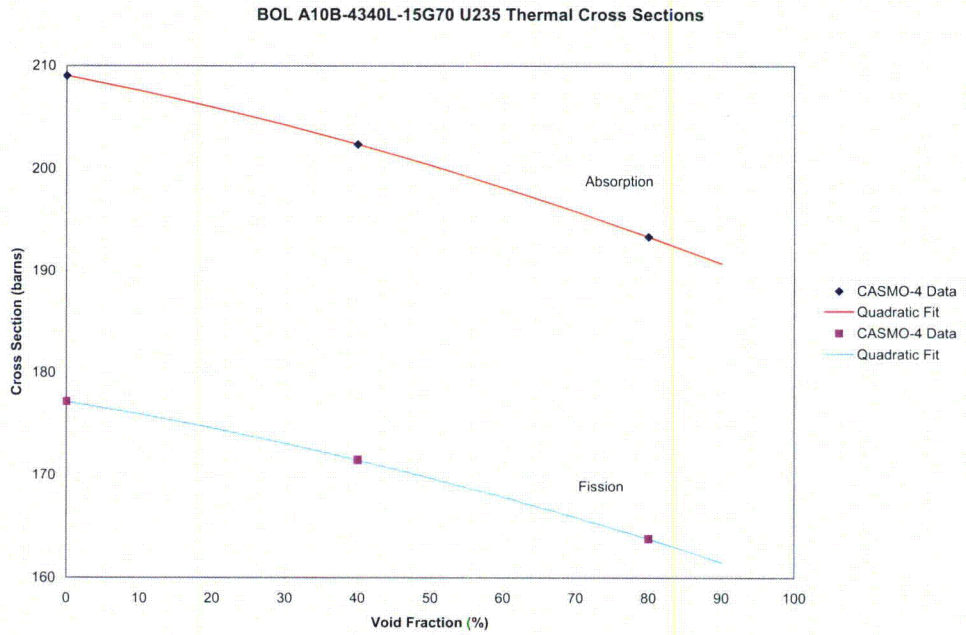

Figure A-3 Microscopic Thermal Cross Section of U-235 at Beginning of Life

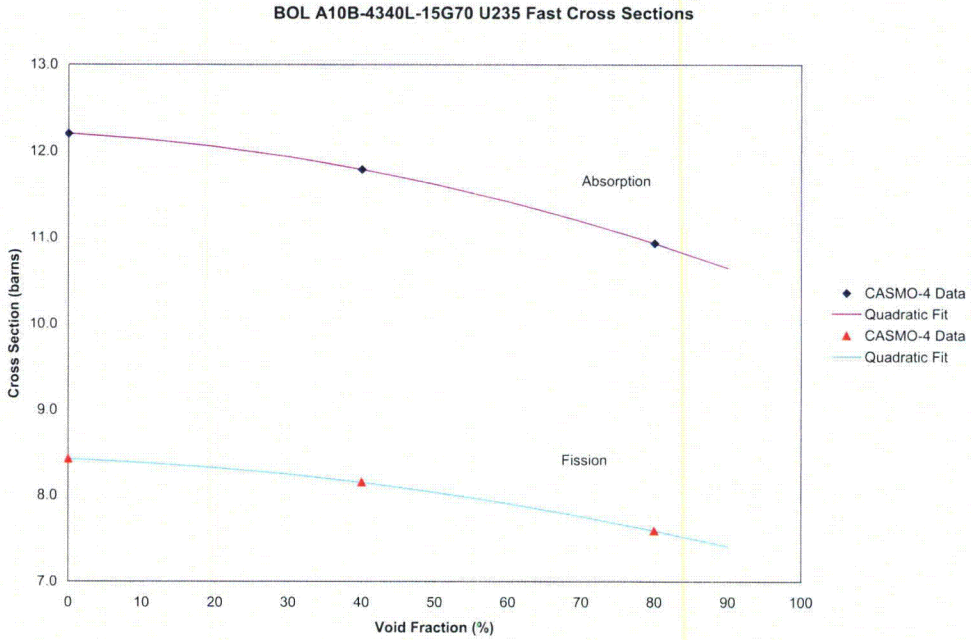

Figure A-4 Microscopic Fast Cross Section of U-235 at Beginning of Life

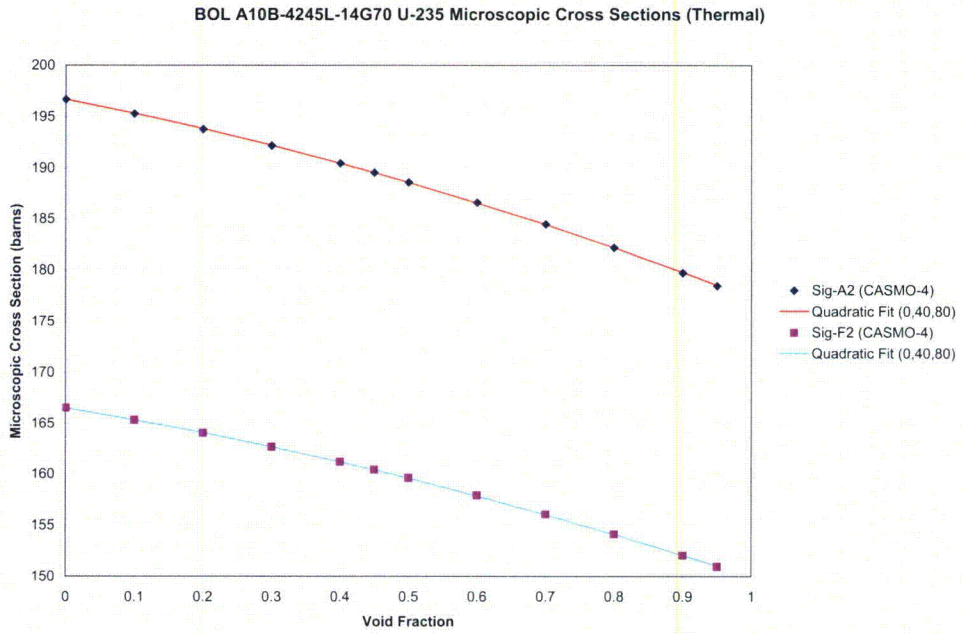

Figure A-5 Microscopic Thermal Cross Section of U-235 Comparison of Quadratic Fit with Explicit Calculations at Various Void Fractions

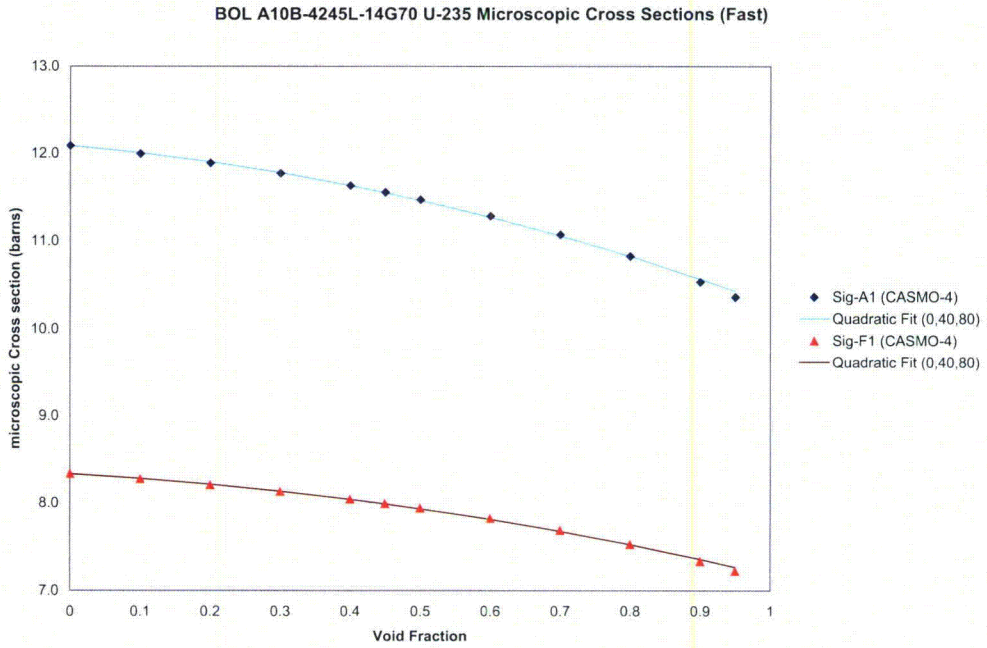

Figure A-6 Microscopic Fast Cross Section of U-235 Comparison of Quadratic Fit with Explicit Calculations at Various Void Fractions

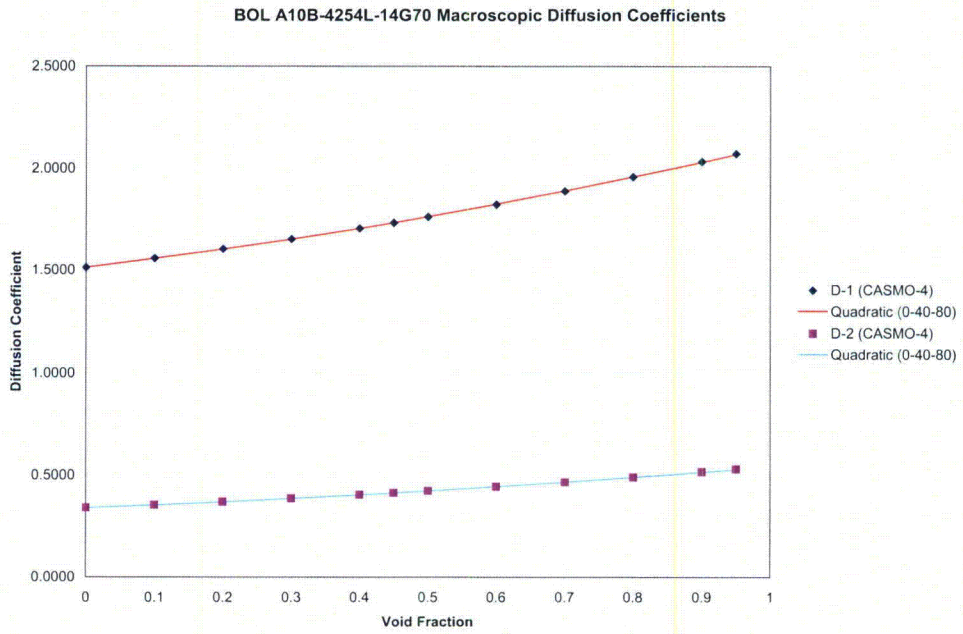

Figure A-7 Macroscopic Diffusion Coefficient (Fast and Thermal) Comparison of Quadratic Fit with Explicit Calculations at Various Void Fractions

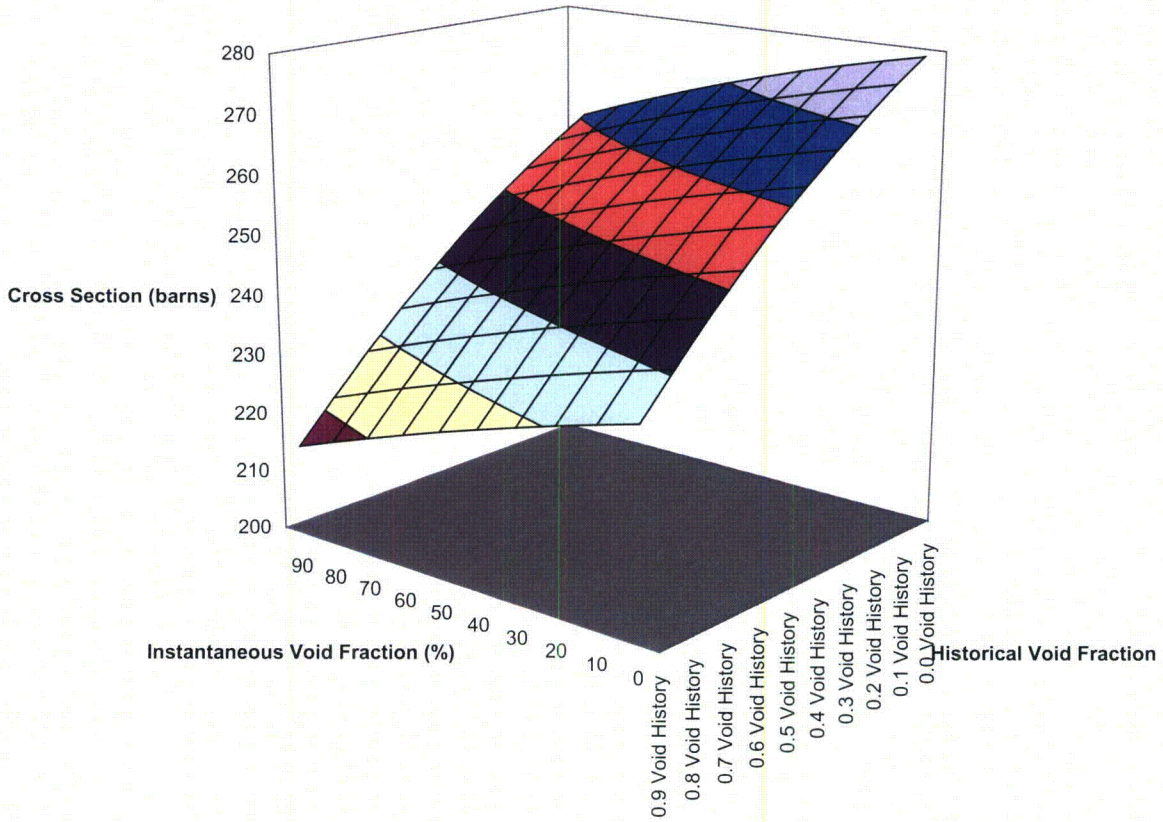

Figure A-8 Microscopic Thermal Cross Section of U-235 at 70 GWd/MTU

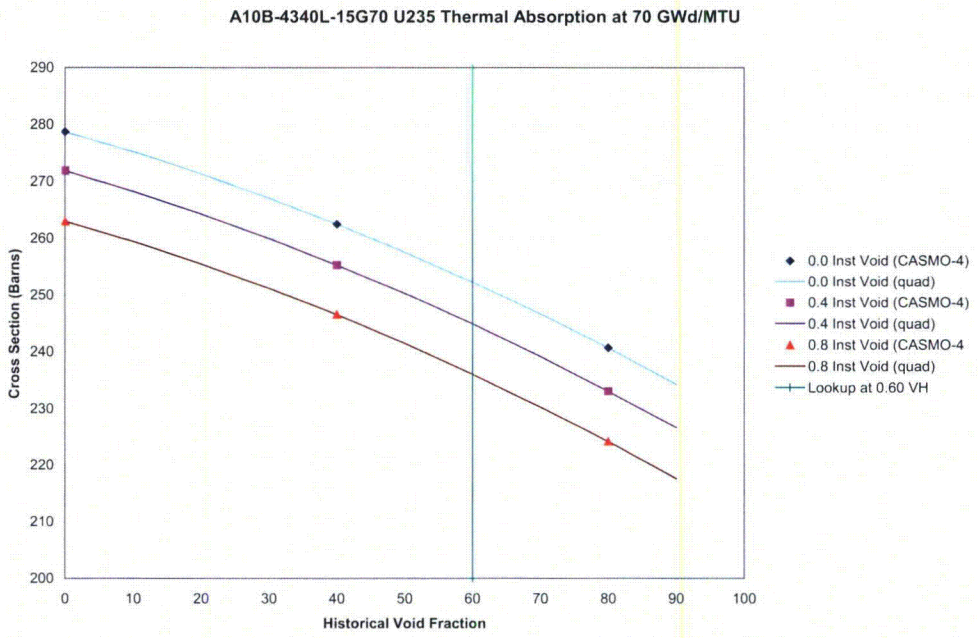

Figure A-9 Quadratic Interpolation Illustration of Microscopic Thermal Cross Section of U-235

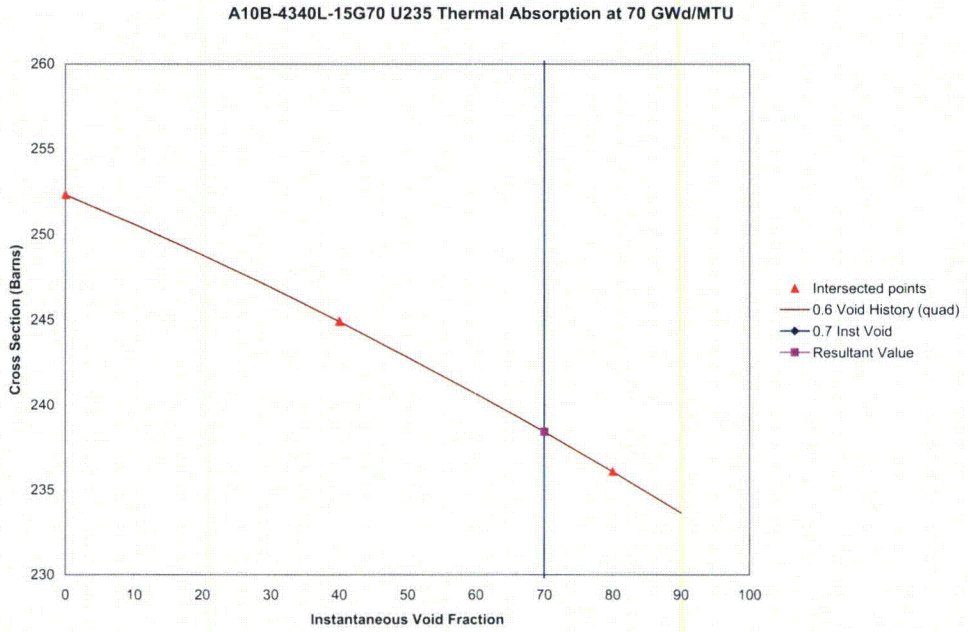

Figure A-10 Illustration of Final Quadratic Interpolation for Microscopic Thermal Cross Section of U-235

Figure A-11 Comparison of k-infinity from MICROBURN-B2 Interpolation Process with CASMO-4 Calculations at Intermediate Void Fractions of 0.2, 0.6 and 0.9

Figure A-12 Comparison of k-infinity from MICROBURN-B2 Interpolation Process with CASMO-4 Calculations at 0.4 Historical Void Fractions and 0.9 Instantaneous Void Fraction

Figure A-13 Delta k-infinity from MICROBURN-B2 Interpolation Process with CASMO-4 Calculations at 0.4 Historical Void Fraction and 0.9 Instantaneous Void Fraction

Figure A-14 Comparison of Interpolation Process Using Void Fractions of 0.0, 0.4 and 0.8 and Void Fractions of 0.0, 0.45 and 0.9

Figure A-15 EMF-2158(P)(A) TIP Statistics by Axial Level

Figure A-16 EMF-2158(P)(A) 2-D TIP Statistics for C-Lattice Plants vs. Core Power

Figure A-17 EMF-2158(P)(A) 2-D TIP Statistics for C-Lattice Plants vs. Core Average Void Fraction

Figure A-18 EMF-2158(P)(A) 2-D TIP Statistics for C-Lattice Plants vs. Core Power/Flow Ratio

Figure A-19 EMF-2158(P)(A) 2-D TIP Statistics for D-Lattice Plants vs. Core Power

Figure A-20 EMF-2158(P)(A) 2-D TIP Statistics for D-Lattice Plants vs. Core Average Void Fraction

Figure A-21 EMF-2158(P)(A) 2-D TIP Statistics for D-Lattice Plants vs. Core Power/Flow Ratio

Figure A-22 EMF-2158(P)(A) 3-D TIP Statistics for C-Lattice Plants vs. Core Power

Figure A-23 EMF-2158(P)(A) 3-D TIP Statistics for C-Lattice Plants vs. Core Average Void Fraction

Figure A-24 EMF-2158(P)(A) 3-D TIP Statistics for C-Lattice Plants vs. Core Power/Flow Ratio

Figure A-25 EMF-2158(P)(A) 3-D TIP Statistics for D-Lattice Plants vs. Core Power

Figure A-26 EMF-2158(P)(A) 3-D TIP Statistics for D-Lattice Plants vs. Core Average Void Fraction

Figure A-27 EMF-2158(P)(A) 3-D TIP Statistics for D-Lattice Plants vs.

Figure A-28 Quad Cities Unit 1 Pin by Pin Gamma Scan Results

Figure A-29 Maximum Assembly Power in Topical Report EMF-2158(P)(A)

Figure A-30 Maximum Exit Void Fraction in Topical Report EMF-2158(P)(A)

Figure A-31 Maximum Assembly Power Observed from Recent Operating Experience

Figure A-32 Void Fractions Observed from Recent Operating Experience

Figure A-33 Axial Power and Void Profile Observed from Recent Design Experience

Figure A-34 Nodal Void Fraction Histogram Observed from Recent Design Experience

Figure A-35 Maximum Assembly Power in an EPFOD Monticello Design

Figure A-36 Maximum Exit Void Fraction in an EPFOD Monticello Design

Figure A-37 Monticello EPFOD Design Axial Profile of Power and Void Fraction

Figure A-38 Monticello EPFOD Design Nodal Void Fraction Histogram

EDIT OF VOID FRACTION IN BYPASS CHANNEL IN UNITS OF %

Figure A-39 Hypothetical MICROBURN-B2 Multi-Channel Average Bypass Void Distribution

Appendix B Non-Linear Stability

This appendix clarifies two topics that have been associated with fuel transitions at Extended Power Uprate. The first is whether the OPRM setpoints account for bypass voiding and the second is the continued applicability of the BWROG analyses (Reference 26) for the Anticipated Transient Analyses Without Scram and Instability (ATWS-I) when AREVA fuel is introduced.

B.1 Bypass voiding

Bypass voiding is not considered in OPRM setpoint analyses. Consideration of bypass voiding is not necessary due to the expected impact discussed below, as well as the overall conservatism of the approved Reference 50 methodology. Examples of conservatism in the Reference 50 methodology approved for application include:

- The reactor is assumed to be operating at the OLMCPR prior to the stability event
- A conservative ΔCPR response (limiting time in cycle) is assumed following a pump trip
- Equilibrium feedwater temperature for off-rated conditions is assumed to be instantaneously achieved following a pump trip
- The statistical analysis selects the hot channel oscillation magnitude value at the 95% probability, 95% confidence level

For Monticello, there is additional conservatism inherent in the DIVOM calculation. The stability analysis of the transition core for Monticello indicates that the global mode is dominant over the regional (out-of-phase) mode where relatively large subcritical reactivity values are calculated with STAIF. Despite the dominance of the global mode, the Monticello DIVOM analyses forced the regional oscillation mode to define the limiting DIVOM slope. Since the regional mode DIVOM slope is typically twice that experienced for the global mode, the OPRM setpoints are expected to be quite conservative.

The impact of localized bypass boiling is a reduction of the LPRM signal due to the decreased local moderation of the fast flux. [

]

[

] Therefore, no degradation in the OPRM signal is expected due to bypass boiling.

B.2 Applicability of ATWS-I

The impact of ATWS with core instability has been addressed in Reference 26. The summary presented on page 3-2 of Reference 26 indicates that for the unmitigated case, a small fraction of the core experiences locally high peak clad temperature (dryout) and some fuel damage cannot be precluded, but the maximum energy deposition meets the licensing limit for reactivity insertion events. Both the ATRIUM 10XM at Monticello and the ATRIUM-10 fuel design are comparable to the current and previous GE fuel designs. The discussion presented on Page 6-7 of Reference 26 indicates that the "Parameters which might vary between fuel designs (e.g., reactivity coefficients) are not expected to significantly change the consequences of large irregular oscillations". Therefore, the generic ATWS stability results of Reference 26 remain applicable upon the introduction of ATRIUM 10XM fuel into Monticello. Therefore, it is assumed that no further evaluations of the ATWS-I are necessary for the introduction of ATRIUM 10XM at Monticello for current conditions.

In support of previous fuel transitions and operation at EPU conditions, the NRC requested comparisons of global and regional ATWS-I scenarios as well as a comparison of the AREVA ATRIUM-10 design relative the GE 8x8 fuel that is a considered as a reference design for stability performance.

The task of evaluating the impact of large regional versus global mode oscillations is first addressed below from an analytical point of view and calculations are presented using a reduced order model. The calculations will also address the effects of the parameters of interest, namely the subcritical reactivity due to core radial power flattening for EPU, increase in void-reactivity coefficient due to increasing the fresh fuel batch size, and fuel geometry effects (part-length rods and reduced pin conduction time constant for an ATRIUM-10 compared with an 8x8 fuel bundle). These effects will be demonstrated to result in equivalent consequences of a postulated ATWS event relative to the results in NEDO-32047-A (Reference 26). Furthermore, the mitigation of the ATWS-I by reducing the core inlet subcooling, as a

consequence of water level reduction by operator action (Reference 28), will be demonstrated to be as effective in suppressing regional mode oscillations as for global mode oscillations.

Analytical Considerations

Unstable global mode oscillations grow exponentially at a fixed rate (decay ratio) from a small perturbation. As the oscillation magnitude increases, nonlinear effects become important. The average power level drifts to higher values as a consequence of the nonlinearity of the neutron kinetics, which results in a negative reactivity feedback due to the increase of void fraction. The negative reactivity superimposed on the oscillating reactivity results in damping the neutron kinetics (References 29, 30, and 31). [

]

[

]

The regional mode oscillations are well understood in the linear limit where the power oscillation is attributed to the excitation of the first azimuthal harmonic mode of the neutron flux. Compared with the fundamental flux mode excitation associated with the global oscillation, the subcritical reactivity of the first azimuthal eigenfunction contributes a damping effect on the neutron kinetics feedback. The hydraulic response is less damped compared to the global mode case due to bypassing the damping effects of the recirculation loop.

[

]

[

]

Description of the Reduced Order Model

The phenomenological description of large power oscillations in the global and regional modes is supported by the results of a reduced order model, which is used here to simulate large global and regional mode oscillations. [

]

[

]

[

]

The reduced order model allows fast and robust simulation of both the global and regional modes and helps to resolve issues that were not apparent at the time NEDO-32047-A (Reference 26) was issued. Most importantly, it helps to explore and provide insight into the differences between the global and regional mode oscillations and their common ultimate limiting mechanism.

Results

The results of several cases performed with the reduced order model are presented. All of these calculations represent unstable oscillations growing to large magnitudes with parameter variations to address the issues of global versus regional and the effect of EPU core loading with fuel design differing from the fuel type used in NEDO-32047-A (Reference 26). These cases are:

[

]

[

]

Conclusions

- Large regional mode oscillations have [ ] effects compared with global mode.
- ATRIUM-10 bundle design differences from an older 8x8 [ ]
- EPU effects (lower subcritical reactivity and higher void reactivity coefficient) [ ]
- [ ]

[

]

Figure B-1 Relative Power for Case 1 Base Global Oscillation

Figure B-2 Relative Power for Case 2 Base Regional Oscillation

Figure B-3 Relative Power for Case 3 Global Oscillation

Figure B-4 Relative Power for Case 4 Regional Oscillation

Figure B-5 Relative Power for Case 5 Regional Oscillation With Decreased Subcriticality

Figure B-6 Relative Power for Case 6 Mitigated Global Oscillation

Figure B-7 Relative Power for Case 7 Mitigated Regional Oscillation

Figure B-8 Relative Power for Case 8 Late-Mitigated Global Oscillation

Figure B-9 Relative Power for Case 9 Late-Mitigated Regional Oscillation

Figure B-10 Inlet Mass Flow Rate for Case 1 Base Global Oscillation

Figure B-11 Inlet Mass Flow Rate for Case 2 Base Regional Oscillation

Figure B-12 Inlet Mass Flow Rate for Case 3 Global Oscillation

Figure B-13 Inlet Mass Flow Rate for Case 4 Regional Oscillation

Figure B-14 Inlet Mass Flow Rate for Case 5 Regional Oscillation With Decreased Subcriticality

Figure B-15 Inlet Mass Flow Rate for Case 6 Mitigated Global Oscillation

Figure B-16 Inlet Mass Flow Rate for Case 7 Mitigated Regional Oscillation

Figure B-17 Inlet Mass Flow Rate for Case 8 Late-Mitigated Global Oscillation

Figure B-18 Inlet Mass Flow Rate for Case 9 Late-Mitigated Regional Oscillation

Figure B-19 Exit Void Fraction for Case 1 Base Global Oscillation

Figure B-20 Exit Void Fraction for Case 2 Base Regional Oscillation

Figure B-21 Exit Void Fraction for Case 3 Global Oscillation

Figure B-22 Exit Void Fraction for Case 4 Regional Oscillation

**Figure B-23 Exit Void Fraction for Case 5
Regional Oscillation With Decreased Subcriticality**

Figure B-24 Exit Void Fraction for Case 6 Mitigated Global Oscillation

Figure B-25 Exit Void Fraction for Case 7 Mitigated Regional Oscillation

Figure B-26 Exit Void Fraction for Case 8 Late-Mitigated Regional Oscillation

Figure B-27 Exit Void Fraction for Case 9 Late-Mitigated Regional Oscillation

Figure B-28 Void Fraction in Selected Nodes for Case 1 Base Global Oscillation

Figure B-29 Void Fraction in Selected Nodes for Case 2 Base Regional Oscillation

Figure B-30 Void Fraction in Selected Nodes for Case 3 Global Oscillation

Figure B-31 Void Fraction in Selected Nodes for Case 4 Regional Oscillation

Figure B-32 Void Fraction in Selected Nodes for Case 5 Regional Oscillation With Decreased Subcriticality

Appendix C Application of AREVA Methodology for Mixed Cores

C.1 Discussion

AREVA has considerable experience analyzing fuel design transition cycles and has methodology and procedures to analyze mixed cores composed of multiple fuel types. For each core design, analyses are performed to confirm that all design and licensing criteria are satisfied. The analyses performed explicitly include each fuel type in the core. The analyses consider the cycle-specific core loading and use input data appropriate for each fuel type in the core. The mixed core analyses are performed using generically approved methodology in a manner consistent with NRC approval of the methodology. Based on results from the analyses, operating limits are established for each fuel type present in the core. During operation, each fuel type is monitored against the appropriate operating limits.

Thermal hydraulic characteristics are determined for each fuel type that will be present in the core. The thermal hydraulic characteristics used in core design, safety analysis, and core monitoring are developed on a consistent basis for both AREVA fuel and other vendor co-resident fuel to minimize variability due to methods. Geometric data for the co-resident fuel is obtained from the utility, generally under a proprietary agreement. The hydraulic characteristics are based on flow test measurements performed for both AREVA fuel and co-resident fuel in the AREVA hydraulic flow test facility. For analyses performed to assess core thermal and hydraulic performance with the XCOBRA computer code, each fuel type in the core is explicitly modeled with the appropriate geometric data and hydraulic characteristics.

The GE14 fuel design will be present during the ATRIUM 10XM transition cycles at Monticello. A GE14 fuel design was flow tested by AREVA in 2002. The GE14 design that will be co-resident with the ATRIUM 10XM fuel at Monticello was confirmed to be thermal hydraulically the same as the GE14 assembly tested by AREVA. The designs differ only by the total axial height, spacer spans are preserved.

For core design and nuclear safety analyses, the neutronic cross-section data is developed for each fuel type in the core using CASMO-4. Geometric and nuclear design data (e.g., enrichment distribution) that is required to prepare CASMO-4 input for the co-resident fuel is obtained from the utility, generally under a proprietary agreement. MICROBURN-B2 is used to

design the core and provide input to safety analyses (core neutronic characteristics, power distributions, etc.). Each fuel assembly is explicitly modeled in MICROBURN-B2 using cross-section data from CASMO-4 and geometric data appropriate for the fuel design.

Fuel assembly thermal mechanical limits for both AREVA and co-resident fuel are verified and monitored for each mixed core designed by AREVA. The thermal mechanical limits established by the co-resident fuel vendor continue to be applicable for mixed (transition) cores. The thermal mechanical limits (steady-state and transient) for the co-resident fuel are provided to AREVA by the utility. AREVA performs design and licensing analyses to demonstrate that the core design meets steady-state limits and that transient limits are not exceeded during anticipated operational occurrences.

The critical power ratio (CPR) is evaluated for each fuel type in the core using calculated local fluid conditions and an appropriate critical power correlation. Fuel type specific correlation coefficients for AREVA fuel are based on data from the AREVA critical power test facility. Unless the co-resident fuel critical power correlation is provided to AREVA, an AREVA critical power correlation is applied to the co-resident fuel. An NRC-approved process for developing correlation coefficients and the associated uncertainty is described in Reference 34 when applying an AREVA critical power correlation for co-resident fuel. If adequate test data is available for the co-resident fuel, the correlation coefficients and uncertainty are determined using the process consistent with the approval of the correlation. When test data for the co-resident fuel is not available to AREVA, fuel type specific correlation coefficients and uncertainty are developed using calculated CPR data provided by the utility based on an alternate (indirect) approach described in Reference 34.

The SPCB critical power correlation will be used for monitoring GE14 fuel present during the ATRIUM 10XM transition cycles at Monticello. Consistent with the NRC-approved methodology, the indirect approach from Reference 34 was used to develop correlation coefficients and uncertainty based on CPR data provided to AREVA by Xcel Energy.

The critical power ratio (CPR) correlation used for the AREVA fuel is based on the ACE/ATRIUM 10XM critical power correlation described in Reference 35. The ACE CPR correlation uses K-factor values to account for rod local peaking, rod location and bundle geometry effects. The K-factor methodology was modified in Reference 36 in response to

deficiencies found in the axial averaging process. In addition, the additive constants were revised as a result of the change to the K-factor model.

The K-factor parameter is described in detail in Section 3.1 of Reference 36.

At the time of the creation of this document, Reference 36 had not yet been generically approved. Reference 23 presents the ACE/ATRIUM 10XM critical power correlation that will be used in licensing analyses for Monticello in the interim. The correlation presented in Reference 23 is exactly the same as that presented in Reference 36.

Analyses performed to determine the safety limit MCPR explicitly address mixed core effects. Each fuel type present in the core is explicitly modeled using appropriate geometric data, thermal hydraulic characteristics, and power distribution information (from CASMO-4 and MICROBURN-B2 analyses). CPR is evaluated for each assembly using fuel type specific correlation coefficients. Plant and fuel type specific uncertainties are considered in the statistical analysis performed to determine the safety limit MCPR. The safety limit MCPR analysis is performed each cycle and uses the cycle specific core configuration.

An operating limit MCPR is established for each fuel type in the core. For fast transients the COTRANSA2 code (Reference 37) is used to determine the overall system response. The core nuclear characteristics used in COTRANSA2 are obtained from MICROBURN-B2 and reflect the actual core loading pattern. Boundary conditions from COTRANSA2 are used with an XCOBRA-T core model. In the XCOBRA-T model, a hot channel with appropriate geometric and thermal hydraulic characteristics is modeled for each fuel type present in the core. Critical power performance is evaluated using local fluid conditions and fuel type specific CPR correlation coefficients. The transient CPR response is used to establish an operating limit MCPR for each fuel type.

For transient events that are sufficiently slow such that the heat transfer remains in phase with changes in neutron flux during the transient, evaluations are performed with MICROBURN-B2 in accordance with NRC approval. Such slow transients are modeled with the MICROBURN-B2 core simulator code by performing a series of steady state solutions with appropriate boundary conditions using the cycle specific design core loading plan. Each fuel assembly type in the core is explicitly modeled. The change in CPR between the initial and final condition after the

transient is determined, and if the CPR change is more severe than those determined from fast transient analyses, the slow transient result is used to determine the MCPR operating limit.

Stability analyses to establish OPRM setpoints and backup stability exclusion regions are performed using the cycle-specific core loading pattern. The stability analyses performed with RAMONA5-FA and STAIF explicitly model each fuel type in the core. Each fuel type is modeled using appropriate geometric, thermal hydraulic and nuclear characteristics determined as described above. The stability OPRM setpoints and exclusion region boundaries are established based on the predicted performance of the actual core composition.

MAPLHGR operating limits are established and monitored for each fuel type in the core to ensure that 10 CFR 50.46 acceptance criteria are met during a postulated LOCA. The AREVA LOCA methodology is used to establish MAPLHGR limits for AREVA fuel. The RELAX code is used to determine the overall system response during a postulated LOCA and provides boundary conditions for a RELAX hot channel model. Results from the hot channel analysis provide boundary conditions to the HUXY computer code. The HUXY model includes fuel type specific input such as dimensions and local power peaking for each fuel rod.

[

]

[

]

The core monitoring system will monitor each fuel assembly in the core. Each assembly is modeled with geometric, thermal hydraulic, neutronic, and CPR correlation input data appropriate for the specific fuel type. Each assembly in the core will be monitored relative to thermal limits that have been explicitly developed for each fuel type.

In summary, AREVA methodology is used consistent with NRC approval to perform design and licensing analyses for mixed cores. The cycle design and licensing analyses explicitly consider each fuel type in mixed core configurations. Co-resident fuel input parameters are developed consistent with the methodology, and in general are developed in the same manner as for AREVA fuel. Limits are established for each fuel type and operation within these limits is verified by the monitoring system during operation.

C.2 Shutdown Margin

In order to accurately determine shutdown margins during transition cycles, AREVA performs detailed benchmarking analyses of the three to five cycles previous to insertion of AREVA fuel in that reactor. This benchmarking is performed with the CASMO-4/MICROBURN-B2 3-D core simulator code system. Hot depletions are performed using actually operated state conditions including as-loaded core configurations, as-operated control rod patterns, and operating power, pressure, flow, and inlet subcooling. To confirm the validity of the hot depletions, comparison of eigenvalue trends and predicted versus measured TIP distributions for the benchmark cycles are performed. These results are used to establish the hot-operating target k-eff for design of the first transition cycle. All cold critical measurements taken during the benchmarking cycles are also modeled in MICROBURN-B2 by restarting from the hot cycle depletions discussed above. The results from the cold critical benchmarks are used to define a cold critical k-eff target. Once the cold target is determined based on the benchmarking, a statistically based design shutdown margin limit is chosen to bound the uncertainty observed by comparing the critical k-effs computed with MICROBURN-B2 to the target selected from the benchmarking. A

typical design target is 1% Δk/k. This ensures that the transition loading fuel design will support the 0.38% Δk/k technical specification cold shutdown margin requirement with additional margin to cover the uncertainty in the design target chosen based on the benchmarking results. Past AREVA experience indicates that the variation in the target cold critical k-eff when transitioning from GE14 to ATRIUM-10 is small (≤ 0.001).

During the design of each transition cycle, shutdown margin is computed by performing restart solutions based on a shuffled core from a short window previous cycle condition. This means that the previous cycle is assumed to shutdown earlier than the nominal planned shutdown for the cycle. The short window shutdown of the previous cycle results in additional carryover reactivity for the shutdown margin analysis of the cycle being designed. Setting the gadolinia design of the fresh fuel and the loading plan to meet the design shutdown margin based on the assumed short window shutdown of the previous cycle assures that adequate shutdown margin exists for the entire cycle at the design stage. Prior to actual startup of the cycle, shutdown margin is recomputed based on the actual previous cycle shutdown exposure. At startup, when each designed cycle reaches cold critical conditions, comparison to the predicted point of criticality to the actual point of criticality is made. High accuracy of the predicted versus actual critical eigenvalue demonstrates the validity of the shutdown margin design for that cycle.

The initial critical and any subsequent cold critical data points achieved in each transition and follow-on cycle are fed back into the cold critical eigenvalue database for the reactor unit, and the target is revised as needed for the design of the subsequent cycle. This method assures continued accuracy in predicting the cold shutdown margin as new fuel is transitioned into the reactor core during the first and second transition cycles and all subsequent cycles.

C.3 Assembly Liftoff

The analysis of record for Monticello has a minimum [ ] margin to assembly liftoff under normal operating conditions and [ ] under anticipated operational occurrences (AOO). The margin to liftoff is the difference between the wet weight of the fuel assembly and hydraulic forces. The hydraulic forces are calculated from conservative thermal-hydraulic evaluations which predict a maximum core pressure drop of [

].

Thermal-hydraulic compatibility studies have shown that the core pressure drop with a typical GNF fuel design could be a maximum of [

] the effect of mixed cores is negligible.

Appendix D Void-Quality Correlations

D.1 AREVA Void Quality Correlations

The Zuber-Findlay drift flux model (Reference 38) is utilized in the AREVA nuclear and safety analysis methods for predicting vapor void fraction in the BWR system. The model has a generalized form that may be applied to two phase flow by defining an appropriate correlation for the void concentration parameter, Co, and the drift flux, Vgj. The model parameters account for the radially non-uniform distribution of velocity and density and the local relative velocity between the phases, respectively. This model has received broad acceptance in the nuclear industry and has been successfully applied to a host of different applications, geometries, and fluid conditions through the application of different parameter correlations (Reference 39).

Two different correlations are utilized at AREVA to describe the drift flux parameters for the analysis of a BWR core. The correlations and treatment of uncertainties are as follows:

- The nuclear design, frequency domain stability, nuclear AOO transient and accident analysis methods use the [ ] void correlation (Reference 40) to predict nuclear parameters. Uncertainties are addressed at the overall methodology and application level rather than individually for the individual correlations of each method. The overall uncertainties are determined statistically by comparing predictions using the methods against measured operating data for the reactors operating throughout the world.

- The thermal-hydraulic design, system AOO transient and accident analysis, and loss of coolant accident (only at specified junctions) methods use the Ohkawa-Lahey void correlation (Reference 41). This correlation is not used in the direct computation of nuclear parameters in any of the methods. Uncertainties are addressed at the overall methodology level through the use of conservative assumptions and biases to assure uncertainties are bounded.

The [ ] void correlation was developed for application to multi-rod geometries operating at typical BWR operating conditions using multi-rod data and was also validated against simple geometry data available in the public domain. The correlation was defined to be functionally dependent on the mass flux, hydraulic diameter, quality, and fluid properties.

The multi-rod database used in the [

]. As a result, the multi-rod database and prediction uncertainties are not available to AREVA. However, the correlation has been independently validated by AREVA against public domain multi-rod data and proprietary data collected for prototypical ATRIUM-10 and ATRIUM 10XM test assemblies. Selected results for the ATRIUM-10 test assembly are reported in the public domain in Reference 42.

The Ohkawa-Lahey void correlation was developed for application in BWR transient calculations. In particular, the correlation was carefully designed to predict the onset of counter current flow limit (CCFL) characteristics during the occurrence of a sudden inlet flow blockage. The correlation was defined to be functionally dependent on the mass flux, quality, and fluid properties.

Independent validation of the correlation was performed by AREVA at the request of the NRC during the NRC review of the XCOBRA-T code. The NRC staff subsequently reviewed and approved Reference 19, which compared the code to a selected test from the FRIGG experiments (Reference 43). More recently the correlation has been independently validated by AREVA against additional public domain multi-rod data and proprietary data collected for prototypic ATRIUM-10 and ATRIUM 10XM test assemblies.

The characteristics of the AREVA multi-rod void fraction validation database are listed in Table D-1.

The FRIGG experiments have been included in the validating database because of the broad industry use of these experiments in benchmarking activities, including TRAC, RETRAN, and S-RELAP5. The experiments include a wide range of pressure, subcooling, and quality from which to validate the general applicability of a void correlation. However, the experiments do not contain features found in modern rod bundles such as part length fuel rods and mixing vane grids. The lack of such features makes the data less useful in validating correlations for modern

fuel designs. Also the reported instrument uncertainty for these tests is provided in Table D-1 based on mockup testing. However, the total uncertainty of the measurements (including power and flow uncertainties) is larger than the indicated values.

Because of its prototypical geometry, the ATRIUM-10 and ATRIUM 10XM void data collected at KATHY was useful in validating void correlation performance in modern rod bundles that include part length fuel rods, mixing vane grids, and prototypic axial/radial power distributions. Void measurements were made at one of three different elevations in the bundle for each test point: just before the end of the part length fuel rods, midway between the last two spacers, and just before the last spacer.

As shown in Figure 2-1, the range of conditions for the ATRIUM void data are valid for typical reactor conditions. This figure compares the equilibrium quality at the plane of measurement for the ATRIUM-10 void data with the exit quality of bundles in the EMF-2158 benchmarks and Monticello operating at EPU conditions. As seen in the figure, the data at the measurement plane covers nearly the entire range of reactor conditions. However, calculations of the exit quality from the void tests show the overall test conditions actually envelope the reactor conditions.

Figure D-1 and Figure D-2 provide comparisons of predicted versus measured void fractions for the AREVA multi-rod void fraction validation database using the [ ] correlation. These figures show the predictions fall within ±0.05 (predicted – measured) error bands with good reliability and with very little bias. Also, there is no observable trend of uncertainty as a function of void fraction.

Figure D-3 and Figure D-4 provide comparisons of predicted versus measured void fractions for the AREVA multi-rod void fraction validation database using the Ohkawa-Lahey correlation. In general, the correlation predicts the void data with a scatter of about ±0.05 (predicted – measured), but a bias in the prediction is evident for voids between 0.5 and 0.8. The observed under prediction is consistent with the observations made in Reference 44.

The comparisons in Figure D-1 through Figure D4 demonstrate that the [ ] and the Ohkawa-Lahey void-quality correlations predict a span of geometries without bias. The cross-sectional views of the FRIGG and ATRIUM-10 test channels are shown in Figure D-5 along with the geometry of the GE14 fuel design. Despite the significantly different geometrical

configurations (between FRIGG and ATRIUM-10), the behavior of the calculations when compared to the measured data is remarkable similar. This similarity indicated that the [ ] and the Ohkawa-Lahey void-quality correlations are applicable to a range of geometries larger than the differences between the ATRIUM-10 and GE14 and therefore are equally applicable to the GE14 fuel design.

In conclusion, validation using the AREVA multi-rod void fraction validation database has shown that both drift flux correlations remain valid for modern fuel designs. Furthermore, there is no observable trend of uncertainty as a function of void fraction. This shows there is no increased uncertainty in the prediction of nuclear parameters at EPU conditions within the nuclear methods when applied to the Monticello reactor.

D.2 Void Quality Correlation Uncertainties

The AREVA NP analyses methods and the correlations used by the methods are applicable for modern fuel designs in both pre-EPU and EPU conditions. The approach for addressing the void-quality correlation bias and uncertainties remains unchanged and is applicable for Monticello operation with the ATRIUM 10XM fuel design.

The OLMCPR is determined based on the safety limit MCPR (SLMCPR) methodology and the transient analysis (ΔCPR) methodology. Void-quality correlation uncertainty is not a direct input to either of these methodologies; however, the impact of void-correlation uncertainty is inherently incorporated in both methodologies as discussed below.

The SLMCPR methodology explicitly considers important uncertainties in the Monte Carlo calculation performed to determine the number of rods in boiling transition. One of the uncertainties considered in the SLMCPR methodology is the bundle power uncertainty. This uncertainty is determined through comparison of calculated to measured core power distributions. Any miscalculation of void conditions will increase the error between the calculated and measured power distributions and be reflected in the bundle power uncertainty. Therefore, void-quality correlation uncertainty is an inherent component of the bundle power uncertainty used in the SLMCPR methodology.

The transient analysis methodology is not a statistical methodology and uncertainties are not directly input to the analyses. The transient analyses methodology is a deterministic, bounding

approach that contains sufficient conservatism to offset uncertainties in individual phenomena. Conservatism is incorporated in the methodology in two ways: (1) computer code models are developed to produce conservative results on an integral basis relative to benchmark tests, and (2) important input parameters are biased in a conservative direction in licensing calculations.

The transient analyses methodology results in predicted power increases that are bounding relative to benchmark tests. In addition, for licensing calculations a 110% multiplier is applied to the calculated integral power to provide additional conservatism to offset uncertainties in the transient analyses methodology. Therefore, uncertainty in the void-quality correlation is inherently incorporated in the transient analysis methodology.

Based on the above discussions, the impact of void-quality correlation uncertainty is inherently incorporated in the analytical methods used to determine the OLMCPR. Biasing of important input parameters in licensing calculations provides additional conservatism in establishing the OLMCPR. No additional adjustments to the OLMCPR are required to address void-quality correlation uncertainty.

D.3 Biasing of the Void-Quality Correlation

AREVA NP has performed studies to determine the OLMCPR sensitivity to biases approaching the upper and lower extremes of the data comparisons shown in Figure D-1 through Figure D-4.

For one of these studies, the transient ΔCPR impact was determined by propagating void-quality biases through three main computer codes: MICROBURN-B2, COTRANSA2, and XCOBRA-T.

The [ ] correlation in MICROBURN-B2 was modified to correct the mean to match the measured ATRIUM-10 void fraction data shown in Figure D-2. The modified [ ] correlation parameters were then modified to generate two bounding correlations for the ATRIUM-10 of ±0.05 void. The results of this modified correlation are presented in Figure D-6.

COTRANSA2 does not have the [ ] correlation. For COTRANSA2 the modified [ ] correlations in MICROBURN-B2 were approximated in COTRANSA2 with [ ]. Figure D-7 shows a comparison of the [ ] ratio results compared to the ATRIUM-10

test data. This approach created equivalent void fractions as the [ ] correlation modifications.

The thermal hydraulic methodology incorporates the effects of subcooled boiling through use of the Levy model. The Levy model predicts a critical subcooling that defines the onset of boiling. The critical subcooling is used with a profile fit model to determine the total flow quality that accounts for the presence of subcooled boiling. The total flow quality is used with the void-quality correlation to determine the void fraction. This void fraction explicitly includes the effects of subcooled boiling. Application of the Levy model results in a continuous void fraction distribution at the boiling boundary.

Like COTRANSA2, XCOBRA-T does not have the [ ] correlation. Unlike COTRANSA2, XCOBRA-T does not have [

]. For the other void scenarios, no correction was done in XCOBRA-T. Not modifying the void-quality correlation for the other void scenarios results in a very small difference in ΔCPR.

The transient response was assessed relative to a limiting uprated BWR plant transient calculation. The impact of the change in the void correlations was also captured in the burn history of the fuel (the results are not for an instantaneous change in the void correlations). The SLMCPR response was also assessed with the new input corresponding to the three different void scenarios. The results are provided in Table D-2.

The major influence that the void-quality models have on scram reactivity worth is through the predicted axial power shape. The void-quality models, used for ATRIUM fuel, result in a very good prediction of the axial power shape.

As seen in the results in Table D-2, modifying the void-quality correlations to correct the mean to match the measured ATRIUM-10 void fraction data results in a very small increase in ΔCPR, a very small decrease in SLMCPR, and a very small increase in OLMCPR for this study; therefore, the impact of the correlation bias is insignificant.

The +0.05 void scenarios show an increase in the OLMCPR; however, as mentioned previously, the transient analysis methodology is a deterministic, bounding approach that contains sufficient

conservatism to offset uncertainties in individual phenomena. Conservatism is incorporated in the models to bound results on an integral basis relative to benchmark tests. For licensing calculations, important input parameters are biased in a conservative direction. In addition, the licensing calculations include a 110% multiplier to the calculated integral power to provide additional conservatism to offset uncertainties in the transient analysis methodology (which includes the void-quality correlation). Even with an extreme bias in the void correlation of +0.05, the conservatism introduced by the 110% multiplier is alone sufficient to offset the increase in results presented in Table D-2. For the study, the conservatism of the 110% multiplier was [ ]. These calculations demonstrate that the overall methodology has sufficient conservatism to account for both the bias and the uncertainty in the void-quality correlation.

To provide a more accurate assessment of the impact of a +0.05 void bias, AREVA NP would need to re-evaluate the Peach Bottom transient benchmarks; it is likely that the +0.05 void scenario would show overconservatism in the benchmarks. Likewise, the pressure drop correlations and core monitoring predictions of power will likely show a bias relative to measured data. Correcting the models to new benchmarks and measured data would further reduce the OLMCPR sensitivity.

D.4 Void-Quality Correlation Uncertainty Summary

Integral power is a parameter obtainable from test measurements that is directly related to ΔCPR and provides a means to assess code uncertainty. The COTRANSA transient analysis methodology was a predecessor to the COTRANSA2 methodology. The integral power figure of merit was introduced with the COTRANSA methodology as a way to assess (not account for) code uncertainty impact on ΔCPR. From COTRANSA analyses of the Peach Bottom turbine trip tests, the mean of the predicted to measured integral power was 99.7% with a standard deviation of 8.1%. AREVA NP (Exxon Nuclear at the time) initially proposed to treat integral power as a statistical parameter. However, following discussions with the NRC, it was agreed to apply a deterministic 110% integral power multiplier (penalty) on COTRANSA calculations for licensing analyses. That increase was sufficient to make the COTRANSA predicted to measured integral power conservative for all of the Peach Bottom turbine trip tests.

COTRANSA2 is not a statistical methodology and uncertainties are not directly input to the analyses. The methodology is a deterministic bounding approach that contains sufficient conservatism to offset uncertainties in individual phenomena. Conservatism is incorporated in

the methodology in two ways: (1) computer code models are developed to produce conservative results on an integral basis relative to benchmark tests, and (2) important input parameters are biased in a conservative direction in licensing calculations. Justification that the integrated effect of all the conservatisms in COTRANSA2 licensing analyses is adequate for EPU operation at Monticello is provided below.

The COTRANSA2 methodology results in predicted power increases that are bounding ([ ] on average) relative to Peach Bottom benchmark tests. In addition, for licensing calculations a 110% multiplier is applied to the calculated integral power to provide additional conservatism. This approach adds significant conservatism to the calculated OLMCPR as discussed previously.

Biasing of important input parameters in licensing calculations provides additional conservatism in establishing the OLMCPR. The Peach Bottom turbine trips were performed assuming the measured performance of important input parameters such as control rod scram speed and turbine valve closing times. For licensing calculations, these (and other) parameters are biased in a conservative bounding direction. These conservative assumptions are not combined statistically; assuming all parameters are bounding at the same time produces very conservative results.

With the ATRIUM 10XM void fraction benchmarks presented in Figures D-2 and D-4, the applicability of the void-quality correlation at high void fractions is confirmed and the uncertainty associated with the application of the correlation to the ATRIUM 10XM design is demonstrated to be equivalent to the data used in the bias assessment. Therefore, the sensitivity studies and conclusions drawn from the study are equally applicable to the ATRIUM 10XM applications at Monticello

Table D-1 AREVA Multi-Rod Void Fraction Validation Database

	FRIGG-2 (Reference 45)	**FRIGG-3 (Reference 43 & 44)**	**ATRIUM-10 KATHY**	**ATRIUM 10XM KATHY**
Axial Power Shape	uniform	uniform	[ ]	[ ]
Radial Power Peaking	uniform	mild peaking	[ ]	[ ]
Bundle Design	circular array with 36 rods + central thimble	circular array with 36 rods + central thimble	[ ]	[ ]
Pressure (psi)	725	725, 1000, and 1260	[ ]	[ ]
Inlet Subcooling (^{0}F)	4.3 to 40.3	4.1 to 54.7	[ ]	[ ]
Mass Flow Rate (lbm/s) *(Based on mass flux assuming ATRIUM-10 inlet area)*	14.3 to 31.0	10.1 to 42.5	[ ]	[ ]
Equilibrium Quality at Measurement Plane (fraction)	-0.036 to 0.203	-0.058 to 0.330	[ ]	[ ]
Max Void at Measurement Plane (fraction)	0.828	0.848	[ ]	[ ]
Reported Instrument Uncertainty (fraction)	0.025	0.016	[ ]	[ ]
Number of Data	27 tests, 174 points	39 tests, 157 points	[ ]	[ ]

Table D-2 Void Sensitivity Results

Parameter	Reference Calculation	Modified V-Q (0.0)	Modified V-Q (+0.05)	Modified V-Q (−0.05)
ΔCPR	0.305	0.307	0.321	0.305
SLMCPR	1.09	1.09	1.09	1.09
ΔSLMCPR	NA	−0.001	−0.002	+0.002
OLMCPR	1.395	1.396	1.409	1.397

Figure D-1 Validation of [ ] using FRIGG-2 and FRIGG-3 Void Data

Figure D-2 Validation of [ ] using ATRIUM-10 and ATRIUM 10XM Void Data

Figure D-3 Validation of Ohkawa-Lahey using FRIGG-2 and FRIGG-3 Void Data

Figure D-4 Validation of Ohkawa-Lahey using ATRIUM-10 and ATRIUM 10XM Void Data

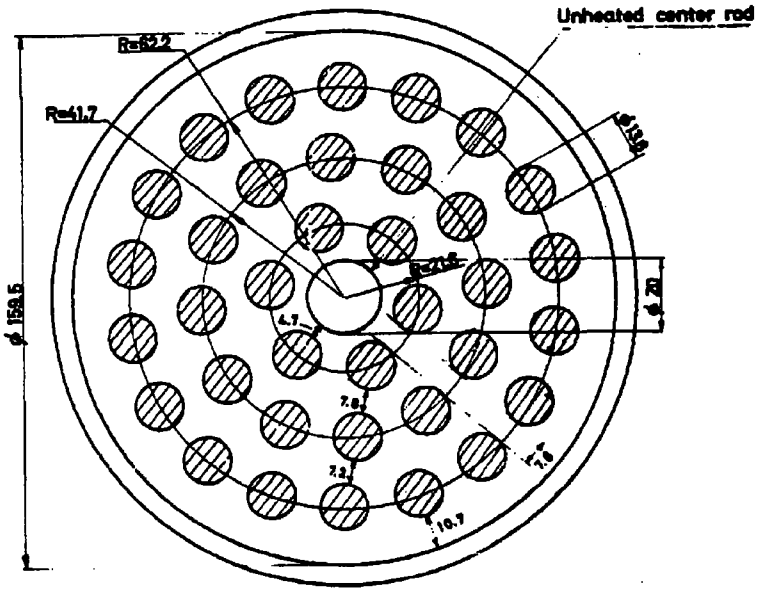

Figure D-5a FRIGG Test Cross Section

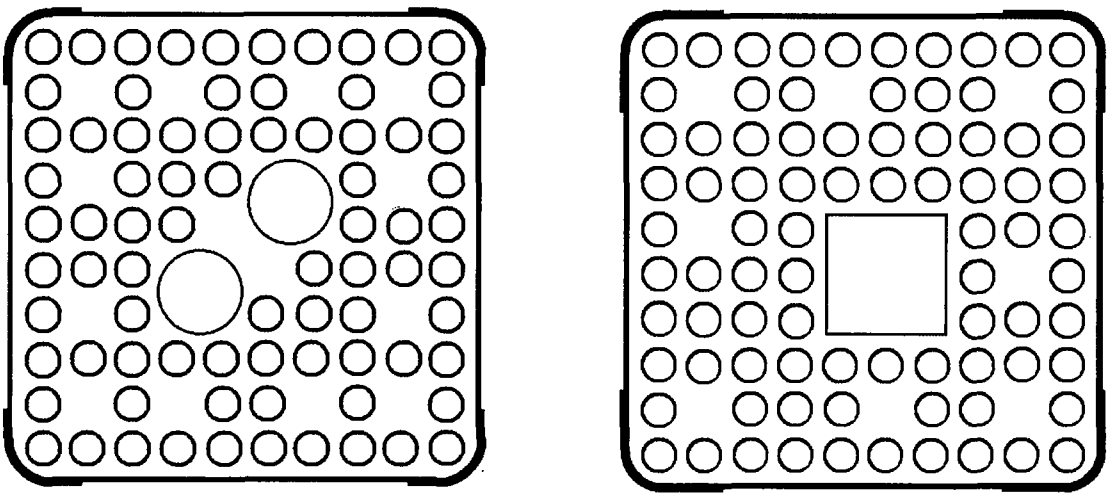

Figure D-5b GE14 (left) and ATRIUM-10 (right)
Top Cross Section

Figure D-6 Modified Void Fraction Correlation Comparison to ATRIUM-10 Test Data

Figure D-7 [ ] Void Fraction Comparison to ATRIUM-10 Test Data

Appendix E Fuel Conductivity Degradation

E.1 Introduction

The U.S. Nuclear Regulatory Commission (NRC) issued Information Notice (IN) 2009-23 (No. ML091550527), dated October 8, 2009, for concerns regarding the use of historical fuel thermal conductivity models in the safety analysis of operating reactor plants. IN 2009-23 discusses how historical fuel thermal mechanical codes may overpredict fuel rod thermal conductivity at higher burn-ups based on new experimental data. This new experimental data showed significant degradation of fuel pellet thermal conductivity with exposure. The NRC staff concluded that the use of the older legacy fuel models will result in predicted fuel pellet conductivities that are higher than the expected values.

The appendix summarizes the impact and treatment of fuel conductivity degradation for licensing safety analyses supporting the ATRIUM 10XM fuel that is being introduced to Monticello.

E.2 Disposition of Licensing Safety Analysis for Monticello ATRIUM 10XM Fuel

RODEX2 and RODEX2A codes were approved by the NRC in the early and mid-1980's, respectively. At that time, thermal conductivity degradation (TCD) with exposure was not well characterized by irradiation tests or post-irradiation specific-effects tests at high burnups. The fuel codes developed at that time did not accurately account for this phenomenon. Analyses performed with RODEX2/2A are impacted by the lack of an accurate thermal conductivity degradation model. Likewise, conductivity models in the transient codes COTRANSA2 and XCOBRA-T do not account for thermal conductivity degradation.

RODEX4 (Topical Report 2-11) is a best-estimate, state-of-the-art fuel code that fully accounts for burnup degradation of fuel thermal conductivity. RODEX4, therefore, can be used to quantify the impact of burnup-dependent fuel thermal conductivity degradation and its effect on key analysis parameters.

Thermal-mechanical licensing safety analyses for the Monticello ATRIUM 10XM are performed with RODEX4 and therefore explicitly account for thermal conductivity degradation. No

additional assessment is needed for those analyses. For thermal-hydraulic and safety analyses an evaluation is needed. The following analysis methodologies use RODEX2 and/or include a separate UO_2 thermal conductivity correlation:

- Anticipated Operational Occurrence (AOO) analysis based on COTRANSA2/RODEX2/XCOBRA-T codes;
- Loss of Coolant Accidents (LOCA) analyses based on RELAX/RODEX2/HUXY codes;
- Overpressurization analyses based on COTRANSA2/RODEX2 codes;
- Stability analyses based on STAIF/RAMONA5-FA codes; and
- Fire event analyses based on RELAX/RODEX2/HUXY codes.

E.3 Assessment of Analyses for Monticello ATRIUM 10XM Fuel

The issues identified in IN 2009-23 were entered into AREVA NP corrective action program in 2009. A summary of the investigation was provided to the NRC in a white paper (Reference 46). The white paper was an extensive evaluation; for BWRs the assessments consisted primarily of ATRIUM-10 fuel. A summary of that evaluation is provided as follows for the items noted in the previous section. In addition, to include the assessment of the ATRIUM 10XM fuel being introduced at Monticello, each subsection ends with a discussion of the impact and treatment of thermal conductivity degradation for ATRIUM 10XM fuel.

The NRC reviewed Reference 46 and provided requests for information in Reference 47. AREVA provided responses in Reference 48. Items relevant from References 47 and 48 are also discussed in the following subsections.

E.3.1 Anticipated Operational Occurrence Analyses

The computer codes COTRANSA2 and XCOBRA-T are used in AOO analyses. Both codes use UO_2 thermal conductivity correlations that do not address TCD. In addition, the core average gap conductance used in the COTRANSA2 system calculations and the hot channel gap conductance used in XCOBRA-T hot channel calculations are obtained from RODEX2 calculations. In general, the sensitivity to conductivity and gap conductance for AOO analyses is in the opposite direction for the core and hot channel, i.e., putting more energy into the coolant (higher thermal conductivity/higher gap conductance) is non-conservative for the system calculation but conservative for the hot channel calculation. The competing effects between the

core and hot channel calculation minimize the overall impact of thermal conductivity degradation.

The assessment of Reference 46 demonstrated that COTRANSA2 uses several conservative assumptions, which results in conservatism relative to the Peach Bottom turbine trip qualification database. The COTRANSA2 methodology results in predicted integral power increases that are bounding relative to the Peach Bottom benchmark tests. With the 110% integral power multiplier used in the methodology, the COTRANSA2 predicted to measured mean integral power is [ ] for the Peach Bottom turbine trip tests. The COTRANSA2 benchmark testing was performed using the same UO_2 conductivity model as used in the current licensing analyses. Therefore, the benchmarking comparisons inherently include any impact of UO_2 conductivity degradation with exposure exhibited in the Peach Bottom tests.

The prior assessment was based on fuel designs current at the time of the Peach Bottom tests. To supplement the assessment with modern fuel, calculations were performed using the as-submitted AURORA-B code (Reference 49). AURORA-B is built from previous NRC approved methods. These methods include codes RODEX4, MICROBURN-B2, and S-RELAP5; UO_2 thermal conductivity degradation is correctly modeled. It is noted that the AURORA-B methodology and application have not yet been reviewed by the NRC; however, the staff accepted its use for sensitivity calculations for this assessment (Reference 47). The AURORA-B sensitivity studies show that the impact of fuel thermal conductivity degradation with exposure results a decrease in the ΔCPR of [ ] increase in the transient LHGR excursion.

Based on the inherent conservatisms associated with the transient analysis codes and the small impact of thermal conductivity degradation with exposure for the AOO analysis, it is concluded that MCPR and LHGR operating limits based on the AOO methodology are not impacted.

The application of the methodology for ATRIUM 10XM fuel does not change the conservatisms nor invalidate the sensitivity; therefore, the AOO methodology remains applicable for ATRIUM 10XM fuel at Monticello. It should be noted that transient LHGR analyses are performed with the RODEX4 code for the Monticello ATRIUM 10XM fuel, which correctly accounts for thermal conductivity degradation.

E.3.2 Loss of Coolant Accident Analyses

LOCA analyses are performed using the EXEM BWR-2000 methodology and include the use of the RODEX2, RELAX and HUXY computer codes. In addition to the initial stored energy, the RODEX2 code is used to calculate fuel mechanical parameters for use in the HUXY computer code that potentially impact the clad ballooning and rupture models. Clad ballooning has a small impact on Peak Cladding Temperature (PCT) and metal water reaction (MWR), but clad rupture can have a significant impact on PCT, depending on event timing.

The LOCA event is divided into two phases: the blowdown and refill/reflood phases. During the initial or blowdown portion of a LOCA, good cooling conditions exist, and the initial stored energy in the fuel is removed. While a decrease in the thermal conductivity increases the overall thermal resistance, heat transfer conditions remain sufficient to remove the initial stored energy. Numerous sensitivity studies have been performed to demonstrate that BWR LOCA analyses are insensitive to initial stored energy. After the initial phase of a LOCA, the heat transfer coefficient at the cladding surface is degraded due to the loss of coolant (low flow and high quality). As a result, the heat transfer from the fuel is primarily controlled by the surface heat flux, and the temperature profile across the pellet is very flat. When compared to the rod surface thermal resistance, the pellet thermal conductivity is not a significant portion of the fuel rod total thermal resistance. Therefore, LOCA calculations are not sensitive to the UO_2 thermal conductivity used in RELAX and HUXY.

To demonstrate that LOCA calculations were not sensitive to UO_2 thermal conductivity, assessments were performed for multiple BWRs. Most LOCA analyses of record are limiting at beginning of life (BOL) conditions. For these cases, increases in PCT at later exposures remained non-limiting. Thermal conductivity degradation may impact calculated PCTs and oxidation at higher exposures; however, since the MAPLHGR limit decreases linearly at higher burnups, significant margin is gained that offsets any decrease in margin associated with thermal conductivity degradation.

Assessments of the potential impact of exposure degradation of UO_2 thermal conductivity on the fuel mechanical parameters were made using the RODEX4 computer code. The RODEX4 code explicitly incorporates the impact of UO_2 thermal conductivity degradation with exposure. RODEX4 calculations were performed with and without the models which account for TCD. The differences in these RODEX4 results were used to adjust the RODEX2 data which is input to

HUXY. The results of these evaluations were summarized to the NRC in References 46 and 48.

The impact of TCD was incorporated in the Monticello ATRIUM 10XM LOCA analysis. For Monticello, an input option was added to RODEX4 to allow the analyst to turn off the models for thermal conductivity degradation with exposure. The impact of TCD was determined by running the nominal RODEX4 fuel rod depletions and then repeating them with the input option selected to turn off TCD. These RODEX4 results were used to increase the stored energy (average pellet temperature) calculated by RODEX2 prior to their input to HUXY. As shown below, this is a very conservative method for evaluating the impact of TCD since RODEX2 was developed to calculate conservatively high stored energy in support of its use as part of the AREVA Appendix K BWR LOCA methodology.

After the NRC approval of RODEX2, more Halden tests were performed with fuel centerline temperature monitoring. As with the RODEX4 submittal, this extended temperature database was used to benchmark RODEX2 over the approved burnup range. The extended temperature benchmarking for RODEX2 shows centerline temperature remains conservative to at least 10 MWd/kgU (Reference 46). Even so, the increase in stored energy predicted with the TCD models in RODEX4 was applied to the RODEX2 calculated stored energy for all nonzero exposures.

The PCT results with and without the impact of TCD are provided in Table E-1. Clad failure and the highest PCT is calculated at 0.0 GWd/MTU, where there is no TCD.

E.3.2.1 Responses to NRC Requests

From the NRC's review of Reference 46, additional information was requested in Reference 47. The information requests and responses are provided as follows:

> *A detailed explanation of the source of the heat transfer coefficients utilized in the HUXY calculation*
>
> This request is answered in Reference 48 and this answer is applicable to Monticello.
>
> *A description of how LOCA analyses are initialized in terms of power distribution; specifically, how thermal limits (such as MLHGR or OLMCPR) are considered in the initialization*

This request is answered in Reference 48. This response explains that AREVA's goal is to establish an MAPLHGR limit that is less restrictive than the LHGR limit and satisfies 10 CFR 50.46 acceptance criteria. When this goal is achieved, some of the rods in the HUXY heatup analysis will have LHGRs higher than the LHGR limit. For some Monticello neutronic lattice designs, the MAPLHGR limit will be more restrictive than the LHGR limit for a small range of exposures. However, the PCT occurs at 0.0 GWd/MTU and at this exposure the MAPLHGR limit is less restrictive than the LHGR limit. For the limiting neutronic lattice, the LHGR of 43 of the 91 rods had initial LHGRs higher than the LHGR limit.

A characterization of the PCT sensitivity to fuel conductivity for plants where early boiling transition is predicted to occur during the early stages of LOCA

The Monticello LOCA break spectrum shows boiling transition occurs as early as 5.8 seconds during two-loop operation and as early as 1.0 seconds during single-loop operation. These calculations used a conservatively high initial stored energy. The highest stored energy occurs at early exposure when the density of the pellet reaches a maximum. The maximum stored energy for Monticello ATRIUM 10XM fuel was calculated with RODEX2 at 2 GWd/MTU. The time of boiling transition was calculated based on a conservatively high stored energy.

The change in stored energy from UO_2 thermal conductivity degradation is of primary concern for the LOCA analyses; however, it is important to note that maximum stored energy would occur between 0 – 15 GWd/MTU. Within this range, maximum stored energy occurs from pellet densification when the gap between the cladding and pellet is at its maximum. This usually occurs before 5 GWd/MTU – an exposure region that is not an issue for conductivity degradation. At later exposures where conductivity degradation is significant, the reduction in power by the MAPLHGR limit would prevent this exposure region from being limiting in terms of stored energy. The RELAX system and RELAX hot channel analyses are performed with stored energy determined from the earlier exposure region. As noted in Reference 46, RODEX2 has an over-prediction of fuel centerline temperature to at least 10 GWd/MTU, therefore stored energy used in the RELAX analyses is conservative.

E.3.3 Overpressurization Analyses

The COTRANSA2 code is used to perform analyses to demonstrate that the reactor vessel pressure will not exceed the ASME vessel pressure limit during specified events. COTRANSA2 is also used to demonstrate that the vessel pressure does not exceed the acceptance criterion for an anticipated transient without scram (ATWS) event.

Analyses using COTRANSA2 are potentially affected by UO_2 thermal conductivity degradation with exposure, as described in Section E.3.1 for AOO analyses. As discussed in Reference 46, the impact on overpressurization analysis was assessed in two ways: using AURORA-B to assess the relative impact of using UO_2 thermal conductivity with exposure degradation; and

decreasing the core average thermal conductivity input into COTRANSA2 to account for the effects of exposure degradation. Reference 46 summarized the increase in pressure as less than a [ ] pressure rise (peak pressure – initial pressure) for the AURORA-B assessment and a pressure rise of [ ] for COTRANSA2 when the core average thermal conductivity assumed a 30% reduction. The Reference 46 evaluations concluded that the impact of UO_2 thermal conductivity degradation with exposure on the peak vessel pressure in overpressurization analyses was a small increase, the increase is less than the existing margins to the acceptance criteria.

In the ASME analysis for Monticello Cycle 28, the impact of TCD was specifically evaluated for ATRIUM 10XM fuel. This evaluation showed that if a 30% reduction in thermal conductivity (due to increased exposure) is applied the ASME overpressure results become slightly less limiting. This is a result of the lower pellet conductivity reducing the moderator feedback and as a consequence the average core peak neutron flux increases faster during the event which in return triggers an earlier scram which improves the overpressure results. No credit was taken for this slight improvement for the reported results. For ATWS analysis, the same 30% reduction in the thermal conductivity resulted in an increase of [ ] of the pressure rise (peak pressure – initial pressure). The effect of TCD will be tracked and applied to the ASME and ATWS overpressure analyses which are performed to support each cycle of operation.

The impact of TCD for the ATRIUM 10XM transition core for Monticello Cycle 28 is [ ].

E.3.3.1 Responses to NRC Requests

From the NRC's review of Reference 46, additional information was requested in Reference 47. The requests and responses to the requests are provided as follows:

> *A comprehensive list of the identified nonconservative biases in the AREVA overpressure analysis methods*
>
> The comprehensive list of items was provided in Reference 48. The biases applicable for Monticello ATRIUM 10XM are summarized as follows. These biases are addressed for each cycle to ensure that the pressure limits are not exceeded.
>
> Void-Quality Correlation: The bias is [ ] for ASME and [ ] for ATWS calculations.

Thermal Conductivity Degradation: In Reference 46 AREVA evaluated the impact of TCD in two ways: using the AURORA-B code (Reference 49) to assess the relative impact of using UO_2 thermal conductivity with exposure degradation; and decreasing the core average thermal conductivity input into COTRANSA2 to account for the effects of exposure degradation. It was noted that changing the UO_2 thermal conductivity model provides a conservative estimate of the impact of exposure degradation on calculated peak vessel pressure. The limiting results obtained for the plants assessed in support of Reference 46 were reported as follows. For ASME, the increase in peak reactor pressure is expected to be less than **[ ]** of the pressure rise (peak pressure – initial pressure). For ATWS, the increase in pressure rise was **[ ]**.

The effect of thermal conductivity degradation for Monticello ASME pressurization was assessed by decreasing the core average thermal conductivity in COTRANSA2 by 30%. The peak pressure did not increase.

The effect of thermal conductivity degradation for Monticello ATWS pressurization was assessed by decreasing the core average thermal conductivity in COTRANSA2 by 30%. The peak pressure increased by **[ ]**.

Doppler Model Mismatch Between MICROBURN-B2 and COTRANSA2: The bias is **[ ]** of the calculated pressure rise from steady-state conditions for the ASME calculation and **[ ]** for the ATWS calculation.

Verification that the nonconservative biases are considered in an integral sense in the safety analyses

Reference 48 demonstrated that it is conservative to add the biases together from separate effect assessments. The integral study demonstrated a decrease in total bias pressure.

E.3.4 Stability Analyses

As summarized in Reference 46, the computer codes STAIF and RAMONA5-FA are used in stability analyses. Both of these codes have fuel models that include UO_2 thermal conductivity degradation with exposure. Therefore, there is no impact on AREVA NP stability analyses.

E.3.5 Fire Event Analyses

The analyses to demonstrate compliance with Appendix R criteria are performed using the LOCA analysis codes. For these analyses, the calculated PCT is much lower than for LOCA analyses. As detailed in Section E.3.2 for the LOCA analyses, the impact of UO_2 thermal conductivity degradation with exposure has only a small impact on calculated PCT. Like the Monticello LOCA analyses, the fire protection analyses are limiting at BOL. Therefore, the conclusions from these analyses would not be affected by UO_2 thermal conductivity degradation with exposure.

Table E-1 Impact of TCD on PCT

Table E-2 Monticello Cycle 28
Overpressurization Biases and Results

Appendix F COTRANSA2 Cross Section Representation

The COTRANSA2 transient simulator solves the one-dimensional neutron diffusion equation to predict the core average power response. In order to accurately capture the core reactivity characteristics, a series of MICROBURN-B2 calculations are performed. These successive calculations are:

1) Nominal initial conditions

The 1½ energy group diffusion equation in steady-state can be written as

$$\nabla \cdot D_1 \nabla \Phi_1 - \left(\Sigma_{a1} + \frac{\Sigma_{1-2}}{\Sigma_{a2}} \cdot \Sigma_{a2} \right) \Phi_1 + \frac{\left(\nu\Sigma_{f2} + \frac{\Sigma_{1-2}}{\Sigma_{a2}} \cdot \nu\Sigma_{f2} \right) \Phi_1}{k_{eff}} = 0$$

The first term is a leakage. This equation is integrated over the cylindrical node depicted in the following figure.

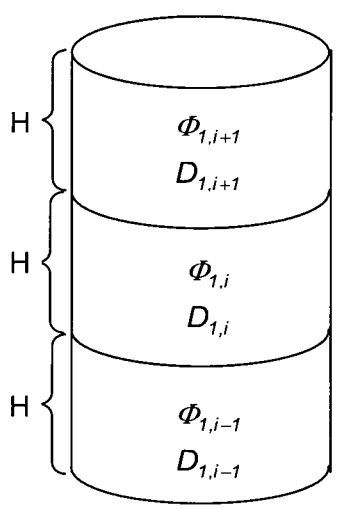

The leakage term is approximated as:

$$-\sum_{j=l}^{3} \frac{2D_{l,i}D_{l,j}(\Phi_{l,i} - \Phi_{l,j})}{(D_{l,i} + D_{l,j})} \frac{A}{HV}$$

where

$D_{1,i}$ = D for plane of interest

$D_{1,j}$ = D for the nodes adjacent to the plane of interest

$\Phi_{1,i}$ = flux in the plane of interest

$\Phi_{1,j}$ = flux in the regions adjacent to the plane of interest

A = surface area between nodes i and j

H = distance between nodes i and nodes j

V = node volume

These final one group cross section and leakage parameters are used in a new 1-dimensional flux solution and the axial power distribution is updated for the next thermal hydraulic solution. The process is repeated for every core solution until a converged core power, power distribution, temperature distribution and density distributions are obtained.

[ ]

Figure F-1 Comparison of Scram Bank Worth for [ ]

Appendix G Extending SPCB/GE14 Low Pressure Boundary

The Pressure Regulator Failure Open (PRFO) event results in depressurization of the Boiling Water Reactor (BWR). The analysis of this event requires that the Critical Power Ratio (CPR) safety limit be maintained during the time that the reactor is above 25% rated thermal power (RTP). This event imposes a requirement that the critical power correlation support pressures lower than the normal operating pressure range.

Co-resident fuel is modeled with an approved AREVA critical power correlation according to the methodology described in Topical Report 2-21. Co-resident GE14 fuel is modeled with the SPCB correlation, Topical Report 2-22. The range of data used to construct additive constants for the Monticello GE14 fuel did not extend below 800 psia. This imposes a low pressure boundary on the SPCB/GE14 correlation of 800 psia, significantly higher than the SPCB correlation low pressure boundary of 571.4 psia.

AREVA analyses indicate the PRFO event can reach pressures below 700 psia, during which, the safety limit must be maintained. Normally, crossing a critical power pressure boundary requires assuming that onset of dryout has occurred. This is not an acceptable outcome for the PRFO event. In this appendix, a method allowing application of the SPCB/GE14 to pressures lower than 800 psia (but remaining within the application range of SPCB) is described and justified. The bases for this justification are:

- Observations of critical power behavior with pressure from the open literature
- Test data observations of critical power behavior as a function of pressure for ATRIUM-10
- SPCB critical power correlation behavior as function of pressure

Collier & Thome (Reference 53) show the influence of pressure on critical heat flux. When the test section is at the critical heat flux, the integrated heat flux over the heated surface area is the critical power. Their figure (reproduced in Figure G-1) shows the characteristic expected behavior in the range of BWR pressure from 40 to 100 bar (approximately 580 to 1450 psia). The dashed line with the inlet subcooling set to zero is the most representative of BWR application. The critical heat flux increases monotonically as the pressure decreases, reaching a maximum near 500 to 600 psia. The curve with the solid line represents an unusual case. The inlet temperature is fixed to the specified value of 174 degC. This means that as the

pressure is increased, the inlet subcooling increases; the decreased inlet subcooling as the pressure is lowered (leading to lower critical power) appears to compete with the effect of pressure, where the critical power increases as the pressure is lowered.

Lahey & Moody (Reference 54) show the influence of pressure on critical power of BWR fuel (reproduced in Figure G-2). It also shows that decreasing the pressure increases the critical power. The data includes two different flow rates and several peaking factors. There is a note in Reference 54, page 113 that says that the behavior continues as the pressure decreases until the trend reverses at a pressure less than 600 psia. Thus, the effect noted by Collier and Thome is observed to be present in BWR fuel assemblies.

Pressure variation of ATRIUM-10 fuel design (test STS-17.8) with an inlet subcooling of approximately 20 Btu/lb and two flow rates are selected from Topical Report 2-22 and plotted in Figure G-3. It shows the ATRIUM-10 critical power data trend with pressure is consistent with that of the open literature – critical power increases as the pressure is decreased.

The bases for the expected behavior of critical power with pressure have been established from the open literature and from BWR fuel critical power test data observations. Now consider the critical power correlation. The SPCB correlation critical power behavior as a function of pressure and flow rate is described in Topical Report 2-22, page 2-28. For the purpose of discussing the low pressure boundary of the SPCB correlation, the critical power is plotted as a function of pressure and mass flow rate with an inlet subcooling of 20 Btu/lb (Figure G-4). The pressure is varied from 1000 psia to the lower boundary of the SPCB correlation. It shows that the SPCB correlation has the expected behavior – that as the pressure is decreased, the critical power increases.

The low pressure boundary of the SPCB/GE14 correlation (800 psia) is well within the range of the SPCB correlation. Thus, an alternative treatment for the low pressure boundary can be described. For pressures that are lower than the SPCB/GE14 800 psia correlation boundary, the critical power will be evaluated as though the pressure was at 800 psia (preserving the same inlet subcooling). The results of applying the SPCB/GE14 correlation to pressures lower than 800 psia is illustrated with dashed lines in Figure G-5 and indicates that the alternative low pressure boundary treatment is conservative. By treating the boundary in this way, the SPCB/GE14 correlation can be applied to system pressures as low as the SPCB correlation lower boundary on pressure.

This application of the SPCB/GE14 correlation to the SPCB lower boundary pressure (571.4 psia) supports the expected system pressure reduction associated with the Pressure Regulator Failure Open event analysis.

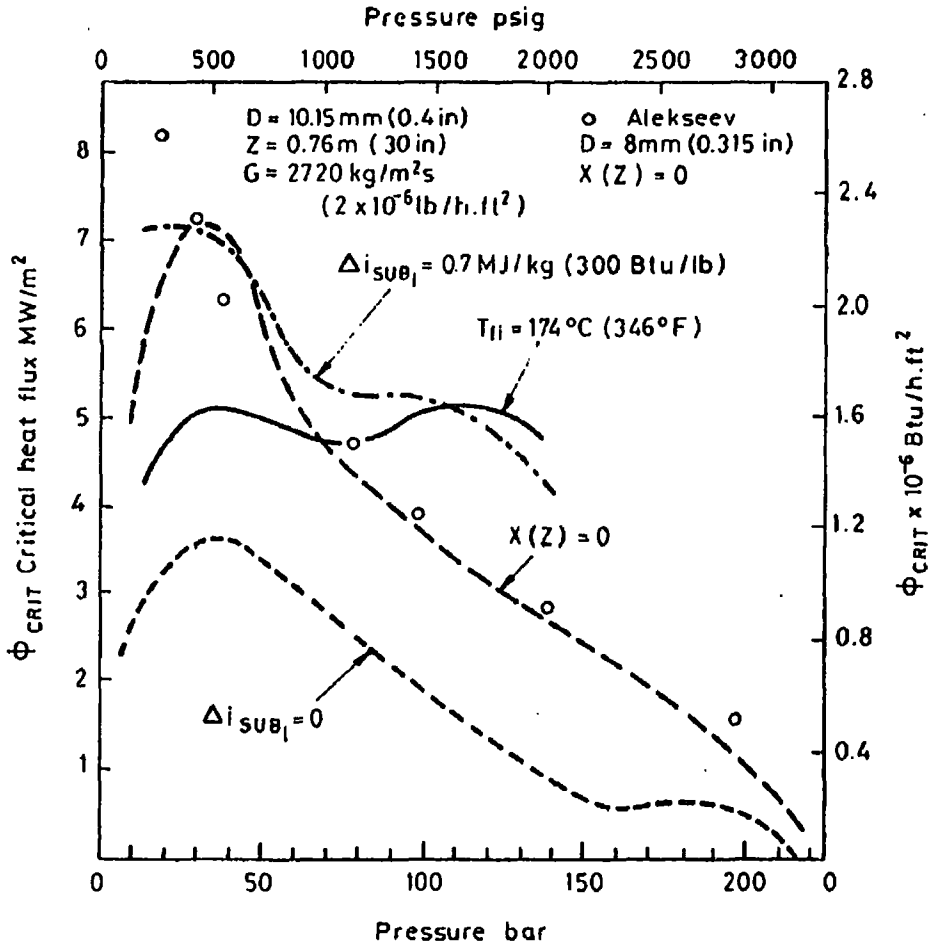

Reproduced from Reference 53, Figure 8.13, page 362.

Figure G-1 The Influence of System Pressure on Critical Heat Flux

Reproduced from Reference 54, Figure 4-36, page 116.

Figure G-2 Normalized Critical Power versus Pressure

Figure G-3 ATRIUM-10 Test STS-17.8 Critical Power versus Pressure

Figure G-4 SPCB Correlation Critical Power as Function of Pressure and Flow Rate

Figure G-5 SPCB/GE14 Correlation With Alternative Treatment of Low Pressure Boundary